SCIENCE CHINA
Information Sciences

• REVIEW •

February 2022, Vol. 65 121301:1–121301:40
https://doi.org/10.1007/s11432-020-3211-8

Multichannel adaptive signal detection: basic theory and literature review

Weijian LIU[1], Jun LIU[2], Chengpeng HAO[3], Yongchan GAO[4] & Yong-Liang WANG[1*]

[1]*Wuhan Electronic Information Institute, Wuhan* 430019*, China;*
[2]*Department of Electronic Engineering and Information Science, University of Science and Technology of China, Hefei* 230027*, China;*
[3]*State Key Laboratory of Acoustics, Institute of Acoustics, Chinese Academy of Sciences, Beijing* 100190*, China;*
[4]*School of Electronic Engineering, Xidian University, Xi'an* 710071*, China*

Received 22 September 2020/Revised 10 January 2021/Accepted 12 March 2021/Published online 19 January 2022

Abstract Multichannel adaptive signal detection uses test and training data jointly to form an adaptive detector to determine whether a target exists. The resulting adaptive detectors typically possess constant false alarm rate (CFAR) properties; thus, no additional CFAR processing is required. In addition, a filtering process is also not required because the filtering function is embedded in the adaptive detector. Adaptive detection typically exhibits better detection performance than the filtering-then-CFAR detection technique. It has been approximately 35 years since the first multichannel adaptive detector was proposed by Kelly in 1986. However, there are few overview articles on this topic. Thus, in this study, we present a tutorial overview of multichannel adaptive signal detection with an emphasis on the Gaussian background. We discuss the main design criteria for adaptive detectors, investigate the relationship between adaptive detection and filtering-then-CFAR detection techniques, investigate the relationship between adaptive detectors and adaptive filters, summarize typical adaptive detectors, present numerical examples, provide a comprehensive literature review, and discuss potential future research tracks.

Keywords constant false alarm rate, multichannel signal, signal mismatch, statistical distribution, subspace signal

Citation Liu W J, Liu J, Hao C P, et al. Multichannel adaptive signal detection: basic theory and literature review. Sci China Inf Sci, 2022, 65(2): 121301, https://doi.org/10.1007/s11432-020-3211-8

1 Introduction

Signal detection in noise is a fundamental problem in various fields, e.g., radar, sonar, communications, optical image, hyperspectral imagery, remote sensing, medical imaging, and subsurface prospecting. Taking the radar system as an example, the received data in early radar systems are single channel data; thus, the data are scalar-valued. In contrast, in applications that employ pulsed Doppler techniques and/or multiple transmit/receive (T/R) modules, in addition to increased computational power and advances in hardware design, the received data for modern radar systems are typically multichannel, i.e., vector-valued or matrix-valued data. In addition, frequency diversity, polarization diversity, and waveform diversity can also lead to multichannel data. Multichannel data contain more information compared to single-channel data. On the one hand, using multichannel data, we have more degrees of freedom (DOFs) to design adaptive processors. On the other hand, with the multichannel data model, it is more convenient to characterize the correlated properties between data in different channels. Using these correlated properties, we can design a filter whose output signal-to-noise (SNR) is frequently greater than that of single-channel data. Similarly, utilizing data correlation, we can design a detector with superior detection performance compared to a detector for single-channel data.

Remarkably, noise is ubiquitous, which, in a general sense, usually includes thermal noise and clutter. For multichannel data in the cell under test (also referred to as primary data), the noise covariance matrix

* Corresponding author (email: ylwangkjld@163.com)

is unknown and must be estimated. Here, a common strategy is to use training data (referred to as secondary data) to form an appropriate estimator. A previous study [1] pointed out that a modern strategy for radar detection should (1) be adaptive to the noise spectral density or its probability density function (PDF), (2) maintain a constant false alarm rate (CFAR), and (3) have a relatively simple processing scheme. Multichannel adaptive signal detection is such a strategy that utilizes test data and training data jointly to design adaptive detectors, which typically possess the CFAR property. The resulting adaptive detector is then compared to a certain detection threshold set to ensure a fixed probability of false alarm (PFA). Finally, a target is declared to be present (absent) if this threshold is exceeded (not exceeded).

Here two points need to be emphasized. One is that the word "adaptive" in the above first feature indicates that the spectrum character of the noise is unknown in advance or changes in the operational environment; thus, adaptive techniques are needed. The other point is that the CFAR property or CFARness[1)], which, for a single-channel signal, means that the detection threshold of a detector is independent of the noise power. Equivalently, the statistical property of the detector is functionally independent of the noise power under the signal-absence hypothesis. In contrast, for multichannel signal detection, CFARness means that the statistical property of the detector is also functionally independent of the structure of the noise covariance matrix under the signal-absence hypothesis. This type of CFARness is referred to as matrix CFAR in [2] and covariance matrix-CFAR in [3].

Multichannel adaptive signal detection was first investigated by Kelly in 1986. In the seminal paper [4], Kelly proposed a famous detector, i.e., Kelly's generalized likelihood ratio test (KGLRT), to detect a rank-one signal in a homogeneous environment (HE). The rank-one signal has a known steering vector but an unknown amplitude. For the HE model, noise in the training and test data is both subject to mean-zero circularly complex Gaussian distribution with the same covariance matrix.

It has been approximately 35 years since Kelly proposed the KGLRT, and multichannel adaptive signal detection has been adopted in various fields. Based on different design criteria, numerous detectors have been proposed for different problems. Recently, an important book about multichannel adaptive signal detection is edited by de Maio and Greco [5]. However, to the best of our knowledge, only a few survey papers have reported on multichannel signal detection. In particular, Refs. [6] and [7] provided overviews of signal detection in compound-Gaussian clutter for subspace signals and rank-one signals, respectively. These papers focused primarily on known clutter or a known noise covariance matrix. In addition, the target was point-like and no signal mismatch was considered. Differing from the above papers, we present a review of multichannel adaptive signal detection in unknown noise with an emphasis on Gaussian background.

In this paper, we provide a tutorial on multichannel adaptive signal detection and present a brief survey of state-of-the-art techniques. For brevity, "adaptive detection" always means "multichannel adaptive signal detection" in the following. The remainder of this paper is organized as follows. In Section 2, we present the basic theory for adaptive detection, including the data model, the primary detector design criteria, the relationship between adaptive detection and filter-then-CFAR detection, and the relationship between adaptive detection and adaptive filtering. In Section 3, we present a comprehensive literature review. In Section 4, we analyze and compare the detection performance of typical adaptive detectors. Finally, Section 5 concludes the paper and presents potential future research tracks to advance adaptive detection techniques.

2 Basic theory

2.1 Main detector design criteria

The GLRT, Rao test, and Wald test are three main detector design criteria [8–25][2)]. These three criteria are referred to as "the Holy Trinity" in statistical inference [26]. Prior to discussing these criteria in detail, we must mathematically formulate a binary hypothesis. A binary hypothesis has two possible cases, i.e., the null (signal-absence) hypothesis and the alternative (signal-presence) hypothesis. Thus, a

1) CFARness is an important property required by an effective detector in practice because the PFA may increase dramatically to an unaffordable value if the detector does not maintain CFARness and noise changes severely.

2) Note that other criteria are often used, e.g., the gradient test [8], Durbin test [9], test based on maximal invariant statistic [10], multifamily likelihood ratio test [11], and other modifications of the likelihood ratio test [11], which are utilized for adaptive detector design [12–25].

binary hypothesis test can be expressed as follows:

$$\begin{cases} \mathrm{H}_0 : \boldsymbol{x} = \boldsymbol{n},\ \boldsymbol{x}_{\mathrm{e},l} = \boldsymbol{n}_{\mathrm{e},l},\ l = 1, 2, \ldots, L, \\ \mathrm{H}_1 : \boldsymbol{x} = \boldsymbol{s} + \boldsymbol{n},\ \boldsymbol{x}_{\mathrm{e},l} = \boldsymbol{n}_{\mathrm{e},l},\ l = 1, 2, \ldots, L, \end{cases} \tag{1}$$

where H_0 denotes the null hypothesis, H_1 denotes the alternative hypothesis, $\boldsymbol{x}$ represents the test data, $\boldsymbol{s}$ is the signal to be detected, $\boldsymbol{n}$ is the noise in the test data, whose covariance matrix $\boldsymbol{R}$, is generally unknown, and $\{\boldsymbol{x}_{\mathrm{e},l}\}_{l=1}^{L}$ are L training data, used to estimate the unknown $\boldsymbol{R}$.

For the detection problem in (1), the GLRT is given as follows [27]:

$$t_{\mathrm{GLRT}} = \frac{\max_{\boldsymbol{\Theta}_1} f_1(\boldsymbol{x}, \boldsymbol{X}_L)}{\max_{\boldsymbol{\Theta}_0} f_0(\boldsymbol{x}, \boldsymbol{X}_L)}, \tag{2}$$

where $\boldsymbol{\Theta}_1$ and $\boldsymbol{\Theta}_0$ denote the unknown parameters under hypotheses H_1 and H_0, respectively, and $f_1(\boldsymbol{x}, \boldsymbol{X}_L)$ and $f_0(\boldsymbol{x}, \boldsymbol{X}_L)$ are the joint PDFs of the test data $\boldsymbol{x}$ and training data $\boldsymbol{X}_L = [\boldsymbol{x}_{\mathrm{e},1}, \boldsymbol{x}_{\mathrm{e},2}, \ldots, \boldsymbol{x}_{\mathrm{e},L}]$ under hypotheses H_1 and H_0, respectively.

To derive the Rao and Wald tests, we require the Fisher information matrix (FIM), which, for circularly symmetric random parameters, is defined as [28]

$$\boldsymbol{I}(\boldsymbol{\Theta}) = \mathrm{E}\left[\frac{\partial \ln f(\boldsymbol{x}, \boldsymbol{X}_L)}{\partial \boldsymbol{\Theta}^*} \frac{\partial \ln f(\boldsymbol{x}, \boldsymbol{X}_L)}{\partial \boldsymbol{\Theta}^{\mathrm{T}}}\right]. \tag{3}$$

For convenience, the FIM is usually partitioned as

$$\boldsymbol{I}(\boldsymbol{\Theta}) = \begin{bmatrix} \boldsymbol{I}_{\boldsymbol{\Theta}_{\mathrm{r}},\boldsymbol{\Theta}_{\mathrm{r}}}(\boldsymbol{\Theta}) & \boldsymbol{I}_{\boldsymbol{\Theta}_{\mathrm{r}},\boldsymbol{\Theta}_{\mathrm{s}}}(\boldsymbol{\Theta}) \\ \boldsymbol{I}_{\boldsymbol{\Theta}_{\mathrm{s}},\boldsymbol{\Theta}_{\mathrm{r}}}(\boldsymbol{\Theta}) & \boldsymbol{I}_{\boldsymbol{\Theta}_{\mathrm{s}},\boldsymbol{\Theta}_{\mathrm{s}}}(\boldsymbol{\Theta}) \end{bmatrix}, \tag{4}$$

where

$$\boldsymbol{\Theta} = [\boldsymbol{\Theta}_{\mathrm{r}}^{\mathrm{T}}, \boldsymbol{\Theta}_{\mathrm{s}}^{\mathrm{T}}]^{\mathrm{T}}, \tag{5}$$

$$\boldsymbol{I}_{\boldsymbol{\Theta}_{\mathrm{r}},\boldsymbol{\Theta}_{\mathrm{r}}}(\boldsymbol{\Theta}) = \mathrm{E}\left[\frac{\partial \ln f(\boldsymbol{x}, \boldsymbol{X}_L)}{\partial \boldsymbol{\Theta}_{\mathrm{r}}^*} \frac{\partial \ln f(\boldsymbol{x}, \boldsymbol{X}_L)}{\partial \boldsymbol{\Theta}_{\mathrm{r}}^{\mathrm{T}}}\right], \tag{6a}$$

$$\boldsymbol{I}_{\boldsymbol{\Theta}_{\mathrm{r}},\boldsymbol{\Theta}_{\mathrm{s}}}(\boldsymbol{\Theta}) = \mathrm{E}\left[\frac{\partial \ln f(\boldsymbol{x}, \boldsymbol{X}_L)}{\partial \boldsymbol{\Theta}_{\mathrm{r}}^*} \frac{\partial \ln f(\boldsymbol{x}, \boldsymbol{X}_L)}{\partial \boldsymbol{\Theta}_{\mathrm{s}}^{\mathrm{T}}}\right], \tag{6b}$$

$$\boldsymbol{I}_{\boldsymbol{\Theta}_{\mathrm{s}},\boldsymbol{\Theta}_{\mathrm{r}}}(\boldsymbol{\Theta}) = \mathrm{E}\left[\frac{\partial \ln f(\boldsymbol{x}, \boldsymbol{X}_L)}{\partial \boldsymbol{\Theta}_{\mathrm{s}}^*} \frac{\partial \ln f(\boldsymbol{x}, \boldsymbol{X}_L)}{\partial \boldsymbol{\Theta}_{\mathrm{r}}^{\mathrm{T}}}\right], \tag{6c}$$

$$\boldsymbol{I}_{\boldsymbol{\Theta}_{\mathrm{s}},\boldsymbol{\Theta}_{\mathrm{s}}}(\boldsymbol{\Theta}) = \mathrm{E}\left[\frac{\partial \ln f(\boldsymbol{x}, \boldsymbol{X}_L)}{\partial \boldsymbol{\Theta}_{\mathrm{s}}^*} \frac{\partial \ln f(\boldsymbol{x}, \boldsymbol{X}_L)}{\partial \boldsymbol{\Theta}_{\mathrm{s}}^{\mathrm{T}}}\right]. \tag{6d}$$

In (5), $\boldsymbol{\Theta}_{\mathrm{r}}$ is the relevant parameter, e.g., the signal amplitude, and $\boldsymbol{\Theta}_{\mathrm{s}}$ is the nuisance parameter, e.g., the noise covariance matrix. Note that if $\ln f(\boldsymbol{x}, \boldsymbol{X}_L)$ is twice differential with respect to $\boldsymbol{\Theta}$, and then the FIM in (3) under the regularity condition can be calculated as follows [29]:

$$\boldsymbol{I}(\boldsymbol{\Theta}) = -\mathrm{E}\left[\frac{\partial^2 \ln f(\boldsymbol{x}, \boldsymbol{X}_L)}{\partial \boldsymbol{\Theta}^* \partial \boldsymbol{\Theta}^{\mathrm{T}}}\right], \tag{7}$$

which is often easier to derive.

Then, the Rao and Wald tests for complex-valued signals are given as follows [29,30][3)]:

$$t_{\mathrm{Rao}} = \left.\frac{\partial \ln f_1(\boldsymbol{x}, \boldsymbol{X}_L)}{\partial \boldsymbol{\Theta}_{\mathrm{r}}}\right|_{\boldsymbol{\Theta}=\hat{\boldsymbol{\Theta}}_0}^{\mathrm{T}} [\boldsymbol{I}^{-1}(\hat{\boldsymbol{\Theta}}_0)]_{\boldsymbol{\Theta}_{\mathrm{r}},\boldsymbol{\Theta}_{\mathrm{r}}} \left.\frac{\partial \ln f_1(\boldsymbol{x}, \boldsymbol{X}_L)}{\partial \boldsymbol{\Theta}_{\mathrm{r}}^*}\right|_{\boldsymbol{\Theta}=\hat{\boldsymbol{\Theta}}_0}, \tag{8}$$

and

$$t_{\mathrm{Wald}} = (\hat{\boldsymbol{\Theta}}_{\mathrm{r}_1} - \boldsymbol{\Theta}_{\mathrm{r}_0})^{\mathrm{H}} \{[\boldsymbol{I}^{-1}(\hat{\boldsymbol{\Theta}}_1)]_{\boldsymbol{\Theta}_{\mathrm{r}},\boldsymbol{\Theta}_{\mathrm{r}}}\}^{-1} (\hat{\boldsymbol{\Theta}}_{\mathrm{r}_1} - \boldsymbol{\Theta}_{\mathrm{r}_0}), \tag{9}$$

3) The complex-valued Rao test is given in [30] for the case of no nuisance parameter, which is suitable for non-circularly symmetric random parameters.

respectively, where $\hat{\boldsymbol{\Theta}}_0$ and $\hat{\boldsymbol{\Theta}}_1$ are the maximum likelihood estimates (MLEs) of $\boldsymbol{\Theta}$ under hypotheses H_0 and H_1, respectively, $\hat{\boldsymbol{\Theta}}_{\mathrm{r}_1}$ is the MLE of $\boldsymbol{\Theta}_{\mathrm{r}}$ under hypothesis H_1, $\boldsymbol{\Theta}_{\mathrm{r}_0}$ is the value of $\boldsymbol{\Theta}_{\mathrm{r}}$ under hypothesis H_0, and $\{[\boldsymbol{I}^{-1}(\boldsymbol{\Theta})]_{\boldsymbol{\Theta}_{\mathrm{r}},\boldsymbol{\Theta}_{\mathrm{r}}}\}^{-1}$ is the Schur complement of $\boldsymbol{I}_{\boldsymbol{\Theta}_{\mathrm{s}},\boldsymbol{\Theta}_{\mathrm{s}}}(\boldsymbol{\Theta})$, namely,

$$\left\{[\boldsymbol{I}^{-1}(\boldsymbol{\Theta})]_{\boldsymbol{\Theta}_{\mathrm{r}},\boldsymbol{\Theta}_{\mathrm{r}}}\right\}^{-1} = \boldsymbol{I}_{\boldsymbol{\Theta}_{\mathrm{r}},\boldsymbol{\Theta}_{\mathrm{r}}}(\boldsymbol{\Theta}) - \boldsymbol{I}_{\boldsymbol{\Theta}_{\mathrm{r}},\boldsymbol{\Theta}_{\mathrm{s}}}(\boldsymbol{\Theta})\ \boldsymbol{I}^{-1}_{\boldsymbol{\Theta}_{\mathrm{s}},\boldsymbol{\Theta}_{\mathrm{s}}}(\boldsymbol{\Theta})\ \boldsymbol{I}_{\boldsymbol{\Theta}_{\mathrm{s}},\boldsymbol{\Theta}_{\mathrm{r}}}(\boldsymbol{\Theta}). \tag{10}$$

In some cases, relevant parameter $\boldsymbol{\Theta}_{\mathrm{r}}$ and/or the nuisance parameter $\boldsymbol{\Theta}_{\mathrm{s}}$ may be known. Obviously, in such cases, we use these true values and do not need to derive their MLEs.

Note that the two-step variations of the three design criteria are also adopted. Specifically, the GLRT, Rao test, or Wald test is first derived under the assumption that the noise covariance matrix is known (or its structure is known). Then, the noise covariance matrix in the corresponding detector is replaced by a proper estimate using the training data. For example, the two-step GLRT (2S-GLRT) can be expressed mathematically as follows:

$$t_{\text{2S-GLRT}} = \left[\frac{\max_{\boldsymbol{\Theta}_1'} f_1(\boldsymbol{x}, \boldsymbol{X}_L)}{\max_{\boldsymbol{\Theta}_0'} f_0(\boldsymbol{x}, \boldsymbol{X}_L)}\right]\Bigg|_{\boldsymbol{R}=\hat{\boldsymbol{R}}}, \tag{11}$$

where $\boldsymbol{\Theta}_1'$ and $\boldsymbol{\Theta}_0'$ denote the unknown parameters except for $\boldsymbol{R}$ under hypotheses H_1 and H_0, respectively, and $\hat{\boldsymbol{R}}$ is an appropriate estimation of $\boldsymbol{R}$.

From the three detector design criteria in (2), (8), and (9), we know that one of the key points is finding the derivatives of scalar real-valued functions, e.g., PDFs, with respect to a complex-valued scalar, vector, or matrix. One of the most useful books on this topic is written by Hjørungnes [31], which was written in an engineering-oriented manner. The theory of finding complex-valued derivatives in [31] is based on the complex differential of the objective function. Using the complex differential, it is much easier to find a derivative than using the component-wise approach, e.g., the book by Magnus and Neudecker [32], which primarily focuses on real-valued derivatives.

The following fact is often used when deriving a detector with a simplified detection statistic or in a form whose statistical distribution can be derived easily. More precisely, if a detector can be expressed as a monotonically increasing function of another detector, then these two detectors are equivalent. We attempted to find a related reference; however, none was found. Therefore, we summarize the above fact in the following theorem.

Theorem 1. Let t_1 and t_2 be two detectors, and

$$t_2 = g(t_1) \tag{12}$$

increases monotonically with t_1. Then, t_1 and t_2 have the same detection performance such that they have identical probability of detection (PD) under the same PFA.

Proof. Let the PFAs of t_1 and t_2 be PFA_1 and PFA_2, respectively. Then,

$$\mathrm{PFA}_1 = \Pr[t_1 > \eta_1; \mathrm{H}_0], \tag{13}$$

$$\mathrm{PFA}_2 = \Pr[t_2 > \eta_2; \mathrm{H}_0], \tag{14}$$

where η_1 and η_2 are the detection thresholds of t_1 and t_2, respectively. According to (12), Eq. (14) can be rewritten as follows:

$$\mathrm{PFA}_2 = \Pr[g(t_1) > \eta_2; \mathrm{H}_0] = \Pr[t_1 > g^{-1}(\eta_2); \mathrm{H}_0], \tag{15}$$

where the second equality is due to the fact that $g(t_1)$ is a monotonically increasing function of t_1, and $g^{-1}(\cdot)$ denotes the inverse function of $g(\cdot)$. By comparing (13) and (15), and using $\mathrm{PFA}_1 = \mathrm{PFA}_2$, we obtain the following:

$$\eta_1 = g^{-1}(\eta_2). \tag{16}$$

The PDs of t_1 and t_2 can be expressed as follows:

$$\mathrm{PD}_1 = \Pr[t_1 > \eta_1; \mathrm{H}_1] \tag{17}$$

and

$$\mathrm{PD}_2 = \Pr[t_2 > \eta_2; \mathrm{H}_1], \tag{18}$$

respectively. Here, $t_2 = g(t_1)$ is a monotonically increasing function of t_1; thus, Eq. (18) can be recast as follows:

$$\mathrm{PD}_2 = \Pr[t_1 > g^{-1}(\eta_2); \mathrm{H}_1] = \Pr[t_1 > \eta_1; \mathrm{H}_1] = \mathrm{PD}_1, \tag{19}$$

where the second equality is obtained according to (16).

Adaptive detection differs from filtering-then-CFAR detection, which is widely adopted in most radar systems. In addition, adaptive detection is highly related to adaptive filtering, although their purposes differ. In Subsection 2.2, we investigate the relationship between adaptive detection and filtering-then-CFAR detection.

2.2 Relationship between adaptive detection and filtering-then-CFAR detection

Currently, the most common detection scheme in most radar systems is the filtering-then-CFAR approach. Here, the test data are first filtered and then processed using CFAR techniques. CFAR processing is a technique that makes the detection threshold of a detector independent of the noise covariance matrix. Equivalently, via CFAR processing, the statistical characteristics of the detector do not depend on the noise covariance matrix under the signal-absence hypothesis. Note that there are many CFAR technologies, e.g., cell-averaging CFAR (CA-CFAR), greatest-of-selection CFAR (GO-CFAR), and ordered statistic CFAR (OS-CFAR) [33,34]. It appears that the filtering-then-CFAR detection scheme is a natural approach to detecting a target in noise because adaptive filtering can obtain high output SNR, which is beneficial to the detection process.

The theoretical basis behind the filtering-then-CFAR detection scheme for multichannel data can be traced back to the classic paper [35]. Precisely, for airborne radar space-time two-dimensional signal processing, the test data, if containing the target signal, can be written as follows:

$$\boldsymbol{x} = a\boldsymbol{s} + \boldsymbol{n}, \tag{20}$$

where $\boldsymbol{x}$ is an $N_\mathrm{a}N_\mathrm{p} \times 1$ test data vector, N_a is the number of antennas, N_p is the number of pulses received by each antenna, $\boldsymbol{s} = \boldsymbol{s}_\mathrm{p} \otimes \boldsymbol{s}_\mathrm{a}$ is an $N_\mathrm{a}N_\mathrm{p} \times 1$ signal space-time steering vector, with $\boldsymbol{s}_\mathrm{p}$ and $\boldsymbol{s}_\mathrm{a}$ being an $N_\mathrm{p} \times 1$ time steering vector and an $N_\mathrm{a} \times 1$ space steering vector, respectively, $\otimes$ denotes the Kronecker product, and $\boldsymbol{n}$ is noise, including clutter and thermal noise, distributed as circularly complex Gaussian distribution with covariance matrix $\boldsymbol{R}$.

In [35], to detect the target in (20), the test data vector $\boldsymbol{x}$ is first filtered by an $N_\mathrm{a}N_\mathrm{p} \times 1$ weight vector $\boldsymbol{w}$. Thus, the output of the filter can be expressed as follows:

$$y = \boldsymbol{w}^\mathrm{H}\boldsymbol{x}. \tag{21}$$

For filtered data y, the optimum detector (in the Neyman-Pearson sense) is the likelihood ratio test, which is given as follows:

$$t_\mathrm{LRT} = \frac{f_1(y|\boldsymbol{x} = a\boldsymbol{s} + \boldsymbol{n})}{f_0(y|\boldsymbol{x} = \boldsymbol{n})}, \tag{22}$$

where $f_1(\cdot)$ and $f_0(\cdot)$ are the PDFs under the signal-presence and signal-absence hypotheses, respectively. Here, the optimum filter weight $\boldsymbol{w}$ can be obtained by maximizing (22), written symbolically as

$$\boldsymbol{w}_\mathrm{opt} = \max_{\boldsymbol{w}} \frac{f_1(y|\boldsymbol{x} = a\boldsymbol{s} + \boldsymbol{n})}{f_0(y|\boldsymbol{x} = \boldsymbol{n})}, \tag{23}$$

which is shown to be equivalent to [35]

$$\boldsymbol{w}_\mathrm{opt} = \max_{\boldsymbol{w}} \frac{|\boldsymbol{w}^\mathrm{H}\boldsymbol{s}|^2}{\boldsymbol{w}^\mathrm{H}\boldsymbol{R}\boldsymbol{w}}, \tag{24}$$

and the solution to (24) is

$$\boldsymbol{w}_\mathrm{opt} = \mu\boldsymbol{R}^{-1}\boldsymbol{s}, \tag{25}$$

where μ is an arbitrary non-zero constant.

A well-known equivalent solution to (24) is the minimum variance distortionless response (MVDR), which is mathematically formed as follows [36]:

$$\begin{cases} \min\limits_{\boldsymbol{w}} \boldsymbol{w}^\mathrm{H}\boldsymbol{R}\boldsymbol{w}, \\ \text{s.t. } \boldsymbol{w}^\mathrm{H}\boldsymbol{s} = 1, \end{cases} \tag{26}$$

and the corresponding solution is given as

$$\boldsymbol{w}_{\mathrm{MVDR}} = \frac{\boldsymbol{R}^{-1}\boldsymbol{s}}{\boldsymbol{s}^{\mathrm{H}}\boldsymbol{R}^{-1}\boldsymbol{s}}. \tag{27}$$

By taking (27) into (21) and performing the norm-squared operation, we obtain the following:

$$t_{\mathrm{MF}} = \frac{|\boldsymbol{s}^{\mathrm{H}}\boldsymbol{R}^{-1}\boldsymbol{x}|^2}{(\boldsymbol{s}^{\mathrm{H}}\boldsymbol{R}^{-1}\boldsymbol{s})^2}. \tag{28}$$

Gathering the above results indicates that the optimum detection in (22) is equivalent to the optimum filtering in (24), and the optimum filter weight is given in (25). Based on the above results, the space-time adaptive processing (STAP) technique came into being, which is considered to be one of the most effective technologies for airborne radar clutter cancellation, and numerous achievements have been obtained using this technique [37–39]. Note that STAP is a filtering technique [40, 41][4)] that attempts to maximize the output SNR. To realize the final target detection, CFAR processing is required.

Note that the above equivalence between optimum detection and optimum filtering holds under certain processing flow and certain assumptions. The specific processing flow is filtering-then-detection. Precisely, the multichannel test data vector $\boldsymbol{x}$ is first filtered by the weight vector $\boldsymbol{w}$, resulting in the scalar-valued data y. Then, a detector is devised based on the filtered data y. Here, the assumption is that the noise $\boldsymbol{n}$ in the test data is Gaussian distributed, and its covariance matrix $\boldsymbol{R}$ is known in advance. Unfortunately, the above assumption is generally not satisfied in practice because radar systems work in varying environments. Typically, when the noise covariance matrix $\boldsymbol{R}$ is unknown, it is replaced by the sample covariance matrix (SCM) formed using the training data received in the vicinity of the test data. Then, the optimum filter in (25) becomes the suboptimum filter of the sample covariance inversion (SMI) [42]. Note that appropriate CFAR processing is required to complete target detection.

In addition, the above filtering-then-CFAR detection scheme adopts adaptive filtering. However, there is another filtering-then-CFAR detection scheme that performs non-adaptive filtering, e.g., moving target indication (MTI), moving target detection (MTD), and pulse Doppler processing. The key point in MTD and pulse Doppler processing is Doppler filtering using multiple pulses. However, the number of pulses used in MTD is much smaller than that used in pulse Doppler processing, and MTD is frequently used by ground-based radar, while pulse Doppler processing is primarily used by airborne radar. This non-adaptive filtering-then-CFAR detection scheme typically has lower complexity than the adaptive filtering-then-CFAR detection scheme; however, it suffers from certain performance loss because its filtering performance is limited.

For unknown noise, if the test and training data are utilized directly to devise multichannel adaptive detectors, then better detection performance can be obtained compared to the above filtering-then-CFAR detection scheme. Adaptive detection is simply a type of this detection scheme. Specifically, for adaptive detection, the test and training data are utilized jointly to design an adaptive detector, which is compared to a detection threshold set according to a pre-assigned PFA. Here, if the value of a detector is greater than the threshold, a target is claimed; otherwise, no target is claimed.

Block diagrams of filtering-then-CFAR detection and adaptive detection schemes are shown in Figure 1. It can be concluded that the filtering-then-CFAR detection approach (adaptive or non-adaptive) requires two independent processing procedures, as its name indicates, i.e., filtering and CFAR processing. In contrast, independent filtering processing is not required for adaptive detection, which achieves the filtering function and CFAR processing simultaneously, both of which are embedded in the detection statistic of the adaptive detection.

2.3 Relationship between adaptive detectors and adaptive filters

As explained previously, adaptive filters and adaptive detectors have different purposes, since the former attempts to maximize the output SNR, and the latter attempts to maximize the PD with a fixed PFA. However, adaptive filters and adaptive detectors have some common features. For example, they both adopt adaptivity. Specifically, they use training data to adaptively estimate the unknown noise covariance matrix, which is the essential point in adaptive processors. In addition, adaptive detectors have the function of adaptive filtering, which is not achieved in an independent procedure, as noted previously.

4) Strictly speaking, the STAP technique is much less than its literal meaning. Precisely, STAP is a filtering technique to reject the clutter and jammer (if present) for airborne radar [40, 41].

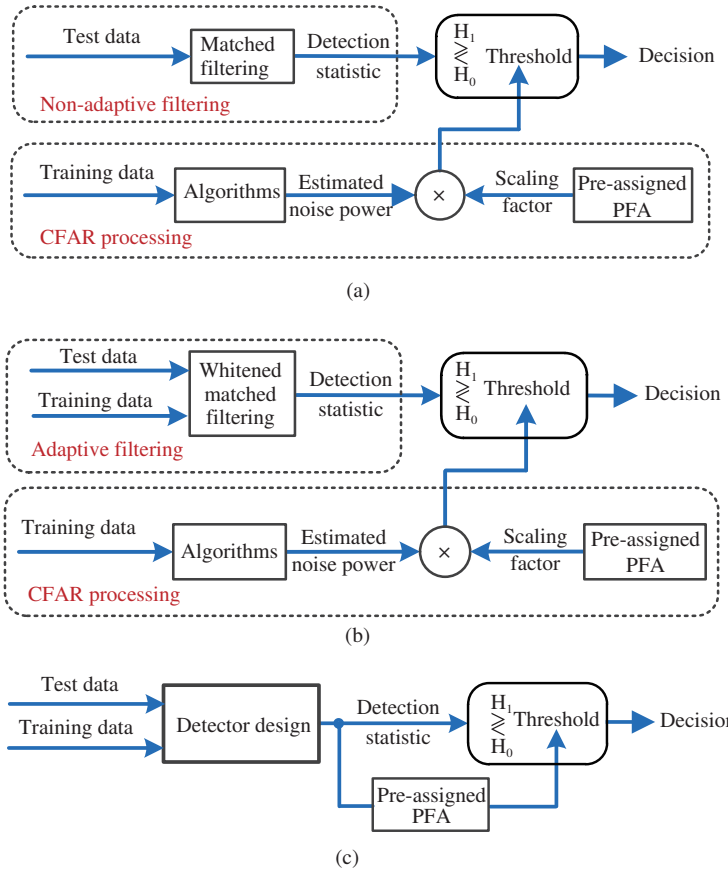

Figure 1 (Color online) Block diagrams of (a) non-adaptive filtering-then-CFAR detection, (b) adaptive filtering-then-CFAR detection, and (c) adaptive detection.

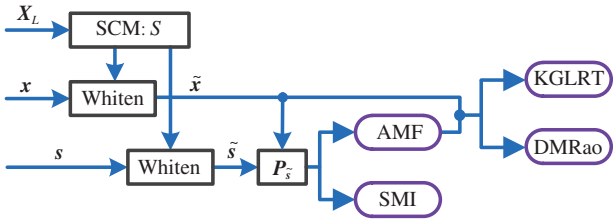

Figure 2 (Color online) Block diagrams for one adaptive filter and three adaptive detectors.

For example, Figure 2 shows block diagrams of one adaptive filter, i.e., the SMI [42], and three adaptive detectors, i.e., the KGLRT [4], adaptive matched filter (AMF) [43,44], and de Maio's Rao (DMRao) [45][5]. The SMI can be obtained by replacing $\boldsymbol{R}$ with the SCM $\boldsymbol{S}$ in (28), which results in the following:

$$t_{\mathrm{SMI}} = \frac{\tilde{\boldsymbol{x}}^{\mathrm{H}} \boldsymbol{P}_{\tilde{\boldsymbol{s}}} \tilde{\boldsymbol{x}}}{\tilde{\boldsymbol{s}}^{\mathrm{H}} \tilde{\boldsymbol{s}}}. \tag{29}$$

In addition, the detection statistics of the KGLRT, AMF, and DMRao are given as follows:

$$t_{\mathrm{KGLRT}} = \frac{\tilde{\boldsymbol{x}}^{\mathrm{H}} \boldsymbol{P}_{\tilde{\boldsymbol{s}}} \tilde{\boldsymbol{x}}}{1 + \tilde{\boldsymbol{x}}^{\mathrm{H}} \tilde{\boldsymbol{x}} - \tilde{\boldsymbol{x}}^{\mathrm{H}} \boldsymbol{P}_{\tilde{\boldsymbol{s}}} \tilde{\boldsymbol{x}}}, \tag{30}$$

$$t_{\mathrm{AMF}} = \tilde{\boldsymbol{x}}^{\mathrm{H}} \boldsymbol{P}_{\tilde{\boldsymbol{s}}} \tilde{\boldsymbol{x}}, \tag{31}$$

and

$$t_{\mathrm{DMRao}} = \frac{\tilde{\boldsymbol{x}}^{\mathrm{H}} \boldsymbol{P}_{\tilde{\boldsymbol{s}}} \tilde{\boldsymbol{x}}}{(1 + \tilde{\boldsymbol{x}}^{\mathrm{H}} \tilde{\boldsymbol{x}})(1 + \tilde{\boldsymbol{x}}^{\mathrm{H}} \tilde{\boldsymbol{x}} - \tilde{\boldsymbol{x}}^{\mathrm{H}} \boldsymbol{P}_{\tilde{\boldsymbol{s}}} \tilde{\boldsymbol{x}})}, \tag{32}$$

5) The KGLRT, AMF and DMRao are proposed for the detection problem given in (1) according to the GLRT, 2S-GLRT, and Rao test criteria, respectively. The AMF can also be obtained according to the Wald test.

Table 1 Related taxonomy in Subsection 3.1

Taxonomy	Meaning
HE	A scenario that test and training data have the same noise covariance matrix.
PHE	A scenario that test and training data have the same noise covariance matrix upon to unknown scaling factor.
Non-homogeneity	A scenario that the data in the collection of test and training data do not have the same noise covariance matrix.
Compound-Gaussian process	A random process which is in the form of a product of two components. One is the square root of a positive scalar random process (called texture, accounting for local power change), while the other is a complex Gaussian process (called speckle, accounting for local scattering).
Rank-one signal	A kind of signal, modeled by the product of a known vector and an unknown scaling factor.
Subspace signal	A kind of signal, modeled by the product of a known matrix and an unknown vector. That is to say, a subspace signal lies in a known subspace but with unknown coordinates.

respectively, where $\tilde{\boldsymbol{x}} = \boldsymbol{S}^{-\frac{1}{2}}\boldsymbol{x}$, $\tilde{\boldsymbol{s}} = \boldsymbol{S}^{-\frac{1}{2}}\boldsymbol{s}$, $\boldsymbol{x}$ is the test data vector, $\boldsymbol{s}$ is the signal steering vector, and $\boldsymbol{S} = \boldsymbol{X}_L\boldsymbol{X}_L^{\mathrm{H}}$ is the SCM[6)], and $\boldsymbol{P}_{\tilde{\boldsymbol{s}}} = \frac{\tilde{\boldsymbol{s}}\tilde{\boldsymbol{s}}^{\mathrm{H}}}{\tilde{\boldsymbol{s}}^{\mathrm{H}}\tilde{\boldsymbol{s}}}$ is the orthogonal projection matrix of $\tilde{\boldsymbol{s}}$.

The SMI and AMF can be taken as the outputs of certain adaptive filters. Then, their corresponding weight vectors[7)] are given as follows:

$$\boldsymbol{w}_{\mathrm{SMI}} = \frac{\boldsymbol{S}^{-1}\boldsymbol{s}}{\boldsymbol{s}^{\mathrm{H}}\boldsymbol{S}^{-1}\boldsymbol{s}} \tag{33}$$

and

$$\boldsymbol{w}_{\mathrm{AMF}} = \frac{\boldsymbol{S}^{-1}\boldsymbol{s}}{\sqrt{\boldsymbol{s}^{\mathrm{H}}\boldsymbol{S}^{-1}\boldsymbol{s}}}, \tag{34}$$

respectively. However, the KGLRT and DMRao cannot be expressed as the output of a filter.

Two key functions of adaptive filtering are clutter rejection and signal integration. The former is achieved using the "whiten" model, which is accomplished by the matrix $\boldsymbol{S}^{-\frac{1}{2}}$, and the latter is achieved using the orthogonal projection matrix $\boldsymbol{P}_{\tilde{\boldsymbol{s}}}$. Figure 2 shows that, along with (29)–(32), the SMI, KGLRT, AMF, and DMRao all have the function of adaptive filtering. In addition, the AMF and SMI demonstrate the same filtering performance because they have the same output SNR, which can be verified by substituting (33) and (34) into the quantity to be maximized in the right-hand side of (24). However, their detection performance differs because the AMF has the CFAR property, whereas the SMI does not [46][8)].

In summary, adaptive detectors use the test and training data to form specific structures, and they have CFAR properties and have the function of filtering, embedded in the detection statistics.

3 Literature review

According to different criteria, the adaptive detection problem can be categorized into different types. For example, according to the extension of a target, adaptive detection can be sorted into point target detection and distributed (spread) target detection. Here, depending on whether the signal is mismatched or not, adaptive detection can be sorted as detection in the absence or presence of signal mismatch. According to the statistical property of the noise, adaptive detection can be sorted into detection in Gaussian noise and detection in non-Gaussian noise, and according to the characters of the test and training data, adaptive detection can be sorted into detection in HE and detection in non-homogeneous (i.e., heterogeneous) environment. However, these classifications are too broad. Thus, we present a literature review in the following six categories[9)]. For convenience, we summarize the corresponding taxonomies in a table in each subsection, namely, Tables 1–6.

3.1 Adaptive detection for point targets in the absence of signal mismatch

In the seminal paper [4], Kelly considered the detection problem for a point target in HE. Here, the point target has a known signal steering vector embedded in Gaussian noise with an unknown covariance matrix.

6) A more common SCM in adaptive filtering is defined as $\boldsymbol{S}' = \frac{1}{L}\boldsymbol{X}_L\boldsymbol{X}_L^{\mathrm{H}}$. However, for adaptive detection, it is generally more convenient to use the SCM defined as $\boldsymbol{S} = \boldsymbol{X}_L\boldsymbol{X}_L^{\mathrm{H}}$.

7) Note that the SMI weight in (33) satisfies the constraint $\boldsymbol{w}_{\mathrm{SMI}}^{\mathrm{H}}\boldsymbol{s} = 1$.

8) The statistical performance analysis of the multi-band generalization of the SMI, referred to as the modified SMI (MSMI), in [46] demonstrates that the detection threshold of the SMI depends on the noise covariance matrix $\boldsymbol{R}$.

9) We apologize to any researcher whose work is overlooked or otherwise not discussed.

To estimate the unknown noise covariance matrix, a set of IID training data was used, which is signal-free and shares the same noise covariance matrix with the test data. Then, Kelly proposed the KGLRT. According to 2S-GLRT, Chen et al. [43] and Robey et al. [44] independently derived the well-known AMF, which has small complexity compared to the KGLRT. The corresponding Rao test was obtained by de Maio [45], i.e., the DMRao, which has lower PD than the KGLRT and AMF. However, the DMRao demonstrates better performance in terms of rejecting mismatched signals. The corresponding Wald test was also derived by de Maio [47], which coincides with the AMF. Notably, in 1994, Gerlach proposed the nonconcurrent mean level adaptive detector (N-MLAD) [48] and concurrent mean level adaptive detector (C-MLAD) [49], which are essentially the AMF and DMRao, respectively (see also [50, 51]). In addition, the AMF was utilized in [52] for simultaneous detection and parameter estimation (i.e., a target's Doppler and bearing).

The KGLRT, DMRao, and AMF detectors were all devised under the HE assumption. However, the data may have different statistical properties due to rapidly changing environmental factors or instrumental factors, e.g., adaptation of conformal array, bistatic radar, or multisite radar [53]. The partially HE (PHE) is a widely used non-homogeneity model that well characterizes the environment for airborne radars with a small amount of training data [54] and is suitable for wireless communications with fades over multiple interference sources [55]. The GLRT for point target detection in PHE was derived by Kraut et al. [56] and is referred to as the adaptive coherent estimator (ACE). It was found in [57] that the Rao and Wald tests in PHE coincide with the ACE. A simple approach was provided in [58] to set the threshold of the ACE and AMF. An invariance property of the ACE was given in [59], and the ACE was shown to be uniformly most powerful invariant (UMPI) in [55]. More recently, it was demonstrated in [60] that the ACE using the fixed-point covariance estimate [61] coincides with a maximal invariant component [62–64][10)]. Note that the ACE is effective in two kinds of non-homogeneous environments, i.e., spherically invariant noise [65] or compound-Gaussian noise [62], and Bayesian heterogeneity, for which the covariance matrix of the training data is subject to inverse complex Wishart distribution proportional to the covariance matrix in the test data [66]. In addition, the ACE is also referred to as the adaptive normalized matched filter (ANMF) [65,67] or normalized AMF (NAMF) [68]. In [69], the CFAR behavior using experimentally measured data was investigated for the KGLRT, AMF, and two variations of the ACE, i.e., recursive ANMF (R-ANMF) [70] and recursive persymmetric ANMF (RP-ANMF) [71]. It was shown in [69] that all of these detectors exhibit a false alarm rate that is greater than the preassigned value, and the RP-ANMF is the most robust among these detectors. More recently, the target separation detection (TSD) problem was considered in [72], where TSD tests were designed according to the GLRT. It was demonstrated that the TSD tests could effectively monitor target separation events.

The above detectors are for rank-one signals, which have a known steering vector. However, a signal may naturally lie in a subspace but with unknown coordinates, e.g., polarimetric target detection [73–77]. This type of signal is referred to as a subspace signal, which can be expressed mathematically as the product of a full-column-rank matrix and a vector. Under the background of polarimetric target detection, Refs. [78,79] generalized the KGLRT and AMF to the case of two-dimensional subspace. Then, Refs. [80, 81] generalized the KGLRT to the case of subspace with dimension greater than two, which is referred to as the subspace-based GLRT (SGLRT). Similarly, the AMF has been generalized to the case of subspace with dimension greater than two in [82], and this detector is referred to as the subspace-based AMF (SAMF). The subspace versions of the DMRao and ACE were given in [83, 84], and the resulting detectors are called the subspace-based Rao (SRao) test and adaptive subspace detector (ASD), respectively. The statistical properties of the SGLRT were given in [80, 85], the statistical properties of the SAMF were given in [82], the statistical properties of the ASD were given in [86, 87], and the statistical properties of the SRao were given in [88].

3.2 Adaptive detection for distributed targets in the absence of signal mismatch

For a high-resolution radar (HRR), a target may be spread in range, especially a large target, e.g., a large ship. It was demonstrated in [89] that a properly designed HRR could provide improved detection performance, which is primarily due to two factors. One is that increasing the capability of range

10) The upper-bound performance of the ACE is provided by the normalized matched filter (NMF), which was given in [62, 63]. In addition, the NMF was shown in [64] to be the UMPI detector in spherically invariant random vector (SIRV) disturbance with a specific texture.

Table 2 Related taxonomy in Subsection 3.2

Taxonomy	Meaning
Distributed target	A target which occupies more than one range bins for a radar system.
DD	A detection problem, for which the received echoes all come from the same direction. However, the corresponding signal steering vector is only known to lie in a given subspace.
GDD	A detection problem, for which both the column and row components of a rank-one matrix-valued signal are constrained to lie in known subspaces, but with unknown coordinates.
DOS signal	A kind of signal, which is matrix-valued and its row and column elements both lie in known subspaces but with unknown coordinates.

resolution of the radar can reduce the amount of energy per range bin backscattered by the clutter, and the other is that a distributed target is typically less fluctuated than an unresolved point target.

It was assumed in [54] that the echoes reflected by the distributed target all came from the same direction, and the GLRT and 2S-GLRT for distributed target detection in HE and PHE were derived. The corresponding Rao and Wald tests in HE were derived in [90], and the Rao and Wald test in PHE were given in [91]. Note that the 2S-GLRT in HE in [54] is referred to as the generalized AMF (GAMF). Similarly, we can refer to the GLRT in HE in [54] as generalized KGLRT (GKGLRT) because it is a generalization of the KGLRT. The GLRT in HE proposed in [54] shares the same form as the multiband GLR (MBGLR) in [92][11)].

Ref. [93] investigated the distributed target detection problem whose signal steering vector was unknown. The GLRT, 2S-GLRT, modified 2S-GLRT (M2S-GLRT), and spectral norm test (SNT) were proposed therein. It was demonstrated in [94] that the 2S-GLRT and M2S-GLRT can be obtained according to the Wald test and Rao test, respectively. Some intuitive interpretations about the detectors were also given in [94]. Recently, Ref. [95] considered the case where the test data matrix was of rank two. In addition, a generalization of ACE was proposed, and its analytical performance was demonstrated.

In [96], it was assumed that echoes backscattered by the distributed target all came from the same direction; however, the corresponding signal steering vector was only known to lie in a given subspace. This corresponding detection problem was referred to as the direction detection (DD), and the so-called generalized adaptive direction detector (GADD) was proposed according to the 2S-GLRT in PHE. From a mathematical perspective, the matrix-valued signal to be detected is of rank one for the DD problem, and its column components are constrained to a known subspace, while its row components are completely unknown. A more general signal model was adapted in [97], where both the column and row components of a rank-one matrix-valued signal are constrained to lie in known subspaces but with unknown coordinates. This kind of problem can be taken as generalized direction detection (GDD); however, it did not use the training data in [97]. Instead, it was assumed that the dimension of the test data satisfied a certain constraint. Then, a set of virtual training data can be obtained using a unitary matrix transformation on the test data. As a result, the row structure of the signal was lost. The corresponding GLRT and 2S-GLRT were then proposed. Essentially, the data model in [97] was equivalent to that in [96]; however, the environments were homogeneous. The Wald test for the DD in HE was proposed in [98], and it was demonstrated that there is no reasonable Rao test for the DD problem. The problem of GDD in HE was exploited in [99], where the corresponding GLRT and 2S-GLRT were proposed. In addition, the 2S-GLRT in PHE for GDD was given in [100].

For the problem of detecting a distributed target, a systematic and comprehensive investigation was reported by Kelly and Forsythe in 1989 [101], where the solid mathematical background for adaptive signal detection was given. In [101], the signal to be detected was matrix-valued, and its row and column elements both lay in known subspaces but with unknown coordinates. This type of signal model is referred to as the double subspace (DOS) signal in [83, 102]. The DOS signal model is very general and includes many types of point targets and distributed targets as special cases. In [101], no training data set was utilized. In contrast, a dimension constraint was posed on the test data. Then, after a unitary matrix transformation on the test data, a set of virtual training data was obtained; however, the row structure of the DOS signal was lost after the unitary matrix transformation. The problem of detecting a DOS signal was generalized in [83, 102], where true training data were assumed to be available, and many detectors were proposed and compared.

Compared to detectors for point targets, the statistical performance of detectors designed for distributed targets is difficult to derive. In particular, the statistical performance of the GLRT and 2S-GLRT

11) The MBGLR was proposed for point target detection when a radar system has multiple frequency bands.

Table 3 Related taxonomy in Subsection 3.3

Taxonomy	Meaning
Signal mismatch	The phenomenon that the actual signal steering vector is not aligned with the nominal one adopted by the radar system.
Robustness	A property that the detection performance of a detector does not decrease severely with the increase of signal mismatch.
Selectivity	A property that the detection performance of a detector decreases rapidly with the increase of signal mismatch.
Directivity	The property (including robustness and selectivity) of a detector when detecting a mismatch signal.
Tunable detector	A kind of detector, which is parameterized by one or more positive scaling factors, called the tunable parameters. By adjusting the tunable parameters, the directivity property of the detector can be changed.
Cascaded detector	A kind of detector, formed by cascading a robust detector and a selective detector.
Weighted detector	A kind of detector, formed by weighting a robust detector and a selective detector.

for distributed target in HE as proposed in [54] was given in [92,103], respectively. In addition, the result in [92] was generalized in [104] to the signal mismatch case. Signal mismatch is explained in detail in Subsection 3.3.

3.3 Adaptive detection in the presence of signal mismatch

In practice, signal mismatch occurs frequently [105]. Specifically, the actual signal steering vector is not aligned with the nominal one adopted by the radar system. The statistical performance analysis of adaptive detectors in the presence of signal mismatch was first handled in [106], where it was demonstrated that a key quantity controlling the detection performance of the KGLRT with mismatched signals is the generalized cosine-squared between the actual signal and the nominal signal in the whitened space. Based on the results in [106], the statistical performance of the AMF and ACE was given in [107], and the performance of the DMRao was analyzed in [45]. The statistical performance of the subspace-based detectors was addressed in [108] for the case of mismatched subspace signals, which is a generalization of the rank-one signal.

Note that signal mismatch can be caused by array error or target maneuvering. In addition, signal mismatch can be caused by jamming signals coming from the radar sidelobe due to electronic countermeasures (ECM). For different sources of signal mismatch, different types of detectors are needed. For the first case, a robust detector is preferred to achieve satisfactory detection performance when signal mismatch occurs. In contrast, for the second case, a selective detector is preferred, whose detection performance decreases rapidly with increasing signal mismatch.

One method to design a robust detector for mismatched signals is adopting a subspace signal model (for rank-one signals) [80] or enlarging the signal subspace (for subspace signals) [109, 110]. Another method is constraining the actual angle or Doppler frequency to a compact interval [111, 112]. Then, maximization of the concentrated likelihood function over the actual angle or Doppler can be formulated as a semidefinite programming (SDP) convex problem and solved easily. A third method is to assume that the actual signal lies in a convex cone, whose axes coincide with the nominal signal steering vector. A robust detector is then designed using second-order cone (SOC) programming [113–117]. A fourth method involves adding a random component in the test data under the signal-presence hypothesis, which makes the hypothesis more plausible when signal mismatch occurs [118].

One approach to designing a selective detector is to modify the original hypothesis test by adding a determinant unknown fictitious signal (or jammer) under the null hypothesis. Here, the fictitious signal satisfies certain constraints. A useful constraint is that the fictitious signal is orthogonal to the nominal signal in quasi-whitened space [119] or whitened space [120]. Then, the resulting detector is inclined to select the null hypothesis when there is no target in the nominal direction but in other directions. Many selective detectors have been proposed based on this idea, e.g., the adaptive beamformer orthogonal rejection test (ABORT) [119], whitened ABORT (W-ABORT) [120], their Bayesian variations [121], and other modifications [122–124]. The selective detectors proposed in the aforementioned studies were primarily under the assumption of the HE. In contrast, a selective detector was proposed in [125] for distributed target detection in PHE; however, the selectivity property of the proposed detector is limited. In [126], a detector with improved selectivity was proposed for distributed target detection in PHE.

Another approach to designing a selective detector is adding a random unknown fictitious signal under both the null and alternative hypotheses. An intuitive interpretation may be lacking. However, it works

in certain parameter settings, e.g., the double-normalized AMF (DN-AMF) [127].

Note that the directivity (robustness or selectivity) of the above detectors cannot be adjusted. In other words, for a given detector, it either works as a robust detector or a selective detector (but not both). This limits the flexibility of the detectors in detecting mismatched signals. Tunable detectors, cascaded detectors, weighted detectors, and their combinations can overcome the above limitation.

Tunable detectors are generally obtained by comparing the similarities in the detection statistics of two or more detectors with different directivity properties, and they (with specific tunable parameters) typically contain conventional detectors as special cases. The directivity property of a tunable detector for mismatched signals can be changed smoothly by adjusting one or two tunable parameters. The first tunable detector was proposed by Kalson in 1992 [128], which contains the KGLRT and AMF as two special cases; however, the selectivity of this tunable detector cannot exceed the KGLRT. Another tunable detector was proposed by Hao et al. in [129], termed as KRAO, which contains the KGLRT and DMRao as two special cases. The KRAO has enhanced selectivity; however, its robustness is limited. In [130] a tunable detector termed as KMABORT, was proposed, which contains the KGLRT, AMF, and ABORT as three special cases. The KMABORT is characterized by two tunable parameters; thus, it has more freedom to detect mismatched signals. However, its best robustness for mismatched signals is tantamount to that of the AMF. Fortunately, the AMF is very robust for mismatched signals, although it was not specifically designed for robust detection of mismatched signals. A tunable detector, called KWA, was proposed in [131], which contains the KGLRT, W-ABORT, and adaptive energy detector (AED) [132] as special cases. The KWA is more robust compared to the AMF. As a special case of the KWA, the AED does not need the nominal signal steering vector. Instead, it only tests whether a signal with sufficient energy exists. In other words, it does not differentiate between matched and mismatched signals. As a result, the AED is the most robust. Note that there are other tunable detectors, such as the ones in [133–136].

A cascaded detector is formed by cascading robust and selective detectors; thus, it has numerous pairs of detection thresholds. By changing the pair of detection thresholds, it can change the directivity property for mismatched signals. This type of cascaded detector is also referred to as a two-stage detector. A two-stage detector that cascades the KGLRT and AMF was proposed in [137]. In [107], a two-stage detector, called adaptive sidelobe blanker (ASB), was proposed, which cascades the AMF and ACE. A two-stage detector called AMF-Rao that cascades the AMF and DMRao was proposed in [45]. In [138], a two-stage detector called WAS-ASB that cascades the SGLRT and W-ABORT was proposed. In addition, in [139], a two-stage detector called S-ASB that cascades the SGLRT and ACE was proposed. In [131], a two-stage detector called KWAS-ASB that cascades the KWA and SGLRT was proposed. In [129], two two-stage detectors were proposed, named the KRAO-ASB and SKRAO-ASB. The former cascades the AMF and KRAO, while the latter cascades the SGLRT and KRAO. In [140], a two-stage detector called SD-RAO that cascades the SGLRT and DMRao was proposed. Note that the above two-stage detectors were all designed for rank-one signals. In contrast, a two-stage detector called AESD was proposed in [141] for mismatched subspace signal by cascading the AED and ASD. A useful lecture [142] summarized the selective detectors ABORT and W-ABORT, the tunable detector KWA, the two-stage detectors ASB, AMF-Rao, S-ASB, and WAS-ASB. A survey on two-stage detectors was recently presented in [143].

A weighted detector is constructed by weighting a robust detector and a selective detector. Here, the directivity can be changed smoothly by adjusting the weight. A weighted detector called SAMF-ASD was proposed in [144].

All of the tunable, two-stage, and weighted detectors are designed for a point target in HE. Note that ABORT was generalized in [125] for distributed target detection in both HE and PHE. For distributed target detection, the W-ABORT was generalized in [126, 145] in HE and PHE, respectively. In addition, a tunable detector called tunable GLRT in PHE (T-GLRT-PHE) for distributed target detection in PHE was proposed in [126].

Note that the robustness or selectivity of two-stage and weighted detectors cannot exceed their corresponding cascaded detectors and weighted detectors, respectively. In contrast, a tunable detector typically has much more freedom to change the directivity for mismatched signals.

3.4 Adaptive detection in interference

Most of the aforementioned detectors are designed without considering the presence of interference. However, in practice, interference can occur, in addition to noise and the possible signal of interest.

Table 4 Related taxonomy in Subsection 3.4

Taxonomy	Meaning
Noise interference	A type of random interference, having the effect of thermal noise or clutter.
Coherent interference	A type of interference, having the effect of deceiving the radar system, which only lies in a direction and occupies a Doppler bin.
Subspace interference	A type of coherent interference, which can be modeled by a subspace model.
Orthogonal interference	A type of coherent interference, which is orthogonal to the signal in some manner.

Interference can be caused by the intentional ECM or unintentional industrial production.

Masking and deception are two main effects of interference on radar systems. Noise interference has the effect of masking the radar system, while coherent interference has the effect of deceiving the radar system. Noise interference plays the role of thermal noise or clutter; thus, it increases the noise level. As a result, to maintain the CFAR property, the radar system must increase the detection threshold, which reduces the radar sensitivity for target detection [146, pp. 114–115]. Typically, coherent interference imitates a real target; thus, it can deceive the radar system. To achieve the above purpose, the interference is required to work coherently with the radar system. Coherent interference is also referred to as false-target interference, including false-range interference, false-velocity interference, and false-direction interference.

From the data model perspective, coherent interference [147][12)] is typically constrained to lie in a known subspace; thus, it is often referred to as subspace interference in the adaptive detection field. Significant work was performed by Scharf et al. [148–150] to detect a multichannel signal in subspace interference and thermal noise (or colored noise with a known covariance matrix). Other relative studies into subspace interference and colored noise with a known covariance matrix can be found in [151–154].

In practical applications, the noise covariance matrix is typically unknown and must be estimated. For distributed target detection in subspace interference, it was assumed in [155] that the noise covariance matrix was unknown. Here, a set of sufficient training data was used to estimate the noise covariance matrix, and the GLRT and 2S-GLRT were derived in both HE and PHE. The PFA of the GLRT in HE was given in [156]. The Rao test-based detectors in HE and PHE were derived in [157], and the Wald test-based detectors for point target detection in subspace interference were derived in [158]. In addition, a modified Rao test that took both the signal coordinate matrix and interference coordinate matrix as the relative parameter was given in [159]. It is shown in [158] that the detectors whiten the noise (or equivalently reject the clutter) in HE in the same manner; however, they reject the subspace interference in different manners. Recently, the statistical performance of the GLRT for subspace interference was analyzed in [160] for a rank-one signal. In addition, the statistical performance of the GLRT-based detectors for point target detection in subspace interference was analyzed in [161] for the signal mismatch case, including signal match as a special case. It was demonstrated in [161] that the coherent interference and signal mismatch affect the detection performance of the GLRT-based detectors through two generalized angles. One angle is between the whitened actual signal and whitened interference subspace, and the other is the angle of the actual signal and nominal signal matrix after being projected onto the interference-orthogonalized subspace. Ref. [162] investigated the detection problem in subspace interference in the presence of signal mismatch. Here, two selective detectors and a tunable detector were proposed, and their statistical performance was also given therein. The detection problem in subspace interference was addressed in [163–167] in the framework of invariance principle. When the subspace interference lies in both the test and training data, it was identified in [23] that there is no effective GLRT, and a modified GLRT was proposed based on the sieves method.

For the DD problem in the presence of subspace interference in HE, the GLRT and 2S-GLRT were developed in [168], and Wald test-based detectors were obtained in [169]. Based on GLRT and Wald test, two detectors were proposed in [170] for the DD problem in PHE.

In the above references, sufficient information about the coherent interference was assumed to be available; however, this is not always the case in practical scenarios. In [171], it was assumed that the interference subspace was unknown except for its dimension, and a GLRT-like detector was proposed. In [88], it was assumed that the coherent interference was unknown but was orthogonal to the signal in

12) Coherent interference shares the same waveform with the radar transmitted signals. Currently, waveform information is generally obtained by digital radio frequency memory (DRFM) technology [147]. For most references, the waveform information is not considered in the adaptive detection field, except for some special cases, e.g., multiple-input multiple-output (MIMO) radar, because that waveform information is consumed by matched filtering in the radar receiver while target detection is performed in the signal processor. Note that the matched filtering concept differs from that described in Section 2.

Table 5 Related taxonomy in Subsection 3.5

Taxonomy	Meaning
Low-rank structure	Noise covariance matrix is a sum of a scaled identity matrix and a low-rank matrix, with eigenvalues much greater than unity.
Persymmetry	Noise covariance matrix is persymmetric about its cross diagonal and Hermitian about its diagonal.
Spectral symmetry	Ground clutter has a symmetric PSD centered around the zero-Doppler frequency.

the whitened space, and this type of interference was referred to as orthogonal interference [172–174][13]. Then, three detectors were proposed based on the GLRT, Rao test, and Wald test criteria. Remarkably, the resulting detectors share the same forms as the SGLRT, SRao, and SAMF, respectively. However, statistical performance analysis indicated that the orthogonal interference could degrade detection performance [88]. In addition, in [175–177], it was assumed that uncertainties exist in signal and coherent interference. To account for these uncertainties, the signal and interference were constrained to certain proper cones, and effective detectors were proposed using convex optimization theory.

The adaptive detection in completely unknown coherent interference was considered in [178]. In the detector design stage, unknown interference was assumed to lie in a subspace orthogonal to the signal. According to the GLRT and Wald test, two detectors were proposed, and the detector derived according to the GLRT was called the adaptive orthogonal rejection detector (AORD). It was demonstrated that the AORD exhibits better detection performance than others in completely unknown interference. Another distinctive feature of the AORD is that it can provide significant performance improvement compared to the KGLRT and AMF in the absence of interference. This was demonstrated in [179], where the statistical performance of the AORD was presented.

The above references primarily deal with coherent interference. In [180], it was assumed there was completely unknown noise interference, and the corresponding GLRT for rank-one signals was shown to be equivalent to the ACE. The corresponding Rao test was given in [127], i.e., the DN-AMF, which was primarily adopted for mismatched signal detection, as explained in Subsection 3.3. The above results were generalized in [181] with additional coherent interference, and the GLRT, Rao test, and Wald test were derived for subspace signals. In [182], noise interference was constrained by the GER, and the GLRT was demonstrated to be the same as the KGLRT. In addition, the corresponding Rao and Wald tests were shown to be the DMRao and AMF, respectively [183]. The results in [182, 183] were generalized in [184] for subspace signals. It was assumed in [185] that the noise interference lies in a subspace orthogonal to the signal subspace, and a detector was proposed according to the two-step Rao (2S-Rao) test, named two-step orthogonal SAMF (2S-OSAMF). Numerical examples demonstrated that the 2S-OSAMF exhibits better detection performance than its competitors even though the noise interference is completely unknown.

In [186], the authors considered the problem of determining whether the test data contained noise interference, and this problem was solved by formulating it as a binary hypothesis test, and a detector was designed according to the GLRT criterion. In [187], the authors considered the problem of detecting a signal in the presence of noise interference, which only occupied parts of the training data. Two GLRT-related detectors were proposed, which were shown to outperform existing detectors. In [188], the authors considered two scenarios for the signal detection problem in interference, i.e., only noise interference existed, and both noise interference and coherent interference existed. For the first scenario, an effective estimate for the interference covariance was proposed and utilized in the AMF, which can mitigate the negative effects of the noise interference. A compressive sensing-based GLRT was proposed for the second scenario. Note that other detection problems involving noise interference were discussed in [189–191].

3.5 Adaptive detection with limited training data

Adaptive processing, e.g., adaptive detection or adaptive filtering, typically requires sufficient training data to estimate the unknown noise covariance matrix. In particular, it was shown in [42] that the adaptive filter SMI requires at least $2N-3$ IID training data to maintain 3 dB SNR loss compared to the optimum filter (with known noise covariance matrix), where N is the dimension of the test data. This is

13) Orthogonal interference satisfies the generalized eigenrelation (GER) defined in [172], which can be approximately met in practice, especially for out-of-mainbeam interference [173]. In [173], it was identified that using secondary data selection strategies, e.g., power selected training [174], results in the orthogonality of the signal and interference in the whitened space.

known as the Reed-Mallett-Brenann (RMB) rule [42, 192][14]. However, this requirement may not always be satisfied in practical application. Take STAP filtering for airborne radar as an example. Here, if the number of antenna elements is 30, the number of pulses is 40, and the system bandwidth is 10 MHz. To satisfy the requirement of the RMB rule, each filter requires received data in the range of roughly 36 km. Typically, the IID assumption cannot be guaranteed in such a wide range [193–195][15].

A priori information-based method and dimension reduction are two main approaches to alleviate the sufficient IID training data requirement.

3.5.1 *Priori information-based methods*

Priori information-based methods include Bayesian methods, parametric methods, special structure-based methods, etc.

For Bayesian methods [196, 197][16], the noise covariance matrix is ruled by a certain statistical distribution [198], and the distribution parameters can be obtained using limited training data. In [199], the noise covariance matrix was assumed to be subject to a given inverse Wishart distribution, and the Bayesian one-step GLRT (B1S-GLRT) and Bayesian 2S-GLRT (B2S-GLRT) were proposed. Using simulated and experimental data, it was demonstrated that these Bayesian detectors could provide better detection performance than the conventional ones with low sample support. Note that the B1S-GLRT and B2S-GLRT can be taken as Bayesian generalizations of the KGLRT and AMF, respectively. The Bayesian version of the ACE was derived in [200, 201]. The Bayesian method was also adopted in [121, 202] to devise selective detectors with limited training data. Notably, the Bayesian method can be used even when no training data are available [203].

The parametric (or model-based) method approximates the interference spectrum with a low-order multichannel autoregressive (AR) model [204]. In other words, the noise covariance matrix can be well characterized using only a few parameters. Thus, this method largely reduces the required training data. Simultaneously, it also reduces computational complexity. The parametric AMF (PAMF) was proposed in [204]. The PAMF was demonstrated to be equivalent to the parametric Rao test in [205], where the asymptotic (in the case of sufficiently large samples) statistical distribution was also derived. The corresponding parametric GLRT was obtained in [206], which was shown to have better detection performance than the PAMF. In [207], the nonstationary PAMF (NS-PAMF) and nonstationary normalized PAMF (NS-PAMF) were proposed for adaptive signal detection in hyperspectral imaging. Note that there are many other parametric detectors [208–223].

The structure for special structure-based methods is for the noise covariance matrix, which may have different special structures for different antenna configurations or different radar operating environments. The special structures for the noise covariance matrix include low-rank structure, Toeplitz [224], Kronecker [225, 226], persymmetry, and spectral symmetry.

For the low-rank structure, which is data-dependent, the noise covariance matrix is a sum of a scaled identity matrix (corresponding to weak thermal noise) and a low-rank matrix (corresponding to strong clutter) with eigenvalues much greater than unity. Then, with limited training data, the principal component approximation of the SCM is generally a better estimation for the noise covariance matrix than the SCM itself [227]. Many reduced-rank approaches have been developed under this guideline. Precisely, the reduced-rank versions of the KGLRT, AMF, and ACE were exploited in [228] for the space-time adaptive detection (STAD) problem in airborne radar with the data received by multiple sensors under different pulses. There are many other well-known reduced-rank detectors or filters, e.g., principal component analysis (PCA) [227], cross-spectral metric (CSM) [229], multistage Wiener filter (MWF) [230, 231], auxiliary-vector filter (AVF) [232], joint iterative optimization (JIO) [233], conjugate gradient (CG)-based AMF (CG-AMF) [234–240][17], and some others [241–245]. In addition, the diagonally loaded versions of

14) Recently, a simple proof of the RMB rule was given in [192]. For adaptive detection, more than $2N-3$ IID training data are required to maintain 3 dB SNR loss compared to the optimum detector, as shown in Figure 3.

15) In other words, in many applications, only a few data are IID. There are many approaches to select qualified data, e.g., reiterative censored fast maximum likelihood (CFML) [193], generalized inner product (GIP) [194], and approximate maximum likelihood (AML) [195].

16) Bayesian methods have also been used to model the detection problem in non-homogeneous environment [196, 197].

17) Note that the MWF, AVF, and CG are equivalent [235, 236], and they belong to the Krylov subspace technique, which was originally used in numerical calculation [237], and have recently been used successfully in signal processing [238]. Remarkably, the Krylov subspace technique does not require matrix inversion nor eigenvalue decomposition (EVD), and it can outperform EVD-based methods [239, 240].

the KGLRT, AMF, and ACE were investigated in [12,246]. Diagonal loading can be considered a type of reduced-rank method because it uses the low-rank structure information of the noise covariance matrix.

Persymmetry is another useful structure for covariance matrix estimation with low sample support. For the persymmetric covariance matrix, it is persymmetric for its cross diagonal and Hermitian for its diagonal. This structure exists when symmetrically spaced linear arrays and/or pulse trains are used. In addition, persymmetry can be observed in other situations, e.g., standard rectangular arrays, uniform cylindrical arrays (with an even number of elements), and some standard exagonal arrays [247]. In [248, 249], the maximum likelihood estimates of persymmetric covariance matrices were provided in the absence and presence of white noise, respectively. It was proven in [250, 251] that exploitation of persymmetry is tantamount to doubling the number of training data in adaptive processing. For target detection by exploiting the persymmetry, Refs. [252–256] considered the point target case with a single observation in HE, and Ref. [257–260] considered the distributed target or point target case with multiple observations/multi-bands in HE. Persymmetric detectors in HE with improved rejection capabilities were given in [261]. For the PHE, several persymmetric detection algorithms were designed in [262–267]. The above studies exploiting persymmetry primarily focused on rank-one signal detection. In contrast, persymmetric detection of subspace signals was considered in [268–273]. In addition, persymmetry can be used in non-Gaussian noise [71, 252, 274–277] or MIMO radar [278–281].

Spectral symmetry exists in ground clutter when it is observed by a stationary monostatic radar system. Precisely, ground clutter has a symmetric power spectral density (PSD) centered around the zero-Doppler frequency, and this special structure was confirmed by real data in [282, 283]. Other situations where spectral symmetry exists have been discussed in detail in [247]. Adaptive detectors that exploit spectral symmetry were proposed for the HE [247, 284] and PHE [285]. Simulation results demonstrate that utilizing spectral symmetry is equivalent to doubling the number of training data.

The above special structures can be combined to further improve detection performance, e.g., the Bayesian and parametric methods [286], the parametric method and persymmetry [287,288], the low-rank structure and persymmetry [289], and persymmetry and spectral symmetry [290–292] can be combined effectively.

3.5.2 *Dimension reduction methods*

Utilizing a priori information may suffer from significant performance loss if the prior information greatly departs from the actual information. Another approach to alleviating the requirement of sufficient IID training data is dimension reduction, which is a data-independent process. Here, reduced-dimension transformation is applied to the test and training data prior to adaptive processing, which has the effect of projecting the noise covariance matrix onto a low-dimension subspace. As a result, the required number of IID training data can be reduced considerably, and computational complexity is also reduced. Various reduced-dimension approaches have been proposed, e.g., the auxiliary channel receiver (ACR) [293], extended factor approach (EFA) [294], space-time multiple-beam (STMB) [295], sum-difference STAP ($\Sigma\Delta$-STAP) [296], best channel method (BCM) [297], alternating low-rank decomposition (ALRD) [298], and others [299].

The aforementioned approaches were proposed for filtering. In contrast, the joint-domain localized GLR (JDL-GLR) detector was proposed for airborne radar target detection in [300]. First, the JDL-GLR transforms the test and training data into reduced-dimension space, and then uses the KGLRT structure to form the final detector. Another similar reduced-dimension GLRT was proposed in [301]. Two reduced-dimension detectors that adopted the AMF structure were proposed in [52]. In [302], a reduced-dimension detector with subarray processing was proposed. Recently, a random matrix-based reduced-dimension detector was given in [303]. This detector also uses the KGLRT structure; however, the reduced-dimension matrix is selected in a different manner. Here, one column of the reduced-dimension matrix is aligned with the signal steering vector, and the other columns are selected randomly in the subspace orthogonal to the signal steering vector.

In [304,305], the test and training data were first projected on one-dimensional signal subspace, thereby resulting in scalar data. Then, two reduced-dimension detectors were designed using the resultant scalar data. Note that these reduced-dimension detectors are primarily for rank-one signals. In contrast, a reduced-dimension detector for subspace signal detection was proposed in [306], which is referred to as the subspace transformation-based detector (STBD). In [306], it was demonstrated that the STBD, which can also serve as a filter, can provide improved detection and filtering performance even in some

Table 6 Related taxonomy in Subsection 3.6

Taxonomy	Meaning
Distributed MIMO radar	MIMO radar with widely separate antennas.
Colocated MIMO radar	MIMO radar with closely spaced antennas.
Spatial diversity	The transmit antennas are far enough from each other, and hence the target radar cross sections can be taken as independent random variables for different transmit-receive paths. With a spatially diverse set of "looks", each set of received data carries independent information about the target.

sample-abundant scenarios, as well as cases with limited training data.

In addition to a priori information-based and dimension reduction methods, some other technologies may alleviate (or even not need) the training data requirement. For example, in [307], the authors considered the problem of detecting a multichannel spatial signal in unknown noise without training data. Here, to estimate the unknown noise covariance matrix, a number of echo signals reflected by the test data were utilized.

3.6 Adaptive detection for MIMO radar

MIMO radar adopts multiple elements at both the transmit and receive antennas, and the transmitted waveforms are linearly independent or orthogonal [308]. According to the antenna configuration, there are two basic categories for MIMO radar, i.e., distributed MIMO radar, where antennas are distant from each other [309], and colocated MIMO radar, where antennas are positioned close to each other [310].

Strictly speaking, a review of MIMO radar target detection can also be carried out from the above five aspects or be included in the above five aspects. However, as an emerging research area, MIMO radar has received considerable attention. Thus, we review MIMO radar target detection in an independent subsection from the three perspectives: adaptive detection for distributed MIMO radar, adaptive detection for colocated MIMO radar, and adaptive detection for other types of MIMO radar.

3.6.1 *Adaptive detection for distributed MIMO radar*

It was demonstrated in [311] that distributed MIMO radar can provide better detection performance than traditional phased-array radar in high SNR regions because spatial diversity can alleviate the impact of target scintillation, and spatial diversity gain is greater than the coherent processing gain of phased-array radar. Based on the results presented in [311], the expressions for the PD of the GLRT were derived in [312] when the target comprises a finite number of small scatterers. In addition, Ref. [313] considered the problem of joint target detection and parameter estimation, and it was demonstrated that distributed MIMO radar provides significant improvement over phased-array radars for distributed targets. Ref. [314] dealt with the MIMO radar detection problem when phase synchronization mismatch occurs between the transmit and receive antennas. Here, phase error was modeled as the von Mises distribution, and the corresponding GLRT was derived. Polarimetric MIMO radar detection in Gaussian noise was investigated in [315], and it was shown that optimal design of the antenna polarization leads to better detection performance than MIMO radar systems that transmit fixed polarized waveforms over all antennas.

Note that the target's movement feature was not considered in the above references. When the transmitted waveform was orthogonal and Doppler processing was adopted, the GLRT and 2S-GLRT were derived in [316] for moving target detection in a Gaussian background, and the expression for the PFA of the GLRT was given in [317]. In addition, it was assumed in [278] that the noise covariance matrix possessed persymmetry, and then the GLRT (and statistical property) was derived for distributed MIMO radar that transmitted orthogonal waveforms and employed Doppler processing. Under the same antenna configuration, as well as adopting the Doppler processing, the 2S-GLRT was given in [318] for compound-Gaussian clutter, and the corresponding 2S-Rao and 2S-Wald tests were derived in [319]. When the distributed MIMO radar transmitted orthogonal waveforms and adopted Doppler processing, Ref. [320] derived the GLRT for polarimetric moving target detection in Gaussian noise. The detection problem in [316] was generalized in [321] by assuming that the target velocity was unknown, and it was demonstrated that distributed MIMO radar exhibits better detection performance than phased-array radar when detecting a target with small radial velocities and the environment is homogeneous. The distributed MIMO radar detection in non-homogeneous clutter was considered in [322], where the corresponding GLRT was derived and evaluated analytically. It was also demonstrated that the GLRT

in [322] exhibited better detection performance than the detector in [321], as well as the corresponding phased-array detector.

Note that orthogonal waveforms were adopted in the above references. Under the assumption of white Gaussian noise, it is demonstrated in [323] that a detector suffers certain detection performance loss if the orthogonality property of the waveforms transmitted by different antennas is not satisfied. However, the above result may not be suitable for colored noise. Ref. [324] derived the GLRT for distributed MIMO radar with arbitrary transmitted waveforms and arbitrary time-correlation of the noise, and it was demonstrated that there exists an inherent trade-off between diversity and integration, and that no uniformly optimum waveform design strategy exists. In addition, in [325], the GLRT was derived for distributed MIMO radar with arbitrary transmit waveform and Doppler processing. Here, it was assumed that all transmit-receive pairs share the same known covariance matrix, and then the expressions for the PD of the GLRT were given [325], according to which the optimum transmit waveform was then given. Ref. [326] generalized the data model in [325] for different transmit-receive pairs with different but known covariance matrices, and then the statistical performance of the corresponding GLRT was given for a Swerling-I target.

The signal model in [325] was also adopted in [327–331]; however, the noise was assumed to be compound-Gaussian. Specifically, the 2S-Rao and 2S-Wald tests for distributed MIMO radar were given in [327], and several Bayesian 2S-GLRTs were derived in [328, 329]. The 2S-Rao and 2S-Wald tests in [327] were generalized to polarimetric distributed MIMO radar detection in [332] for point targets and [333] for distributed targets. In addition, Ref. [330] derived the 2S-GLRT for point target detection with polarimetric distributed MIMO radar in compound-Gaussian clutter, and it was generalized in [331] for distributed target detection.

3.6.2 *Adaptive detection for colocated MIMO radar*

For the colocated MIMO radar detection, Ref. [334] derived the GLRT and its asymptotic statistical distribution for colocated MIMO radar after beamforming in white Gaussian noise. In addition, Ref. [335] proposed three 2S-GLRTs for colocated MIMO radar with randomly distributed arrays in compound-Gaussian clutter, and it was demonstrated that the configuration of randomly distributed arrays achieved detection performance improvement at directions with strong clutter.

Remarkably, in [336], it was shown that colocated MIMO radar enables target detection and parameter estimation without the need for training data or even range compression. Without training data, the parameter estimation problem for colocated MIMO radar was addressed in [337], where the GLRT was derived to suppress the false peak induced by a strong jammer. The corresponding Rao and Wald tests, and their statistical properties, were given in [338]. When signal mismatch occurs, a tunable MIMO radar detector was proposed in [136], which includes the Rao and Wald tests in [338] as special cases. The tunable detector proposed in [136] has flexibility in controlling the direction property, selectivity, or robustness for mismatched signals. In addition, two robust detectors were proposed in [339] for mismatched signals by assuming the actual signal lying in certain subspaces. The GLRT in [337] was generalized in [279] when the persymmetry of noise covariance matrix was exploited. It was demonstrated by simulation and experimental data that the detector proposed in [279] could achieve better detection performance by utilizing persymmetry. The corresponding persymmetric Rao test and Wald test were given in [280, 281], respectively, and a two-stage detector was also given in [281] for mismatched signal detection by cascading the above persymmetric Rao and Wald tests.

More recently, for a colocated MIMO radar, a robust Wald-type test was proposed in [340]. Performance analysis demonstrated that there always exists a sufficient number of (virtual) antennas such that the required performance is realized without prior knowledge of the noise statistical property. This type of MIMO radar was referred to as the massive MIMO radar. In addition, three adaptive GLRTs were proposed in [341] for colocated MIMO radar equipped with a frequency diverse array (FDA).

3.6.3 *Adaptive detection for other types of MIMO radar*

There are several variations of the distributed MIMO radar and colocated MIMO radar, e.g., phased MIMO (Phased-MIMO) radar [342], hybrid MIMO phased array radar (HMPAR) [343], transmit sub-aperturing MIMO (TS-MIMO) radar [344], and multi-site radar system MIMO (MSRS-MIMO) [345]. The MSRS-MIMO radar has multiple widely separate sub-arrays, and each sub-array has multiple colocated antennas. According to the waveforms, the MSRS-MIMO radar can be classified into two groups.

Table 7 Important progress in multichannel adaptive signal detection

Year	Important progress	Author	Ref.
1986	The first paper on adaptive detection	Kelly	[4]
1989	Solid mathematical background for adaptive signal detection	Kelly and Rorsythe	[101]
1991/1992	Well-known detector for point targets: AMF	Chen et al. and Fobey et al.	[43, 44]
1992	Tunable detector for mismatched signals	Kalson	[128]
1992	Persymmetry structure based detector with limited training data	Cai and Wang	[258]
1995/1999	Well-known detector for point targets: ACE	Kraut et al. and Conte et al.	[56, 62]
1996	Subspace-based signal detection	Raghavan et al.	[80]
1996	Direction detection	Bose and Steinhardt	[97]
1997	Distributed target detection	Gerlach et al.	[355]
2000	Two-stage detector for mismatched signals	Pulsone and Zatman	[137]
2000	Low-rank structure based detector with limited training data	Ayoub and Haimovich	[301]
2000	Parametric detector with limited training data	Roman et al.	[204]
2001	Selective detector for mismatched signals	Pulsone and Rader	[119]
2003	Adatpive detectors based on Rao and Wald tests	Conte and de Maio	[274]
2004	Multiple target detection	Gini et al.	[356]
2005	Adaptive detection based on convex optimization	de Maio	[113]
2007	Adaptive detection in subspace interference	Bandiera et al.	[155]
2007	Bayesian detector in heterogeneous environment	Besson et al.	[196]
2008	MIMO radar detection in unknown noise	Xu et al.	[337]
2010	Spectral symmetry based detector with limited training data	de Maio et al.	[247]
2014	Rao and Wald tests for complex-valued signals with circularly symmetric random parameters	Liu et al.	[29]
2014	Double subspace signal detection	Liu et al.	[83, 102]
2016	Rao test for complex-valued signals with circularly or non-circularly symmetric random parameters	Kay and Zhu	[30]
2016	Statistical performance of adaptive subspace detectors for point targets in the presence of signal mismatch	Liu et al.	[108]
2016	Adaptive detection based on covariance structure classification	Carotenuto et al.	[357]

In the first group, the waveforms differ or are orthogonal in different transmit antennas [346]. In the other group, the waveforms transmitted by the antennas are scaled versions of a single waveform [347]. For convenience, the first type of MSRS-MIMO radar is referred to as distributed-colocated MIMO radar, and the latter is referred to as distributed-phased MIMO radar [322, 348, 349][18)].

When the waveforms are orthogonal, the GLRT for distributed-colocated MIMO radar was obtained in a non-Gaussian environment in [2], and the expression for the PFA was given under the constraint that the product of the number of transmit elements and receive elements is the same for each pair of transmit-receive sub-arrays. The result for the PFA in [2] was generalized in [350] by eliminating the above constraint. For distributed-colocated MIMO radar with a non-orthogonal waveform, the GLRT in Gaussian noise was derived in [351], and the two-step Rao and Wald tests were given in [352]. In the non-Gaussian background, the 2S-GLRT, Rao test, and Wald test were exploited in [353] for distributed-colocated MIMO radar with a non-orthogonal waveform. In addition, Ref. [354] considered the problem of detecting a mismatched signal in distributed-phased MIMO radar and proposed three selective detectors.

Before closing this section, we summarize important progress in Table 7 [4, 29, 30, 43, 44, 56, 62, 80, 83, 97, 101, 102, 108, 113, 119, 128, 137, 155, 196, 204, 247, 258, 274, 301, 337, 355–357].

4 Typical adaptive detectors for different detection problems

Multichannel adaptive signal detection was first investigated for a point target by Kelly in 1986 [4]. Based on Kelly's work, all kinds of problems were considered, and numerous detectors have been proposed. Here, we first summarize the statistical properties of many well-known detectors for point targets because such properties are the primary tool to evaluate detection performance. We then generalize the point target detection case to distributed target detection and signal detection in the presence of interference[19)].

18) Note that the data model of distributed-phased MIMO radar is the same as the conventional distributed MIMO radar, which adopts coherent pulse processing in each sub-array [322, 348, 349].

19) We select the above cases because they are representative in the adaptive detection field and have been studied extensively.

4.1 Adaptive detectors for point targets and their statistical distributions

The subspace signal model is more general than the rank-one signal model adopted in (20). In [148], it is pointed out that the matched subspace detector is the general building block of signal processing, and it contains the rank-one matched filter or detector as a special case. Thus, here, the detectors for point targets are all based on the subspace signal model.

For the detection problem in (1), if signal $\boldsymbol{s}$ lies in a known subspace spanned by an $N\times p$ full-column-rank matrix $\boldsymbol{H}$, we have $\boldsymbol{s}=\boldsymbol{H}\boldsymbol{\theta}$, where $\boldsymbol{\theta}$ is a $p\times 1$ unknown coordinate vector. In the HE, the noise covariance matrix in the test data $\boldsymbol{x}$ is the same as that in the training data $\boldsymbol{x}_{\mathrm{e},l}$. Then, for the detection problem in (1) with $\boldsymbol{s}$ replaced by $\boldsymbol{H}\boldsymbol{\theta}$, the GLRT [85], Rao test [83], and Wald test [83] are given as follows:

$$t_{\mathrm{SGLRT}}=\frac{\tilde{\boldsymbol{x}}^{\mathrm{H}}\boldsymbol{P}_{\tilde{\boldsymbol{H}}}\tilde{\boldsymbol{x}}}{1+\tilde{\boldsymbol{x}}^{\mathrm{H}}\tilde{\boldsymbol{x}}-\tilde{\boldsymbol{x}}^{\mathrm{H}}\boldsymbol{P}_{\tilde{\boldsymbol{H}}}\tilde{\boldsymbol{x}}}, \tag{35}$$

$$t_{\mathrm{SRao}}=\frac{\tilde{\boldsymbol{x}}^{\mathrm{H}}\boldsymbol{P}_{\tilde{\boldsymbol{H}}}\tilde{\boldsymbol{x}}}{(1+\tilde{\boldsymbol{x}}^{\mathrm{H}}\tilde{\boldsymbol{x}})(1+\tilde{\boldsymbol{x}}^{\mathrm{H}}\tilde{\boldsymbol{x}}-\tilde{\boldsymbol{x}}^{\mathrm{H}}\boldsymbol{P}_{\tilde{\boldsymbol{H}}}\tilde{\boldsymbol{x}})}, \tag{36}$$

and

$$t_{\mathrm{SAMF}}=\tilde{\boldsymbol{x}}^{\mathrm{H}}\boldsymbol{P}_{\tilde{\boldsymbol{H}}}\tilde{\boldsymbol{x}}, \tag{37}$$

respectively, where $\tilde{\boldsymbol{H}}=\boldsymbol{S}^{-\frac{1}{2}}\boldsymbol{H}$ and $\boldsymbol{P}_{\tilde{\boldsymbol{H}}}=\tilde{\boldsymbol{H}}(\tilde{\boldsymbol{H}}^{\mathrm{H}}\tilde{\boldsymbol{H}})^{-1}\tilde{\boldsymbol{H}}^{\mathrm{H}}$. Note that the detectors in (35)–(37) are referred to as SGLRT, SRao, and SAMF, respectively.

In the PHE, the noise covariance matrices in the test and training data can be modified as $\boldsymbol{R}_{\mathrm{e}}=\sigma^2\boldsymbol{R}$ and $\boldsymbol{R}$, respectively, where σ^2 is an unknown positive scaling factor representing power mismatch between the test and training data. In the PHE, the GLRT, Rao test, and Wald test coincide with each other and are found to be [102]

$$t_{\mathrm{ASD}}=\frac{\tilde{\boldsymbol{x}}^{\mathrm{H}}\boldsymbol{P}_{\tilde{\boldsymbol{H}}}\tilde{\boldsymbol{x}}}{\tilde{\boldsymbol{x}}^{\mathrm{H}}\tilde{\boldsymbol{x}}}, \tag{38}$$

which is called ASD in [84]. Note that the SGLRT, SRao, SAMF, and ASD are the subspace generalizations of the KGLRT, DMRao, AMF, and ACE, respectively.

The above four detectors are designed without considering the possibility of signal mismatch. On the one hand, signal mismatch may be caused by antenna error, mutual coupling, or target maneuvering. On the other hand, signal mismatch can also be caused by a strong target or a jamming signal located in the radar sidelobe generated by the ECM. For different signal mismatch sources, different directivity properties (the capability of selectivity or robustness to signal mismatch) of the detector are preferred. For the first case, a robust detector is required to maintain good detection performance in the presence of signal mismatch. In contrast, for the second case, a selective detector is preferred, whose detection performance decreases rapidly with increasing signal mismatch.

To design selective detectors that consider signal mismatch, an effective approach is to add an artificially determinant factitious jammer under hypothesis H_0 [119]. Then, the detection problem in (1) can be modified as follows:

$$\begin{cases}\mathrm{H}_0:\boldsymbol{x}=\boldsymbol{n}+\boldsymbol{q},\ \boldsymbol{x}_{\mathrm{e},l}=\boldsymbol{n}_{\mathrm{e},l},\ l=1,2,\ldots,L,\\ \mathrm{H}_1:\boldsymbol{x}=\boldsymbol{H}\boldsymbol{\theta}+\boldsymbol{n},\ \boldsymbol{x}_{\mathrm{e},l}=\boldsymbol{n}_{\mathrm{e},l},\ l=1,2,\ldots,L,\end{cases} \tag{39}$$

where the $N\times 1$ unknown vector $\boldsymbol{q}$ denotes the artificially injected determinant factitious jammer. Note that the injection of factitious jammer $\boldsymbol{q}$ makes the resulting detector tend to select hypothesis H_0 if signal mismatch occurs. When $\boldsymbol{q}$ is constrained to be orthogonal to the signal subspace in the quasi-whitened space, i.e.,

$$\boldsymbol{H}^{\mathrm{H}}\boldsymbol{S}^{-1}\boldsymbol{q}=\boldsymbol{0}_{p\times 1}, \tag{40}$$

the GLRT for the detection problem in (39) is given as follows:

$$t_{\mathrm{SABORT}}=\frac{1+\tilde{\boldsymbol{x}}^{\mathrm{H}}\boldsymbol{P}_{\tilde{\boldsymbol{H}}}\tilde{\boldsymbol{x}}}{1+\tilde{\boldsymbol{x}}^{\mathrm{H}}\tilde{\boldsymbol{x}}-\tilde{\boldsymbol{x}}^{\mathrm{H}}\boldsymbol{P}_{\tilde{\boldsymbol{H}}}\tilde{\boldsymbol{x}}}, \tag{41}$$

which is a special case of the adaptive direction detector with mismatched signal rejection of type 2 (ADDMSR2) in [124] and a subspace generalization of the ABORT proposed in [119]. Thus, for convenience, the detector in (41) is referred to as the subspace-based ABORT (SABORT).

The determinant factitious jammer in (40) can be modified as follows:

$$\boldsymbol{H}^{\mathrm{H}}\boldsymbol{R}^{-1}\boldsymbol{q}=\boldsymbol{0}_{p\times 1}. \tag{42}$$

In other words, the factitious jammer is orthogonal to the signal subspace in the truly whitened space. Then the GLRT for the detection problem in (39) is expressed as follows:

$$t_{\text{W-SABORT}}=\frac{1+\tilde{\boldsymbol{x}}^{\mathrm{H}}\tilde{\boldsymbol{x}}}{(1+\tilde{\boldsymbol{x}}^{\mathrm{H}}\tilde{\boldsymbol{x}}-\tilde{\boldsymbol{x}}^{\mathrm{H}}\boldsymbol{P}_{\tilde{\boldsymbol{H}}}\tilde{\boldsymbol{x}})^2}, \tag{43}$$

which is a special case of the adaptive direction detector with mismatched signal rejection of type 1 (ADD-MSR1) in [124] and a subspace generalization of the W-ABORT in [120]. The detector in (43) is referred to as the whitened SABORT (W-SABORT) for convenience.

In addition, another approach to devise a selective detector is injecting an unknown, rank-one, noise-like, fictitious jammer $\boldsymbol{v}$ under both hypotheses. As a result, the noise covariance matrix in the test data becomes $\boldsymbol{R}=\boldsymbol{R}_{\mathrm{e}}+\boldsymbol{v}\boldsymbol{v}^{\mathrm{H}}$. Then, the selective detector derived according to the Rao test is expressed as follows:

$$t_{\text{DN-SAMF}}=\frac{\tilde{\boldsymbol{x}}^{\mathrm{H}}\boldsymbol{P}_{\tilde{\boldsymbol{H}}}\tilde{\boldsymbol{x}}}{\tilde{\boldsymbol{x}}^{\mathrm{H}}\tilde{\boldsymbol{x}}(1+\tilde{\boldsymbol{x}}^{\mathrm{H}}\tilde{\boldsymbol{x}}-\tilde{\boldsymbol{x}}^{\mathrm{H}}\boldsymbol{P}_{\tilde{\boldsymbol{H}}}\tilde{\boldsymbol{x}})}, \tag{44}$$

which is a special case of the Rao test in [181] and a subspace generalization of the DN-AMF in [127]. For convenience, the detector in (44) is referred to as the doubly normalized SAMF (DN-SAMF).

Differing from the above devised selective detectors, a detector that is robust against signal mismatch may be preferable in many applications. A robust detector can be designed by assuming the desired signal to be detected is completely unknown. In other words, the signal $\boldsymbol{s}$ in (1) is unknown, or equivalently, the dimension of signal matrix $\boldsymbol{H}$ is $N\times N$. Then, the corresponding GLRT is given as follows [132]:

$$t_{\text{AED}}=\tilde{\boldsymbol{x}}^{\mathrm{H}}\tilde{\boldsymbol{x}}, \tag{45}$$

which can be referred to as the AED. It was demonstrated in [83] that the Rao and Wald tests are equivalent to the GLRT, i.e., the AED in (45).

The signal match case can be taken as a special case of signal mismatch (i.e., the mismatched angle is zero); thus, we only summarize the statistical properties of the above detectors in the presence of signal mismatch. As mentioned above, the statical performance of detectors in the presence of signal mismatch was first addressed by Kelly in [106] for the KGLRT in the rank-one signal case. Based on this result, the statistical performance of the SGLRT, SAMF, and ASD was given in [108]. In the following, we summarize the statical properties of the above eight detectors, some of which were not found in the open literature.

To obtain the statical distributions of the detectors, it is convenient to introduce the following quantity:

$$\beta=\frac{1}{1+\tilde{\boldsymbol{x}}^{\mathrm{H}}\tilde{\boldsymbol{x}}-\tilde{\boldsymbol{x}}^{\mathrm{H}}\boldsymbol{P}_{\tilde{\boldsymbol{H}}}\tilde{\boldsymbol{x}}}, \tag{46}$$

which can be taken as a loss factor.

If signal mismatch occurs, the actual signal, denoted by $\boldsymbol{s}_0$, may not completely lie in the signal subspace spanned by the columns of $\boldsymbol{H}$. Then, it is demonstrated in [108] that the statistical distribution of the SGLRT in (35) with β given under hypothesis H_1 is a complex noncentral F-distribution, with p and $L-N+1$ DOF, and a noncentrality parameter $\beta\rho\cos^2\phi$, written symbolically as follows:

$$t_{\text{SGLRT}}|[\beta,\mathrm{H}_1]\sim\mathcal{CF}_{p,L-N+1}\left(\beta\rho_{\text{pnt}}\cos^2\phi\right), \tag{47}$$

where ρ_{pnt} is the output SNR, defined as follows:

$$\rho_{\text{pnt}}=\boldsymbol{s}_0^{\mathrm{H}}\boldsymbol{R}^{-1}\boldsymbol{s}_0, \tag{48}$$

$$\cos^2\phi=\frac{\boldsymbol{s}_0^{\mathrm{H}}\boldsymbol{R}^{-1}\boldsymbol{H}(\boldsymbol{H}^{\mathrm{H}}\boldsymbol{R}^{-1}\boldsymbol{H})^{-1}\boldsymbol{H}^{\mathrm{H}}\boldsymbol{R}^{-1}\boldsymbol{s}_0}{\boldsymbol{s}_0^{\mathrm{H}}\boldsymbol{R}^{-1}\boldsymbol{s}_0}, \tag{49}$$

and the notation $|[\beta, \mathrm{H}_1]$ denotes the fact that the above statistical distribution holds under hypothesis H_1 under the condition that β is given. Eq. (49) can be rewritten as follows:

$$\cos^2\phi = \frac{\bar{\boldsymbol{s}}_0^{\mathrm{H}} \boldsymbol{P}_{\bar{\boldsymbol{H}}} \bar{\boldsymbol{s}}_0}{\bar{\boldsymbol{s}}_0^{\mathrm{H}} \bar{\boldsymbol{s}}_0}, \tag{50}$$

where $\bar{\boldsymbol{s}}_0 = \boldsymbol{R}^{-\frac{1}{2}} \boldsymbol{s}_0$, $\bar{\boldsymbol{H}} = \boldsymbol{R}^{-\frac{1}{2}} \boldsymbol{H}$, $\boldsymbol{P}_{\bar{\boldsymbol{H}}} = \bar{\boldsymbol{H}} (\bar{\boldsymbol{H}}^{\mathrm{H}} \bar{\boldsymbol{H}})^{-1} \bar{\boldsymbol{H}}^{\mathrm{H}}$. From (50), it follows that the quantity $\cos^2\phi$ measures the cosine-squared of the angle between the whitened actual signal $\bar{\boldsymbol{s}}_0$ and the whitened nominal signal subspace spanned by the columns of $\bar{\boldsymbol{H}}$. Here, $\cos^2\phi$ plays a key role in controlling detection performance in the presence of signal mismatch. This is demonstrated numerically in Subsection 4.2.

In addition, it is shown in [108] that the statistical distribution of the loss factor β in (46) under hypothesis H_1 is a complex noncentral Beta distribution, with $L - N + p + 1$ and $N - p$ DOFs and a noncentrality parameter δ^2, expressed symbolically as follows:

$$\beta|\mathrm{H}_1 \sim \mathcal{CB}_{L-N+p+1, N-p}(\delta^2), \tag{51}$$

where

$$\delta^2 = \rho_{\mathrm{pnt}} \sin^2\phi, \tag{52}$$

and $\sin^2\phi = 1 - \cos^2\phi$.

In contrast, under hypothesis H_0, the statistical distributions of the SGLRT in (35) and the loss factor β in (46) become

$$t_{\mathrm{SGLRT}}|[\beta, \mathrm{H}_0] \sim \mathcal{CF}_{p, L-N+1}, \tag{53}$$

and

$$\beta|\mathrm{H}_0 \sim \mathcal{CB}_{L-N+p+1, N-p}, \tag{54}$$

respectively.

The analytical expressions for the PDF and cumulative distribution function (CDF) of the complex noncentral F-distribution and complex noncentral Beta distribution were exploited in detail in Kelly and Forsythe's classic report [101], and were summarized in [107, 142]. These CDFs and PDFs can be used to derive the expressions for the PDs and PFAs of the above detectors.

It is straightforward to verify that the following seven equations hold:

$$t_{\mathrm{SAMF}} = \frac{t_{\mathrm{SGLRT}}}{\beta}, \tag{55}$$

$$t_{\mathrm{ASD}} = \frac{t_{\mathrm{SGLRT}}}{1 - \beta}, \tag{56}$$

$$t_{\mathrm{SRao}} = \frac{\beta t_{\mathrm{SGLRT}}}{1 + t_{\mathrm{SGLRT}}}, \tag{57}$$

$$t_{\mathrm{SABORT}} = \beta + t_{\mathrm{SGLRT}}, \tag{58}$$

$$t_{\text{W-SABORT}} = (1 + t_{\mathrm{SGLRT}})\beta, \tag{59}$$

$$t_{\text{DN-SAMF}} = \frac{\beta t_{\mathrm{SGLRT}}}{(1 - \beta)(1 - \beta + t_{\mathrm{SGLRT}})}, \tag{60}$$

$$t_{\mathrm{AED}} = \frac{1 - \beta + t_{\mathrm{SGLRT}}}{\beta}. \tag{61}$$

Based on the conditional distribution of the SGLRT in (47) and the statistical distribution of the loss factor β in (51), as well as the statistical dependencies in (55)–(61), one can readily obtain analytical expressions for the PDs and PFAs of the detectors. Interested readers are referred to [108] for examples. Note that the expressions for the PD and PFA of the AED can be obtained more directly by deriving the statistical distribution of the AED [358]. Specifically, according to Theorem 3.2.13 in [359, p.98] or Theorem 5.2.2 in [360, p.176], the statistical distributions of the AED in (45) under hypotheses H_1 and H_0 are given as follows:

$$t_{\mathrm{AED}}|\mathrm{H}_1 \sim \mathcal{CF}_{N, L-N+1}(\rho_{\mathrm{pnt}}) \tag{62}$$

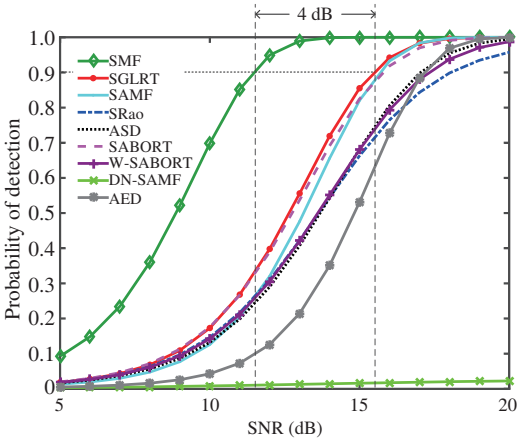

Figure 3 (Color online) PD versus SNR. $N = 12$, $p = 2$, $L = 2N$, and PFA $= 10^{-3}$.

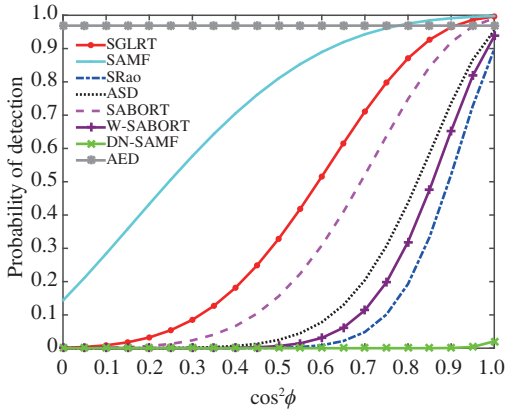

Figure 4 (Color online) PD versus $\cos^2\phi$. $N = 12$, $p = 2$, $L = 2N$, SNR $= 18$ dB, and PFA $= 10^{-3}$.

and

$$t_{\mathrm{AED}}|\mathrm{H}_0 \sim \mathcal{C}\mathcal{F}_{N,L-N+1}, \tag{63}$$

respectively.

To evaluate detection performance under different amounts of training data, we consider the detector with known noise covariance matrix. Here, when $\boldsymbol{R}$ is known, the GLRT for the detection problem in (1) with $\boldsymbol{s}$ replaced by $\boldsymbol{H\theta}$ is given as follows:

$$t_{\mathrm{SMF}} = \boldsymbol{x}^{\mathrm{H}}\boldsymbol{R}^{-1}\boldsymbol{H}(\boldsymbol{H}^{\mathrm{H}}\boldsymbol{R}^{-1}\boldsymbol{H})^{-1}\boldsymbol{H}^{\mathrm{H}}\boldsymbol{R}^{-1}\boldsymbol{x}, \tag{64}$$

which is referred to as the subspace-based matched filter (SMF). It can also be obtained by the criteria of GLRT, Rao and Wald tests. The statistical distribution of the SMF in (64) under hypothesis H_1 is a complex noncentral Chi-square distribution with p DOFs and a noncentrality parameter ρ [88], expressed symbolically as follows:

$$t_{\mathrm{SMF}}|\mathrm{H}_1 \sim \mathcal{C}\chi_p^2(\rho_{\mathrm{pnt}}). \tag{65}$$

Under hypothesis H_0, the above distribution becomes central, i.e.,

$$t_{\mathrm{SMF}}|\mathrm{H}_0 \sim \mathcal{C}\chi_p^2. \tag{66}$$

4.2 Numerical examples

Here, we compare the detection performance using numerical examples and focus on the HE case. Two cases are considered, i.e., without and with signal mismatch. The PD curves of all detectors are obtained using the theoretical results and confirmed via Monte Carlo simulations; however, the Monte Carlo simulation results are not shown for a clear display.

Figure 3 compares the detection performance of the adaptive detectors under different SNRs in the absence of signal mismatch. For comparison, the results for the SMF are also reported. Among the eight adaptive detectors, the results demonstrate that, for the selected parameters, the SGLRT has the highest PD and is slightly better than the SAMF and SABORT. The DN-SAMF has the lowest PD, and the PDs of the ASD, W-SABORT, SRao, and AED are in between. In addition, the detection performance loss of the SGLRT in terms of SNR is approximately 4 dB when PD $= 0.9$ compared to the SMF. This is quite different from adaptive filtering because, from the RMB rule [42], it is well-known that $2N$ independent identically distributed (IID) training data can maintain 3 dB SNR loss compared to the optimum filter. The above detection loss is caused by two factors [4], i.e., the effective SNR loss factor (similar to adaptive filtering) and the CFAR loss of the adaptive detectors. The effective SNR loss factor is generally dependent on the ratio of L to N, and the CFAR loss is entirely dependent on L, whose increase results in decreased CFAR loss.

Figure 4 shows the detection performance of the adaptive detectors under different amounts of signal mismatch. As expected, the AED is the most robust, and its PD does not vary with varying $\cos^2\phi$.

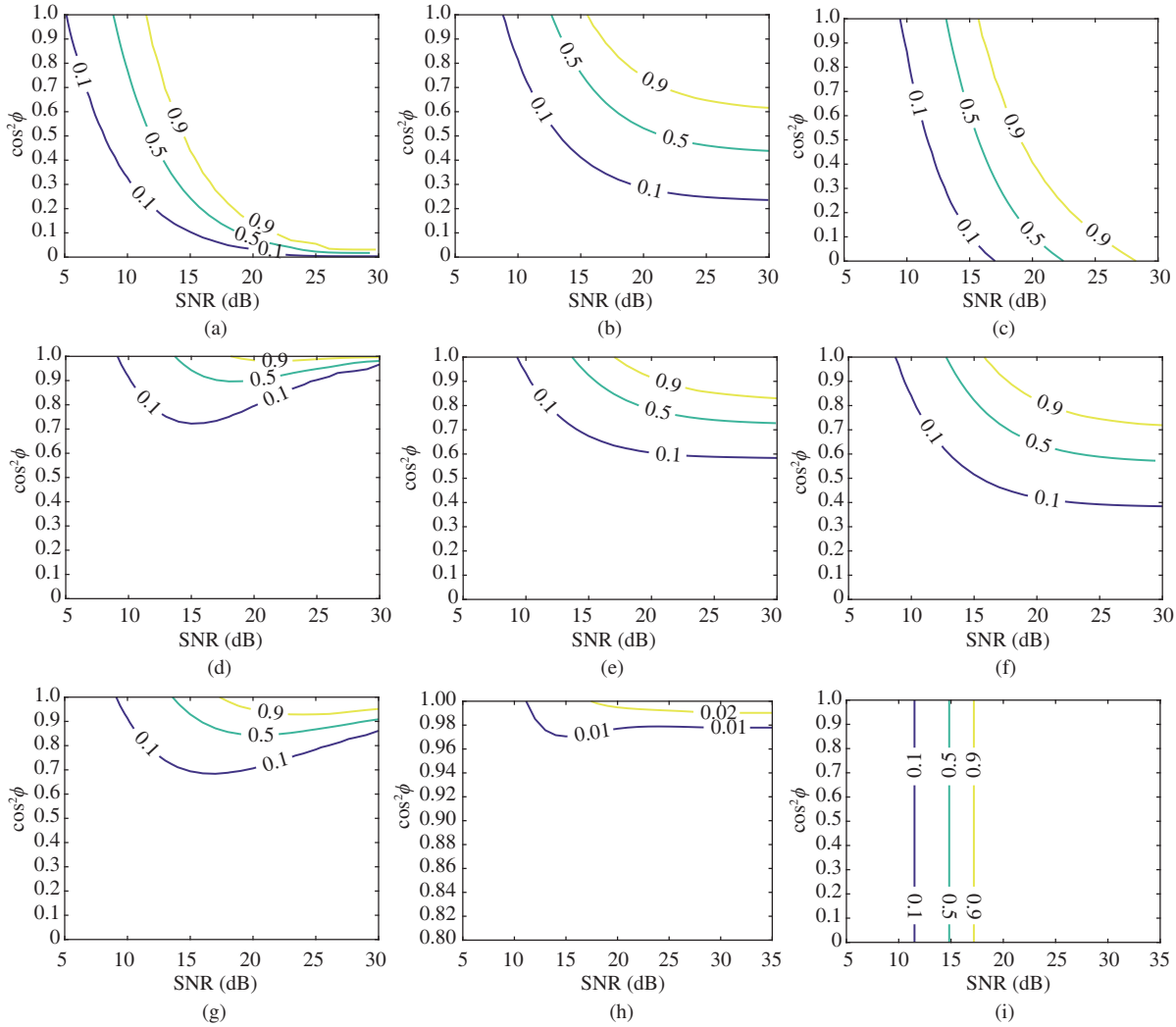

Figure 5 (Color online) Contours of the PDs versus SNR and $\cos^2\phi$. $N = 12$, $p = 2$, $L = 2N$, and PFA $= 10^{-3}$. (a) SMF; (b) SGLRT; (c) SAMF; (d) SRao; (e) ASD; (f) SABORT; (g) W-SABORT; (h) DN-SAMF; (i) AED.

However, its PD cannot attain unity for the selected parameters. Note that the robustness of the SAMF, SGLRT, SABORT, ASD, W-SABORT, SRao, and DN-SAMF reduces in sequence.

Another method to illustrate the detection performance for mismatched signals is the contours of PDs as functions of SNR and $\cos^2\phi$, which was first introduced in [119]. This is referred to as a mesa plot. The mesa plot is shown in Figure 5 for the above detectors. Here, the directivities of the detectors are the same as those in Figure 4; however, more information can be inferred from Figure 5. Taking the SAMF as an example, we observe that it is very robust against signal mismatch. It can provide a PD as high as 0.9 if the SNR is sufficiently high; even the whitened actual signal is orthogonal to the whitened nominal signal subspace, i.e., the case of $\cos^2\phi = 0$. In contrast, for a selective detector, such as the SABORT, it does not achieve a PD higher than 0.5 when $\cos^2\phi < 0.55$, regardless of how high the SNR is. For the selected parameters, the SAMF and SABORT exhibit comparable PDs for matched signals, as shown in Figure 3. Thus, if a selective detector is required, the SABORT is a better candidate than the SAMF.

Prior to closing this section, we provide the following remarks. First, from (53), (54), and (55)–(61), it is known that all adaptive detectors exploited above have the CFAR property with respect to the noise covariance matrix $\boldsymbol{R}$. Second, among the above eight adaptive detectors, only the ASD possesses the CFAR property in PHE, although the ASD has lower PD than some other detectors in HE. Third, the DN-SAMF can behave quite well when the system dimension N is sufficiently large, as demonstrated in [127].

4.3 Generations of point-target-based adaptive detectors

The detection problem in (1) has been generalized in many aspects. Distributed target detection (without interference) and signal detection in interference are two import generations, which are discussed in the following.

4.3.1 *Adaptive detectors for distributed targets*

A large target typically occupies multiple range bins, especially for high-resolution radar systems [361]. In such cases, the detection problem in (1) should be modified as follows:

$$\begin{cases} \mathrm{H}_0 : \boldsymbol{X} = \boldsymbol{N},\ \boldsymbol{x}_{\mathrm{e},l} = \boldsymbol{n}_{\mathrm{e},l},\ l = 1, 2, \ldots, L, \\ \mathrm{H}_1 : \boldsymbol{X} = \boldsymbol{s}\boldsymbol{a}^{\mathrm{H}} + \boldsymbol{N},\ \boldsymbol{x}_{\mathrm{e},l} = \boldsymbol{n}_{\mathrm{e},l},\ l = 1, 2, \ldots, L, \end{cases} \tag{67}$$

where $\boldsymbol{X}$ is an $N \times K$ matrix denoting the test data, with N being the number of system channels and K being the number of range bins occupied by the distributed target, $\boldsymbol{N}$ is the noise in the test data, $\boldsymbol{s}$ is the signal steering vector, $\boldsymbol{a}$ is the coordinate vector of the signal, $\boldsymbol{x}_{\mathrm{e},l}$ is the lth training data vector, and $\boldsymbol{n}_{\mathrm{e},l}$ is the noise in $\boldsymbol{x}_{\mathrm{e},l}$. The columns of $\boldsymbol{N}$ are IID with noise covariance matrix $\boldsymbol{R}_t$. The noise covariance matrix of $\boldsymbol{n}_{\mathrm{e},l}$ is denoted as $\boldsymbol{R}$. Then, in HE, $\boldsymbol{R}_t = \boldsymbol{R}$, while in PHE $\boldsymbol{R}_t = \sigma^2\boldsymbol{R}$, with σ^2 being the unknown power mismatch between the test data and training data.

For the detection problem in (67), the GLRT and its two-step variation for the HE and PHE were proposed in [54]. Specifically, for the HE, the GLRT and 2S-GLRT are given as follows:

$$t_{\mathrm{GKGLRT}} = \frac{\tilde{\boldsymbol{s}}^{\mathrm{H}}\tilde{\boldsymbol{X}}(\boldsymbol{I}_K + \tilde{\boldsymbol{X}}^{\mathrm{H}}\tilde{\boldsymbol{X}})^{-1}\tilde{\boldsymbol{X}}^{\mathrm{H}}\tilde{\boldsymbol{s}}}{\tilde{\boldsymbol{s}}^{\mathrm{H}}\tilde{\boldsymbol{s}} - \tilde{\boldsymbol{s}}^{\mathrm{H}}\tilde{\boldsymbol{X}}(\boldsymbol{I}_K + \tilde{\boldsymbol{X}}^{\mathrm{H}}\tilde{\boldsymbol{X}})^{-1}\tilde{\boldsymbol{X}}^{\mathrm{H}}\tilde{\boldsymbol{s}}} \tag{68}$$

and

$$t_{\mathrm{GAMF}} = \frac{\tilde{\boldsymbol{s}}^{\mathrm{H}}\tilde{\boldsymbol{X}}\tilde{\boldsymbol{X}}^{\mathrm{H}}\tilde{\boldsymbol{s}}}{\tilde{\boldsymbol{s}}^{\mathrm{H}}\tilde{\boldsymbol{s}}}, \tag{69}$$

respectively. In addition, for the PHE, the GLRT, and 2S-GLRT are given as

$$t_{\mathrm{GLRT\text{-}PHE}} = \frac{(\hat{\sigma}_0^2)^{\frac{NK}{L+K}}|\boldsymbol{I}_K + \frac{1}{\hat{\sigma}_0^2}\tilde{\boldsymbol{X}}^{\mathrm{H}}\tilde{\boldsymbol{X}}|}{(\hat{\sigma}_1^2)^{\frac{NK}{L+K}}|\boldsymbol{I}_K + \frac{1}{\hat{\sigma}_1^2}\tilde{\boldsymbol{X}}^{\mathrm{H}}\boldsymbol{P}_{\tilde{\boldsymbol{s}}}^{\perp}\tilde{\boldsymbol{X}}|} \tag{70}$$

and

$$t_{\mathrm{GASD}} = \frac{\tilde{\boldsymbol{s}}^{\mathrm{H}}\tilde{\boldsymbol{X}}\tilde{\boldsymbol{X}}^{\mathrm{H}}\tilde{\boldsymbol{s}}}{\tilde{\boldsymbol{s}}^{\mathrm{H}}\tilde{\boldsymbol{s}}\ \mathrm{tr}(\tilde{\boldsymbol{X}}^{\mathrm{H}}\tilde{\boldsymbol{X}})}, \tag{71}$$

respectively. In (70), $\hat{\sigma}_0^2$ and $\hat{\sigma}_1^2$ are the sole solutions of

$$\sum_{k_0=1}^{r_0}\frac{\lambda_{k_0}}{\lambda_{k_0}+\sigma^2} = \frac{NK}{L+K} \tag{72}$$

and

$$\sum_{k_1=1}^{r_1}\frac{\xi_{k_1}}{\xi_{k_1}+\sigma^2} = \frac{NK}{L+K}, \tag{73}$$

respectively, where $r_0 = \min(N, K)$, $r_1 = \min(N-1, K)$, λ_{k_0} is the k_0th non-zero eigenvalue of $\tilde{\boldsymbol{X}}^{\mathrm{H}}\tilde{\boldsymbol{X}}$, $k_0 = 1, 2, \ldots, r_0$, and ξ_{k_1} is the k_1th non-zero eigenvalue of $\tilde{\boldsymbol{X}}^{\mathrm{H}}\boldsymbol{P}_{\tilde{\boldsymbol{s}}}^{\perp}\tilde{\boldsymbol{X}}$, $k_1 = 1, 2, \ldots, r_1$.

The detectors in (69) and (71) are referred to as generalized AMF (GAMF) and generalized adaptive subspace detector (GASD), respectively, in [54]. For convenience, the detector in (68) is denoted by GKGLRT in this study.

In addition, for the detection problem in (67) in HE, the Wald test is the same as the GAMF, while the Rao test was proposed in [90], which is described as follows[20)]:

$$t_{\text{Rao-HE}} = \frac{\boldsymbol{s}^{\mathrm{H}}(\boldsymbol{S}+\boldsymbol{X}\boldsymbol{X}^{\mathrm{H}})^{-1}\boldsymbol{X}\boldsymbol{X}^{\mathrm{H}}(\boldsymbol{S}+\boldsymbol{X}\boldsymbol{X}^{\mathrm{H}})^{-1}\boldsymbol{s}}{\boldsymbol{s}^{\mathrm{H}}(\boldsymbol{S}+\boldsymbol{X}\boldsymbol{X}^{\mathrm{H}})^{-1}\boldsymbol{s}}. \tag{74}$$

20) Using the matrix inversion lemma, it is easy to demonstrate that Eq. (74) can be recast as $t_{\text{Rao-HE}} = \frac{\tilde{\boldsymbol{s}}^{\mathrm{H}}\tilde{\boldsymbol{X}}(\boldsymbol{I}_K+\tilde{\boldsymbol{X}}^{\mathrm{H}}\boldsymbol{P}_{\tilde{\boldsymbol{s}}}^{\perp}\tilde{\boldsymbol{X}})^{-1}(\boldsymbol{I}_K+\tilde{\boldsymbol{X}}^{\mathrm{H}}\tilde{\boldsymbol{X}})^{-1}\tilde{\boldsymbol{X}}^{\mathrm{H}}\tilde{\boldsymbol{s}}}{\tilde{\boldsymbol{s}}^{\mathrm{H}}\tilde{\boldsymbol{s}}}$.

For the detection problem in (67) in PHE, the Rao and Wald tests were proposed in [91] and are given as follows:

$$t_{\text{Rao-PHE}} = \frac{\boldsymbol{s}^{\text{H}}\hat{\boldsymbol{R}}_0^{-1}\boldsymbol{X}\boldsymbol{X}^{\text{H}}\hat{\boldsymbol{R}}_0^{-1}\boldsymbol{s}}{\hat{\sigma}_0^2\ \boldsymbol{s}^{\text{H}}\hat{\boldsymbol{R}}_0^{-1}\boldsymbol{s}} \tag{75}$$

and

$$t_{\text{Wald-PHE}} = \frac{\boldsymbol{s}^{\text{H}}\hat{\boldsymbol{R}}_1^{-1}\boldsymbol{X}\boldsymbol{X}^{\text{H}}\hat{\boldsymbol{R}}_1^{-1}\boldsymbol{s}}{\hat{\sigma}_1^2\ \boldsymbol{s}^{\text{H}}\hat{\boldsymbol{R}}_1^{-1}\boldsymbol{s}}, \tag{76}$$

respectively, where $\hat{\sigma}_0^2$ and $\hat{\sigma}_1^2$ are the sole solutions of (72) and (73), respectively,

$$\hat{\boldsymbol{R}}_0 = \frac{1}{L+K}\left(\boldsymbol{S} + \frac{1}{\hat{\sigma}^2}\boldsymbol{X}\boldsymbol{X}^{\text{H}}\right) \tag{77}$$

and

$$\hat{\boldsymbol{R}}_1 = \frac{1}{L+K}\boldsymbol{S}^{\frac{1}{2}}\left(\boldsymbol{I}_N + \frac{1}{\hat{\sigma}_1^2}\boldsymbol{P}_{\tilde{\boldsymbol{s}}}^{\perp}\tilde{\boldsymbol{X}}\tilde{\boldsymbol{X}}^{\text{H}}\boldsymbol{P}_{\tilde{\boldsymbol{s}}}^{\perp}\right)\boldsymbol{S}^{\frac{1}{2}}. \tag{78}$$

Differing from the point target case, it is more difficult to derive the statistical performance of distributed-target-based detectors. Currently, only the statistical performance of the GKGLRT and GAMF is known. The statistical distribution of the GKGLRT was first proposed in [92] for the case of no signal mismatch, and then it was generalized to the case of signal mismatch in [104]. In addition, the statistical distribution of the GAMF in the absence of signal mismatch was given in [103]. Specifically, under hypothesis H_1, the conditional distribution of the GKGLRT in (68) is given as follows:

$$t_{\text{GKGLRT}}|\text{H}_1 \sim \mathcal{CF}_{K,L-N+1}\left(\rho_{\text{dstr}}\cos^2\phi_{\text{rk1}}\beta_{\text{GKGLRT}}\right), \tag{79}$$

where

$$\rho_{\text{dstr}} = \boldsymbol{a}^{\text{H}}\boldsymbol{a}\cdot\boldsymbol{s}_0^{\text{H}}\boldsymbol{R}^{-1}\boldsymbol{s}_0 \tag{80}$$

can be taken as the output SNR, where $\boldsymbol{s}_0$ is the actual signal steering vector,

$$\cos^2\phi_{\text{rk1}} = \frac{|\boldsymbol{s}_0^{\text{H}}\boldsymbol{R}^{-1}\boldsymbol{s}|^2}{\boldsymbol{s}_0^{\text{H}}\boldsymbol{R}^{-1}\boldsymbol{s}_0\ \boldsymbol{s}^{\text{H}}\boldsymbol{R}^{-1}\boldsymbol{s}} \tag{81}$$

is generalized cosine-squared between the actual signal $\boldsymbol{s}_0$ and nominal signal $\boldsymbol{s}$ in the whitened space, and β_{GKGLRT} is a loss factor for the GKGLRT taking the following statistical distribution:

$$\beta_{\text{GKGLRT}}|\text{H}_1 \sim \mathcal{CB}_{L+K-N+1,N-1}(\rho\sin^2\phi_{\text{rk1}}), \tag{82}$$

with $\sin^2\phi_{\text{rk1}} = 1-\cos^2\phi_{\text{rk1}}$. Under hypothesis H_0, Eqs. (79) and (82) become

$$t_{\text{GKGLRT}}|\text{H}_0 \sim \mathcal{CF}_{K,L-N+1} \tag{83}$$

and

$$\beta_{\text{GKGLRT}}|\text{H}_0 \sim \mathcal{CB}_{L+K-N+1,N-1}, \tag{84}$$

respectively. In addition, under hypothesis H_1, the conditional distribution of the GAMF in (69) for the case of no signal mismatch is given as follows:

$$\beta_{\text{GAMF}}\ t_{\text{GAMF}}|\text{H}_1 \sim \mathcal{CF}_{K,L-N+1}(\beta_{\text{GAMF}}\rho_{\text{dstr}}), \tag{85}$$

where β_{GAMF} is a loss factor for the GAMF, with the following statistical distribution:

$$\beta_{\text{GAMF}}|[\text{H}_1 \text{ and } \text{H}_0] \sim \mathcal{CB}_{L-N+2,N-1}. \tag{86}$$

Under hypothesis H_0, Eq. (85) becomes

$$\beta_{\text{GAMF}}\ t_{\text{GAMF}}|\text{H}_0 \sim \mathcal{CF}_{K,L-N+1}. \tag{87}$$

There are two further generalizations of the detection problem in (67). One is that the signal steering vector $\boldsymbol{s}$ lies in a given subspace spanned by an $N \times p$ full-column matrix $\boldsymbol{H}$; thus, $\boldsymbol{s}$ can be expressed as $\boldsymbol{s} = \boldsymbol{H}\boldsymbol{\theta}$, where $\boldsymbol{\theta}$ represents the $p \times 1$ unknown coordinates. It follows that Eq. (67) becomes

$$\begin{cases} \mathrm{H}_0 : \boldsymbol{X} = \boldsymbol{N},\ \boldsymbol{x}_{\mathrm{e},l} = \boldsymbol{n}_{\mathrm{e},l},\ l = 1, 2, \ldots, L, \\ \mathrm{H}_1 : \boldsymbol{X} = \boldsymbol{H}\boldsymbol{\theta}\boldsymbol{a}^{\mathrm{H}} + \boldsymbol{N},\ \boldsymbol{x}_{\mathrm{e},l} = \boldsymbol{n}_{\mathrm{e},l},\ l = 1, 2, \ldots, L. \end{cases} \tag{88}$$

The GLRT and 2S-GLRT in HE were proposed in [97] and are described as follows:

$$t_{\mathrm{GLRDD}} = \lambda_{\max}\left[\tilde{\boldsymbol{X}}^{\mathrm{H}}\boldsymbol{P}_{\tilde{\boldsymbol{H}}}\tilde{\boldsymbol{X}}(\boldsymbol{I}_K + \tilde{\boldsymbol{X}}^{\mathrm{H}}\tilde{\boldsymbol{X}})^{-1}\right] \tag{89}$$

and

$$t_{\mathrm{AMDD}} = \lambda_{\max}\left(\tilde{\boldsymbol{X}}^{\mathrm{H}}\boldsymbol{P}_{\tilde{\boldsymbol{H}}}\tilde{\boldsymbol{X}}\right), \tag{90}$$

respectively, where $\lambda_{\max}(\cdot)$ denotes the maximum eigenvalue of the matrix argument. It was demonstrated in [98] that there is no reasonable Rao test for the detection problem in (88), the 2S-Wald test is the same as the detector in (90), and the Wald test is given as follows:

$$t_{\mathrm{SNRDD}} = \frac{\boldsymbol{\theta}_{\max}^{\mathrm{H}}\tilde{\boldsymbol{H}}^{\mathrm{H}}\tilde{\boldsymbol{X}}\tilde{\boldsymbol{X}}^{\mathrm{H}}\tilde{\boldsymbol{H}}\boldsymbol{\theta}_{\max}}{\boldsymbol{\theta}_{\max}^{\mathrm{H}}\tilde{\boldsymbol{H}}^{\mathrm{H}}\tilde{\boldsymbol{H}}\boldsymbol{\theta}_{\max}}, \tag{91}$$

where $\boldsymbol{\theta}_{\max}$ is a principal eigenvector (i.e., eigenvector corresponding to the maximum eigenvalue) of the matrix $(\tilde{\boldsymbol{H}}^{\mathrm{H}}\tilde{\boldsymbol{H}})^{-1}\tilde{\boldsymbol{H}}^{\mathrm{H}}\tilde{\boldsymbol{X}}(\boldsymbol{I}_K + \tilde{\boldsymbol{X}}^{\mathrm{H}}\tilde{\boldsymbol{X}})^{-1}\tilde{\boldsymbol{X}}^{\mathrm{H}}\tilde{\boldsymbol{H}}$. The detectors in (89), (90), and (91) are referred to as GLR-based direction detector (GLRDD), adaptive matched direction detector (AMDD), SNR-based direction detector (SNRDD), respectively in [98]. The 2S-GLRT for the detection problem in (88) in PHE was proposed in [96], given by[21)]

$$t_{\mathrm{GADD}} = \frac{\lambda_{\max}(\tilde{\boldsymbol{X}}^{\mathrm{H}}\boldsymbol{P}_{\tilde{\boldsymbol{H}}}\tilde{\boldsymbol{X}})}{\mathrm{tr}(\tilde{\boldsymbol{X}}^{\mathrm{H}}\tilde{\boldsymbol{X}})}, \tag{92}$$

which was denoted by GADD therein.

From (89) to (92), it follows that the detectors select a direction among the subspace spanned by the columns of $\boldsymbol{H}$. In other words, the detection problem in (88) is tantamount to finding a direction with the largest possibility in a given subspace; thus, it is referred to as direction detection in [96].

The direction detection problem can be further generalized when both the column and row components of the signal to be detected lie in given subspaces. Here, the test data under hypothesis H_1 becomes $\boldsymbol{X} = \boldsymbol{H}\boldsymbol{\theta}\boldsymbol{\alpha}^{\mathrm{H}}\boldsymbol{C} + \boldsymbol{N}$, where $\boldsymbol{C}$ is a given $M \times K$ full-row-rank matrix and $\boldsymbol{\alpha}$ is an $M \times 1$ vector. This type of problem is referred to as generalized direction detection in [99], where the GLRT and 2S-GLRT in HE were proposed. In addition, the Wald test in HE was given in [362], and the 2S-GLRT in PHE was derived in [100].

Differing from (88), another generalization of (67) is the case where each column of the test data $\boldsymbol{X}$ has a slightly different steering vector in the sense that these steering vectors differ but all come from the same subspace. Thus, the detection model in (67) can be modified as follows:

$$\begin{cases} \mathrm{H}_0 : \boldsymbol{X} = \boldsymbol{N},\ \boldsymbol{x}_{\mathrm{e},l} = \boldsymbol{n}_{\mathrm{e},l},\ l = 1, 2, \ldots, L, \\ \mathrm{H}_1 : \boldsymbol{X} = \boldsymbol{H}\boldsymbol{\Phi} + \boldsymbol{N},\ \boldsymbol{x}_{\mathrm{e},l} = \boldsymbol{n}_{\mathrm{e},l},\ l = 1, 2, \ldots, L, \end{cases} \tag{93}$$

where $\boldsymbol{H}$ is an $N \times p$ full-column-rank matrix, and $\boldsymbol{\Phi}$ is a $p \times K$ matrix representing the coordinates. The GLRT in HE was proposed in Kelly and Forsythes classic report [101], while the Rao and Wald tests in HE can be obtained according to the results presented in [83]. Specifically, the GLRT, Rao test, and Wald test are given as follows:

$$t_{\mathrm{GLRT}} = \frac{\left|\boldsymbol{I}_K + \boldsymbol{X}^{\mathrm{H}}\boldsymbol{S}^{-1}\boldsymbol{X}\right|}{\left|\boldsymbol{I}_K + \boldsymbol{X}^{\mathrm{H}}\boldsymbol{S}^{-1}\boldsymbol{X} - \boldsymbol{X}^{\mathrm{H}}\boldsymbol{S}^{-1}\boldsymbol{H}(\boldsymbol{H}^{\mathrm{H}}\boldsymbol{S}^{-1}\boldsymbol{H})^{-1}\boldsymbol{H}^{\mathrm{H}}\boldsymbol{S}^{-1}\boldsymbol{X}\right|}, \tag{94}$$

21) Note that the GADD in (92) can be also derived according to the 2S-Wald test.

$$t_{\mathrm{Rao}}=\mathrm{tr}\left\{\boldsymbol{X}^{\mathrm{H}}(\boldsymbol{S}+\boldsymbol{X}\boldsymbol{X}^{\mathrm{H}})^{-1}\boldsymbol{H}\left[\boldsymbol{H}^{\mathrm{H}}(\boldsymbol{S}+\boldsymbol{X}\boldsymbol{X}^{\mathrm{H}})^{-1}\boldsymbol{H}\right]^{-1}\boldsymbol{H}^{\mathrm{H}}(\boldsymbol{S}+\boldsymbol{X}\boldsymbol{X}^{\mathrm{H}})^{-1}\boldsymbol{X}\right\},\tag{95}$$

and

$$t_{\mathrm{Wald}}=\mathrm{tr}\left[\boldsymbol{X}^{\mathrm{H}}\boldsymbol{S}^{-1}\boldsymbol{H}(\boldsymbol{H}^{\mathrm{H}}\boldsymbol{S}^{-1}\boldsymbol{H})^{-1}\boldsymbol{H}^{\mathrm{H}}\boldsymbol{S}^{-1}\boldsymbol{X}\right],\tag{96}$$

respectively.

Note that when $p=N$ in the detection problem in (93), the signal steering vectors lie in the entire observation space. Equivalently, the steering vectors are completely unknown. The corresponding GLRT, 2S-GLRT, and a modified 2S-GLRT (M2S-GLRT) in HE were proposed in [93]. It was also demonstrated in [94] that the M2S-GLRT is essentially the corresponding Rao test, and the 2S-GLRT can also be derived according to the Wald test. In addition, in [83,102], the test data in (93) were generalized to the case $\boldsymbol{X}=\boldsymbol{H}\boldsymbol{\Phi}\boldsymbol{C}+\boldsymbol{N}$, where $\boldsymbol{\Phi}$ is a $p\times M$ unknown matrix, and $\boldsymbol{C}$ is an $M\times K$ known full-row-rank matrix. The corresponding signal model was called the DOS model [101][22)] in [83, 102], where many adaptive detectors were proposed.

4.3.2 *Adaptive detectors in the presence of interference*

Most of the above detectors were designed without considering the possibility of interference, which typically exists in practical applications. Interference can be caused intentionally (jamming due to the ECM) or unintentionally (communication signals or radar signals transmitted by other radar systems). In this case, the detection problem in (1) can be modified as follows:

$$\begin{cases}\mathrm{H}_0:\boldsymbol{x}=\boldsymbol{n},\ \boldsymbol{x}_{\mathrm{e},l}=\boldsymbol{n}_{\mathrm{e},l},\ l=1,2,\ldots,L,\\ \mathrm{H}_1:\boldsymbol{x}=\boldsymbol{s}+\boldsymbol{j}+\boldsymbol{n},\ \boldsymbol{x}_{\mathrm{e},l}=\boldsymbol{n}_{\mathrm{e},l},\ l=1,2,\ldots,L,\end{cases}\tag{97}$$

where $\boldsymbol{j}$ represents the interference. Generally, there are two primary types of interference, i.e., coherent interference and noise interference. The former works like a real target that typically lies in a certain spatially direction and/or occupies a Doppler bin. Thus, coherent interference can be modeled by a subspace model. The latter works like thermal noise or clutter. As a result, the noise interference changes the noise covariance matrix of the test data.

Based on the above analysis, coherent interference can be modeled as $\boldsymbol{j}=\boldsymbol{J}\boldsymbol{\phi}$, where the $N\times q$ full-column-rank matrix spans the subspace where the interference lies, and the $q\times 1$ vector $\boldsymbol{\phi}$ denotes the unknown coordinates. For coherent interference and subspace signals (i.e., the signal in (97) can be expressed as $\boldsymbol{s}=\boldsymbol{H}\boldsymbol{\theta}$), the GLRT and 2S-GLRT in HE and PHE for the detection problem in (97) were proposed in [155], and the GLRT and 2S-GLRT in PHE coincide with each other. Specifically, the GLRT and 2S-GLRT in HE are given as follows:

$$t_{\text{GLRT-HE-I}}=\frac{\tilde{\boldsymbol{x}}^{\mathrm{H}}\boldsymbol{P}_{\boldsymbol{P}_{\tilde{\boldsymbol{J}}}^{\perp}\tilde{\boldsymbol{H}}}\tilde{\boldsymbol{x}}}{1+\tilde{\boldsymbol{x}}^{\mathrm{H}}\boldsymbol{P}_{\tilde{\boldsymbol{J}}}^{\perp}\tilde{\boldsymbol{x}}-\tilde{\boldsymbol{x}}^{\mathrm{H}}\boldsymbol{P}_{\boldsymbol{P}_{\tilde{\boldsymbol{J}}}^{\perp}\tilde{\boldsymbol{H}}}\tilde{\boldsymbol{x}}}\tag{98}$$

and

$$t_{\text{2S-GLRT-HE-I}}=\tilde{\boldsymbol{x}}^{\mathrm{H}}\boldsymbol{P}_{\boldsymbol{P}_{\tilde{\boldsymbol{J}}}^{\perp}\tilde{\boldsymbol{H}}}\tilde{\boldsymbol{x}},\tag{99}$$

respectively, while the GLRT in PHE is given as

$$t_{\text{GLRT-PHE-I}}=\frac{\tilde{\boldsymbol{x}}^{\mathrm{H}}\boldsymbol{P}_{\boldsymbol{P}_{\tilde{\boldsymbol{J}}}^{\perp}\tilde{\boldsymbol{H}}}\tilde{\boldsymbol{x}}}{\tilde{\boldsymbol{x}}^{\mathrm{H}}\boldsymbol{P}_{\tilde{\boldsymbol{J}}}^{\perp}\tilde{\boldsymbol{x}}},\tag{100}$$

where $\boldsymbol{P}_{\boldsymbol{P}_{\tilde{\boldsymbol{J}}}^{\perp}\tilde{\boldsymbol{H}}}=\boldsymbol{P}_{\tilde{\boldsymbol{J}}}^{\perp}\tilde{\boldsymbol{H}}(\tilde{\boldsymbol{H}}^{\mathrm{H}}\boldsymbol{P}_{\tilde{\boldsymbol{J}}}^{\perp}\tilde{\boldsymbol{H}})^{-1}\tilde{\boldsymbol{H}}^{\mathrm{H}}\boldsymbol{P}_{\tilde{\boldsymbol{J}}}^{\perp}$, $\boldsymbol{P}_{\tilde{\boldsymbol{J}}}^{\perp}=\boldsymbol{I}_N-\boldsymbol{P}_{\tilde{\boldsymbol{J}}}$, and $\boldsymbol{P}_{\tilde{\boldsymbol{J}}}=\tilde{\boldsymbol{J}}(\tilde{\boldsymbol{J}}^{\mathrm{H}}\tilde{\boldsymbol{J}})^{-1}\tilde{\boldsymbol{J}}^{\mathrm{H}}$. For convenience, the detectors in (98)–(100) are referred to as the GLRT in HE with interference rejection (GLRT-HE-I), 2S-GLRT in HE with interference rejection (2S-GLRT-HE-I), and GLRT in PHE with interference rejection (GLRT-PHE-I), respectively.

22) The DOS signal model was first introduced in [101]. However, in [101], it was assumed that no training data were available. Instead, it was assumed that $K\geqslant M+N$, and this constraint ensures the existence of a set of virtual training data generated by a certain unitary matrix to the test data.

For coherent interference, the Rao and 2S-Rao tests were proposed in [157], and the Wald and 2S-Wald tests were derived in [158]. Specifically, in HE the Rao test and 2S-Rao test are given as follows:

$$t_{\text{Rao-HE-I}} = \frac{\tilde{\boldsymbol{x}}^{\text{H}}\boldsymbol{P}_{\tilde{\boldsymbol{J}}}^{\perp}\boldsymbol{P}_{\tilde{\boldsymbol{H}}}\boldsymbol{P}_{\tilde{\boldsymbol{J}}}^{\perp}\tilde{\boldsymbol{x}}}{(1+\tilde{\boldsymbol{x}}^{\text{H}}\boldsymbol{P}_{\tilde{\boldsymbol{J}}}^{\perp}\tilde{\boldsymbol{x}})(1+\tilde{\boldsymbol{x}}^{\text{H}}\boldsymbol{P}_{\tilde{\boldsymbol{J}}}^{\perp}\boldsymbol{P}_{\tilde{\boldsymbol{H}}}^{\perp}\boldsymbol{P}_{\tilde{\boldsymbol{J}}}^{\perp}\tilde{\boldsymbol{x}})} \tag{101}$$

and

$$t_{\text{2S-Rao-HE-I}} = \tilde{\boldsymbol{x}}^{\text{H}}\boldsymbol{P}_{\tilde{\boldsymbol{J}}}^{\perp}\boldsymbol{P}_{\tilde{\boldsymbol{H}}}\boldsymbol{P}_{\tilde{\boldsymbol{J}}}^{\perp}\tilde{\boldsymbol{x}}, \tag{102}$$

respectively, and in PHE, the Rao test is the same as the 2S-Rao test, given as follows:

$$t_{\text{Rao-PHE-I}} = \frac{\tilde{\boldsymbol{x}}^{\text{H}}\boldsymbol{P}_{\tilde{\boldsymbol{J}}}^{\perp}\boldsymbol{P}_{\tilde{\boldsymbol{H}}}\boldsymbol{P}_{\tilde{\boldsymbol{J}}}^{\perp}\tilde{\boldsymbol{x}}}{\tilde{\boldsymbol{x}}^{\text{H}}\boldsymbol{P}_{\tilde{\boldsymbol{J}}}^{\perp}\tilde{\boldsymbol{x}}}. \tag{103}$$

In addition, the Wald test is the same as the 2S-Wald test in both HE and PHE, given as follows:

$$t_{\text{Wald-HE-I}} = \tilde{\boldsymbol{x}}^{\text{H}}\boldsymbol{P}_{\tilde{\boldsymbol{H}}|\tilde{\boldsymbol{J}}}^{\text{H}}\boldsymbol{P}_{\tilde{\boldsymbol{H}}|\tilde{\boldsymbol{J}}}\tilde{\boldsymbol{x}} \tag{104}$$

and

$$t_{\text{Wald-PHE-I}} = \frac{\tilde{\boldsymbol{x}}^{\text{H}}\boldsymbol{P}_{\tilde{\boldsymbol{H}}|\tilde{\boldsymbol{J}}}^{\text{H}}\boldsymbol{P}_{\tilde{\boldsymbol{H}}|\tilde{\boldsymbol{J}}}\tilde{\boldsymbol{x}}}{\tilde{\boldsymbol{x}}^{\text{H}}\boldsymbol{P}_{\tilde{\mathbf{B}}}^{\perp}\tilde{\boldsymbol{x}}}, \tag{105}$$

respectively, where $\boldsymbol{P}_{\tilde{\boldsymbol{H}}|\tilde{\boldsymbol{J}}} = \tilde{\boldsymbol{H}}(\tilde{\mathbf{H}}^{\text{H}}\boldsymbol{P}_{\tilde{\boldsymbol{J}}}^{\perp}\tilde{\boldsymbol{H}})^{-1}\tilde{\boldsymbol{H}}^{\text{H}}\boldsymbol{P}_{\tilde{\mathbf{J}}}^{\perp}$ is the oblique projection matrix onto the subspace spanned by $\tilde{\boldsymbol{H}}$ along the subspace spanned by $\tilde{\boldsymbol{J}}$. A detailed analysis and comparison of the above detectors can be found in [158].

Currently, only the GLRT-HE-I, 2S-GLRT-HE-I, and GLRT-PHE-I have known statistical properties [161]. Specifically, the conditional distribution of the GLRT-HE-I in (98) with a fixed β_{I} under hypothesis H_1 is given as follows:

$$t_{\text{GLRT-HE-I}}|[\beta_{\text{I}}, \text{H}_1] \sim \mathcal{CF}_{p,L-N+q+1}(\rho_{\text{eff}}\beta_{\text{I}}), \tag{106}$$

where

$$\rho_{\text{eff}} = \bar{\boldsymbol{s}}_0^{\text{H}}\boldsymbol{P}_{\tilde{\boldsymbol{J}}}^{\perp}\boldsymbol{P}_{\boldsymbol{P}_{\tilde{\boldsymbol{J}}}^{\perp}\tilde{\boldsymbol{H}}}\boldsymbol{P}_{\tilde{\boldsymbol{J}}}^{\perp}\bar{\boldsymbol{s}}_0 \tag{107}$$

is defined as the effective SNR (eSNR), and β_{I} is loss factor defined as follows:

$$\beta_{\text{I}} = \frac{1}{1+\tilde{\boldsymbol{x}}^{\text{H}}\boldsymbol{P}_{\tilde{\boldsymbol{J}}}^{\perp}\tilde{\boldsymbol{x}} - \tilde{\boldsymbol{x}}^{\text{H}}\boldsymbol{P}_{\boldsymbol{P}_{\tilde{\boldsymbol{J}}}^{\perp}\tilde{\boldsymbol{H}}}\tilde{\boldsymbol{x}}}. \tag{108}$$

The statistical distribution of β_{I} under hypothesis H_1 is given as follows:

$$\beta_{\text{I}}|\text{H}_1 \sim \mathcal{CB}_{L-N+p+q+1,N-p-q}(\delta_{\text{I}}^2), \tag{109}$$

where

$$\delta_{\text{I}}^2 = \bar{\boldsymbol{s}}_0^{\text{H}}\boldsymbol{P}_{\tilde{\boldsymbol{J}}}^{\perp}\boldsymbol{P}_{\boldsymbol{P}_{\tilde{\boldsymbol{J}}}^{\perp}\tilde{\boldsymbol{H}}}^{\perp}\boldsymbol{P}_{\tilde{\boldsymbol{J}}}^{\perp}\bar{\boldsymbol{s}}_0, \tag{110}$$

with $\boldsymbol{P}_{\boldsymbol{P}_{\tilde{\boldsymbol{J}}}^{\perp}\tilde{\boldsymbol{H}}}^{\perp} = \boldsymbol{I}_N - \boldsymbol{P}_{\boldsymbol{P}_{\tilde{\boldsymbol{J}}}^{\perp}\tilde{\boldsymbol{H}}}$. Under hypothesis H_0, Eqs. (106) and (109) can be reduced as follows:

$$t_{\text{GLRT–HE–I}}|[\beta_{\text{I}}, \text{H}_0] \sim \mathcal{CF}_{p,L-N+q+1} \tag{111}$$

and

$$\beta_{\text{I}}|\text{H}_0 \sim \mathcal{CB}_{L-N+p+q+1,N-p-q}, \tag{112}$$

respectively.

More geometric interpretation about the eSNR in (107) can be found in [161].

In addition, the following equations can be verified easily:

$$t_{\text{2S-GLRT-HE-I}} = \frac{t_{\text{GLRT-HE-I}}}{\beta_{\text{I}}}, \tag{113}$$

$$t_{\text{GLRT-PHE-I}} = \frac{t_{\text{GLRT-HE-I}}}{1-\beta_{\text{I}}}. \tag{114}$$

Using (113) and (114), as well (106), (109), (111), and (112), we can obtain the analytical expressions for the PDs and PFAs of the 2S-GLRT-HE-I and GLRT-PHE-I.

In [180], it was demonstrated that the GLRT for rank-one signals is equivalent to the ACE for completely unknown noise interference. The corresponding Rao test was derived in [127], i.e., the DN-AMF, which was originally adopted for mismatched signal detection. The results in [127, 180] were generalized in [181] when additional coherent interference existed. In [182], the noise interference was assumed to be orthogonal to the target signal in the whitened space, and it was demonstrated that the GLRT coincides with the KGLRT. In addition, in [183], it was shown that the corresponding Rao and Wald tests are the same as the DMRao and AMF, respectively. The results in [182,183] were generalized in [184] for the case of subspace signals. Note that other generalizations for noise interference can be found in [185, 187–191].

5 Conclusion

In this study, we have investigated detector design criteria for adaptive detection, analyzed the relationship between adaptive detection and the filtering-then-CFAR detection approach, as well as the relationship between adaptive detectors and adaptive filters, provided a comprehensive literature review, and summarized and compared typical adaptive detectors. Adaptive detection uses test and training data jointly to form an adaptive detector. Adaptive detection has many distinct features compared to the filtering-then-CFAR detection approach (adaptive or non-adaptive). Specifically, adaptive detection achieves the function of filtering and CFAR processing simultaneously; thus, it involves a simple detection procedure. In addition, it can provide better detection performance compared to the filtering-then-CFAR detection approach.

We hope that this study will stimulate new studies into adaptive detection. In the following, we list potential future research tracks. (1) The statistical performance of many adaptive detectors are unknown, such as the Rao and Wald tests in subspace interference [157,158] and the 2S-GLRT in HE in the presence of signal mismatch [54]. Obtaining such results is expected to reveal how signal mismatch and/or interference affect detection performance. (2) Multichannel signal detection has been combined with compressive sensing or sparse representation, which is an emerging signal processing technique to acquire and reconstruct a compressible signal efficiently using much fewer samples than conventional methods. Several compressive sensing-based detectors have been proposed, e.g., [363–369] and the references therein. However, most proposed detectors based on compressive sensing are for known noise or white Gaussian noise with unknown variance. A significantly challenging task is handling colored noise with an unknown covariance matrix. (3) Most existing adaptive detectors were designed under specific assumptions about the noise, either homogeneous, partially homogeneous, compound-Gaussian, or structure non-homogeneity. However, the actual noise may differ from the assumed noise due to both system and environment uncertainties. Consequently, the designed detectors may suffer from significant performance loss. Therefore, it is necessary to develop fully adaptive detection approaches that can adjust the detection strategy to accommodate changing environments. Recently, preliminary analysis of the classification of the noise covariance structure in Gaussian background was given in [292, 357, 370, 371]. (4) Recently, preliminary machine learning results were utilized in adaptive detection [372–374]; however, these studies did not fully address the fundamental problem regarding how and why detection performance can be improved using machine learning technologies.

In this study, we have primarily focused on the Gaussian background. In practice, the environment may exhibit non-Gaussian characteristics [61, 62, 375–381]. Interested readers can refer to a recent overview paper [7] on compound-Gaussian clutter, where the relevant properties of clutter are assumed to be known in advance.

Acknowledgements This work was supported in part by National Natural Science Foundation of China (Grant Nos. 62071482, 61871469), National Natural Science Foundation of China and Civil Aviation Administration of China (Grant No. U1733116), Youth Innovation Promotion Association CAS (Grant No. CX2100060053), National Key Research and Development Program of China (Grant No. 2018YFB1801105), and China Postdoctoral Science Foundation (Grant No. 2020T130493).

References

1 Gini F, Greco M V. Suboptimum approach to adaptive coherent radar detection in compound-Gaussian clutter. IEEE Trans Aerosp Electron Syst, 1999, 35: 1095–1104

2 Chong C Y, Pascal F, Ovarlez J P, et al. MIMO radar detection in non-Gaussian and heterogeneous clutter. IEEE J Sel Top Signal Process, 2010, 4: 115–126
3 Palam R, Greco M, Gini F. Multistatic adaptive CFAR detection in non-Gaussian clutter. EURASIP Journal on Advances in Signal Processing. 2016, 2016: 107
4 Kelly E J. An adaptive detection algorithm. IEEE Trans Aerosp Electron Syst, 1986, 22: 115–127
5 de Maio A, Greco M S. Modern Radar Detection Theory. Raleigh: SciTech Publishing, 2016
6 Gini F, Farina A. Vector subspace detection in compound-Gaussian clutter. Part I: survey and new results. IEEE Trans Aerosp Electron Syst, 2002, 38: 1295–1311
7 Sangston K J, Farina A. Coherent radar detection in compound-Gaussian clutter: Clairvoyant detectors. IEEE Aerosp Electron Syst Mag, 2016, 31: 42–63
8 Lemonte A J. The Gradient Test: Another Likelihood-Based Test. Cambridge: Cambridge University Press, 2016
9 Durbin J. Testing for serial correlation in least-squares regression when some of the regressors are lagged dependent variables. Econometrica, 1970, 38: 410–421
10 Scharf L L. Statistical Signal Processing: Detection, Estimation, and Times Series Analysis. New York: Addison-Wesley Publishing Company, 1991
11 Kay S M. The multifamily likelihood ratio test for multiple signal model detection. IEEE Signal Process Lett, 2005, 12: 369–371
12 Abramovich Y I, Spencer N K, Gorokhov A Y. Modified GLRT and AMF framework for adaptive detectors. IEEE Trans Aerosp Electron Syst, 2007, 43: 1017–1051
13 Carotenuto V, de Maio A, Clemente C, et al. Invariant rules for multipolarization SAR change detection. IEEE Trans Geosci Remote Sens, 2015, 53: 3294–3311
14 Carotenuto V, de Maio A, Clemente C, et al. Unstructured versus structured GLRT for multipolarization SAR change detection. IEEE Geosci Remote Sens Lett, 2015, 12: 1665–1669
15 Carotenuto V, de Maio A, Clemente C, et al. Forcing scale invariance in multipolarization SAR change detection. IEEE Trans Geosci Remote Sens, 2016, 54: 36–50
16 Ciuonzo D, Carotenuto V, de Maio A. On multiple covariance equality testing with application to SAR change detection. IEEE Trans Signal Process, 2017, 65: 5078–5091
17 de Maio A, de Nicola S, Farina A. GLRT versus MFLRT for adaptive CFAR radar detection with conic uncertainty. IEEE Signal Process Lett, 2009, 16: 707–710
18 de Maio A, Orlando D, Pallotta L, et al. A multifamily GLRT for oil spill detection. IEEE Trans Geosci Remote Sens, 2017, 55: 63–79
19 de Maio A, Han S, Orlando D. Adaptive radar detectors based on the observed FIM. IEEE Trans Signal Process, 2018, 66: 3838–3847
20 Gerlach K, Steiner M J. Adaptive detection of range distributed targets. IEEE Trans Signal Process, 1999, 47: 1844–1851
21 de Maio A. Polarimetric adaptive detection of range-distributed targets. IEEE Trans Signal Process, 2002, 50: 2152–2159
22 de Maio A, Farina A, Gerlach K. Adaptive detection of range spread targets with orthogonal rejection. IEEE Trans Aerosp Electron Syst, 2007, 43: 738–752
23 Aubry A, de Maio A, Orlando D, et al. Adaptive detection of point-like targets in the presence of homogeneous clutter and subspace interference. IEEE Signal Process Lett, 2014, 21: 848–852
24 Aubry A, de Maio A, Foglia G, et al. Diffuse multipath exploitation for adaptive radar detection. IEEE Trans Signal Process, 2015, 63: 1268–1281
25 Rong Y, Aubry A, de Maio A, et al. Diffuse multipath exploitation for adaptive detection of range distributed targets. IEEE Trans Signal Process, 2020, 68: 1197–1212
26 Rao C R. Score test: historical review and recent developments. In: Proceedings of Advances in Ranking and Selection, Multiple Comparisons, and Reliability. Boston: Birkhäuser, 2005. 3–20
27 Kay S M. Fundamentals of Statistical Signal Processing: Detection Theory. Englewood Cliffs: Prentice-Hall, 1998
28 Pagadarai S, Wyglinski A, Anderson C. An evaluation of the Bayesian CRLB for time-varying MIMO channel estimation using complex-valued differentials. In: Proceedings of IEEE Pacific Rim Conference on Communications, Computers and Signal Processing, 2011. 818–823
29 Liu W, Wang Y, Xie W. Fisher information matrix, Rao test, and Wald test for complex-valued signals and their applications. Signal Process, 2014, 94: 1–5
30 Kay S, Zhu Z. The complex parameter Rao test. IEEE Trans Signal Process, 2016, 64: 6580–6588
31 Hjørungnes A. Complex-Valued Matrix Derivatives: With Applications in Signal Processing and Communications. New York: Cambridge University Press, 2011
32 Magnus J R, Neudecker H. Matrix Differential Calculus with Applications in Statistics and Econometrics. 3rd ed. New York: Wiley, 2007
33 Richards M A, Scheer J A, Holm W A. Principles of Modern Radar, Volume I - Basic Principles. Raleigh: SciTech Publishing, 2010
34 Weinberg G. Radar Detection Theory of Sliding Window Processes. Boca Raton: CRC Press, 2017
35 Brennan L E, Reed L S. Theory of adaptive radar. IEEE Trans Aerosp Electron Syst, 1973, 9: 237–252
36 Li J, Stoica P. Robust Adaptive Beamforming. Hoboken: Wiley, 2006
37 Wang Y, Peng Y. Space-Time Adaptive Processing. Beijing: Tsinghua University Press, 2000
38 Klemm R. Principles of Space-Time Adaptive Processing. 3rd ed. London: The Institution of Electrical Engineers, 2006
39 Guerci J R. Space-Time Adaptive Processing for Radar. 2nd ed. Boston: Artech House, 2015
40 Ward J. Space-time Adaptive Processing for Airborne Radar. Technical Report. Lexington: MIT Lincoln Laboratory, 1994
41 Melvin W L. A STAP overview. IEEE Aerosp Electron Syst Mag, 2004, 19: 19–35
42 Reed I S, Mallett J D, Brennan L E. Rapid convergence rate in adaptive arrays. IEEE Trans Aerosp Electron Syst, 1974, 10: 853–863
43 Chen W S, Reed I S. A new CFAR detection test for radar. Digital Signal Process, 1991, 1: 198–214
44 Robey F C, Fuhrmann D R, Kelly E J, et al. A CFAR adaptive matched filter detector. IEEE Trans Aerosp Electron Syst, 1992, 28: 208–216
45 de Maio A. Rao test for adaptive detection in Gaussian interference with unknown covariance matrix. IEEE Trans Signal Process, 2007, 55: 3577–3584
46 Wang H, Cai L. On adaptive multiband signal detection with the SMI algorithm. IEEE Trans Aerosp Electron Syst, 1990,

26: 768–773
47 de Maio A. A new derivation of the adaptive matched filter. IEEE Signal Process Lett, 2004, 11: 792–793
48 Gerlach K. A mean level adaptive detector using nonconcurrent data. IEEE Trans Aerosp Electron Syst, 1994, 30: 258–265
49 Gerlach K. A comparison of two adaptive detection schemes. IEEE Trans Aerosp Electron Syst, 1994, 30: 30–40
50 Gerlach K. Effects of signal contamination on two adaptive detectors. IEEE Trans Aerosp Electron Syst, 1995, 31: 297–309
51 Gerlach K, Lin F C. Convergence performance of binary adaptive detectors. IEEE Trans Aerosp Electron Syst, 1995, 31: 329–340
52 Reed I S, Gau Y L, Truong T K. CFAR detection and estimation for STAP radar. IEEE Trans Aerosp Electron Syst, 1998, 34: 722–735
53 Wang Y-L, Bao Z, Peng Y-N. STAP with medium PRF mode for non-side-looking airborne radar. IEEE Trans Aerosp Electron Syst, 2000, 36: 609–620
54 Conte E, de Maio A, Ricci G. GLRT-based adaptive detection algorithms for range-spread targets. IEEE Trans Signal Process, 2001, 49: 1336–1348
55 Kraut S, Scharf L L, Butler R W. The adaptive coherence estimator: a uniformly most-powerful-invariant adaptive detection statistic. IEEE Trans Signal Process, 2005, 53: 427–438
56 Kraut S, Scharf L L. The CFAR adaptive subspace detector is a scale-invariant GLRT. IEEE Trans Signal Process, 1999, 47: 2538–2541
57 de Maio A, Iommelli S. Coincidence of the Rao test, Wald test, and GLRT in partially homogeneous environment. IEEE Signal Process Lett, 2008, 15: 385–388
58 Liu J, Li H, Himed B. Threshold setting for adaptive matched filter and adaptive coherence estimator. IEEE Signal Process Lett, 2015, 22: 11–15
59 Conte E, de Maio A. An invariant framework for adaptive detection in partially homogeneous environment. WSEAS Trans Circ, 2003, 2: 282–287
60 de Maio A. Invariance theory for adaptive radar detection in heterogeneous environment. IEEE Signal Process Lett, 2019, 26: 996–1000
61 Pascal F, Chitour Y, Ovarlez J P, et al. Covariance structure maximum-likelihood estimates in compound Gaussian noise: existence and algorithm analysis. IEEE Trans Signal Process, 2008, 56: 34–48
62 Conte E, Lops M, Ricci G. Asymptotically optimum radar detection in compound-Gaussian clutter. IEEE Trans Aerosp Electron Syst, 1995, 31: 617–625
63 Gini F. Sub-optimum coherent radar detection in a mixture of K-distributed and Gaussian clutter. IEE Proc Radar Sonar Navig, 1997, 144: 39
64 de Maio A, Conte E. Uniformly most powerful invariant detection in spherically invariant random vector distributed clutter. IET Radar Sonar Navig, 2010, 4: 560–563
65 Conte E, Lops M, Ricci G. Adaptive matched filter detection in spherically invariant noise. IEEE Signal Process Lett, 1996, 3: 248–250
66 Bidon S, Besson O, Tourneret J Y. The adaptive coherence estimator is the generalized likelihood ratio test for a class of heterogeneous environments. IEEE Signal Process Lett, 2008, 15: 281–284
67 Conte E, Lops M, Ricci G. Adaptive detection schemes in compound-Gaussian clutter. IEEE Trans Aerosp Electron Syst, 1998, 34: 1058–1069
68 Rangaswamy M. Statistical analysis of the nonhomogeneity detector for non-Gaussian interference backgrounds. IEEE Trans Signal Process, 2005, 53: 2101–2111
69 de Maio A, Foglia G, Conte E, et al. CFAR behavior of adaptive detectors: an experimental analysis. IEEE Trans Aerosp Electron Syst, 2005, 41: 233–251
70 Conte E, de Maio A, Ricci G. Recursive estimation of the covariance matrix of a compound-Gaussian process and its application to adaptive CFAR detection. IEEE Trans Signal Process, 2002, 50: 1908–1915
71 Conte E, de Maio A. Mitigation techniques for non-Gaussian sea clutter. IEEE J Ocean Eng, 2004, 29: 284–302
72 Gao Y, Aubry A, de Maio A, et al. Adaptive target separation detection. IEEE Trans Aerosp Electron Syst, 2021, 57: 293–309
73 de Maio A, Alfano G. Polarimetric adaptive detection in non-Gaussian noise. Signal Process, 2003, 83: 297–306
74 de Maio A, Alfano G, Conte E. Polarization diversity detection in compound-gaussian clutter. IEEE Trans Aerosp Electron Syst, 2004, 40: 114–131
75 Alfano G, de Maio A, Conte E. Polarization diversity detection of distributed targets in compound-Gaussian clutter. IEEE Trans Aerosp Electron Syst, 2004, 40: 755–765
76 Liu J, Zhang Z J, Yang Y. Performance enhancement of subspace detection with a diversely polarized antenna. IEEE Signal Process Lett, 2012, 19: 4–7
77 Hao C, Gazor S, Ma X, et al. Polarimetric detection and range estimation of a point-like target. IEEE Trans Aerosp Electron Syst, 2016, 52: 603–616
78 Park H R, Li J, Wang H. Polarization-space-time domain generalized likelihood ratio detection of radar targets. Signal Process, 1995, 41: 153–164
79 de Maio A, Ricci G. A polarimetric adaptive matched filter. Signal Process, 2001, 81: 2583–2589
80 Raghavan R S, Pulsone N, McLaughlin D J. Performance of the GLRT for adaptive vector subspace detection. IEEE Trans Aerosp Electron Syst, 1996, 32: 1473–1487
81 Lombardo P, Pastina D, Bucciarelli T. Adaptive polarimetric target detection with coherent radar. II. Detection against non-Gaussian background. IEEE Trans Aerosp Electron Syst, 2001, 37: 1207–1220
82 Liu J, Zhang Z J, Yang Y. Optimal waveform design for generalized likelihood ratio and adaptive matched filter detectors using a diversely polarized antenna. Signal Processing, 2012, 92: 1126–1131
83 Liu W, Xie W, Liu J, et al. Adaptive double subspace signal detection in Gaussian background-Part I: homogeneous environments. IEEE Trans Signal Process, 2014, 62: 2345–2357
84 Kraut S, Scharf L L, McWhorter L T. Adaptive subspace detectors. IEEE Trans Signal Process, 2001, 49: 1–16
85 Pastina D, Lombardo P, Bucciarelli T. Adaptive polarimetric target detection with coherent radar. I. Detection against Gaussian background. IEEE Trans Aerosp Electron Syst, 2001, 37: 1194–1206
86 Liu J, Zhang Z-J, Yang Y, et al. A CFAR adaptive subspace detector for first-order or second-order Gaussian signals based on a single observation. IEEE Trans Signal Process, 2011, 59: 5126–5140
87 Liu J, Zhang Z-J, Shui P L, et al. Exact performance analysis of an adaptive subspace detector. IEEE Trans Signal Process,

2012, 60: 4945–4950
88 Liu W, Wang Y L, Liu J, et al. Design and performance analysis of adaptive subspace detectors in orthogonal interference and gaussian noise. IEEE Trans Aerosp Electron Syst, 2016, 52: 2068–2079
89 Hughes P K. A high-resolution radar detection strategy. IEEE Trans Aerosp Electron Syst, 1983, 19: 663–667
90 Shuai X F, Kong L J, Yang J Y. Adaptive detection for distributed targets in Gaussian noise with Rao and Wald tests. Sci China Inf Sci, 2012, 55: 1290–1300
91 Hao C, Ma X, Shang X, et al. Adaptive detection of distributed targets in partially homogeneous environment with Rao and Wald tests. Signal Process, 2012, 92: 926–930
92 Wang H, Cai L. On adaptive multiband signal detection with GLR algorithm. IEEE Trans Aerosp Electron Syst, 1991, 27: 225–233
93 Conte E, de Maio A, Galdi C. CFAR detection of multidimensional signals: an invariant approach. IEEE Trans Signal Process, 2003, 51: 142–151
94 Liu W J, Xie W C, Wang Y L. Rao and Wald tests for distributed targets detection with unknown signal steering. IEEE Signal Process Lett, 2013, 20: 1086–1089
95 Raghavan R S. A generalized version of ACE and performance analysis. IEEE Trans Signal Process, 2020, 68: 2574–2585
96 Besson O, Scharf L L, Kraut S. Adaptive detection of a signal known only to lie on a line in a known subspace, when primary and secondary data are partially homogeneous. IEEE Trans Signal Process, 2006, 54: 4698–4705
97 Bose S, Steinhardt A O. Adaptive array detection of uncertain rank one waveforms. IEEE Trans Signal Process, 1996, 44: 2801–2809
98 Liu W, Xie W, Liu J, et al. Detection of a distributed target with direction uncertainty. IET Radar Sonar Navig, 2014, 8: 1177–1183
99 Liu W, Liu J, Huang L, et al. Robust GLRT approaches to signal detection in the presence of spatial-temporal uncertainty. Signal Process, 2016, 118: 272–284
100 Liu W J, Gao F, Luo Y W, et al. GLRT-based generalized direction detector in partially homogeneous environment. Sci China Inf Sci, 2019, 62: 209303
101 Kelly E J, Forsythe K M. Adaptive Detection and Parameter Estimation for Multidimensional Signal Models. Technical Report. Lexington: Lincoln Laboratory, 1989
102 Liu W, Xie W, Liu J, et al. Adaptive double subspace signal detection in Gaussian background-Part II: partially homogeneous environments. IEEE Trans Signal Process, 2014, 62: 2358–2369
103 Raghavan R S. Maximal invariants and performance of some invariant hypothesis tests for an adaptive detection problem. IEEE Trans Signal Process, 2013, 61: 3607–3619
104 Raghavan R. Analysis of steering vector mismatch on adaptive noncoherent integration. IEEE Trans Aerosp Electron Syst, 2013, 49: 2496–2508
105 Liu J, Liu W, Chen B, et al. Detection probability of a CFAR matched filter with signal steering vector errors. IEEE Signal Process Lett, 2015, 22: 2474–2478
106 Kelly E J. Performance of an adaptive detection algorithm — rejection of unwanted signals. IEEE Trans Aerosp Electron Syst, 1989, 25: 122–133
107 Richmond C D. Performance of the adaptive sidelobe blanker detection algorithm in homogeneous environments. IEEE Trans Signal Process, 2000, 48: 1235–1247
108 Liu W, Liu J, Zhang C, et al. Performance prediction of subspace-based adaptive detectors with signal mismatch. Signal Process, 2016, 123: 122–126
109 Zeira A, Friedlander B. Robust subspace detectors. In: Proceedings of the 31st Asilomar Conference on Signals, Systems and Computers, 1997. 778–782
110 Zeira A, Friedlander B. Robust adaptive subspace detectors for space time processing. In: Proceedings of IEEE International Conference on Acoustics, Speech and Signal Processing (ICASSP), 1998. 1965–1968
111 de Maio A, de Nicola S, Farina A, et al. Adaptive detection of a signal with angle uncertainty. IET Radar Sonar Navig, 2010, 4: 537–547
112 Lee S, Nguyen M, Song I, et al. Detection schemes for range-spread targets based on the semidefinite problem. IEEE Trans Aerosp Electron Syst, 2019, 55: 57–69
113 de Maio A. Robust adaptive radar detection in the presence of steering vector mismatches. IEEE Trans Aerosp Electron Syst, 2005, 41: 1322–1337
114 Besson O. Detection of a signal in linear subspace with bounded mismatch. IEEE Trans Aerosp Electron Syst, 2006, 42: 1131–1139
115 Besson O. Adaptive detection with bounded steering vectors mismatch angle. IEEE Trans Signal Process, 2007, 55: 1560–1564
116 de Maio A, Huang Y, Palomar D P, et al. Fractional QCQP with applications in ML steering direction estimation for radar detection. IEEE Trans Signal Process, 2011, 59: 172–185
117 Hao C, Bandiera F, Yang J, et al. Adaptive detection of multiple point-like targets under conic constraints. Progress In Electromagnetics Res, 2012, 129: 231–250
118 Coluccia A, Ricci G, Besson O. Design of robust radar detectors through random perturbation of the target signature. IEEE Trans Signal Process, 2019, 67: 5118–5129
119 Pulsone N B, Rader C M. Adaptive beamformer orthogonal rejection test. IEEE Trans Signal Process, 2001, 49: 521–529
120 Bandiera F, Besson O, Orlando D, et al. Derivation and analysis of an adaptive detector with enhanced mismatched signals rejection capabilities. In: Proceedings of the 41st Asilomar Conference on Signals, Systems and Computers, 2007. 2182–2186
121 Hao C, Shang X, Bandiera F, et al. Bayesian radar detection with orthogonal rejection. IEICE Trans Fundamentals, 2012, 95: 596–599
122 Coluccia A, Ricci G. A tunable W-ABORT-like detector with improved detection vs rejection capabilities trade-off. IEEE Signal Process Lett, 2015, 22: 713–717
123 Liu J, Zhao H Y, Liu W, et al. Adaptive detection using both the test and training data for disturbance correlation estimation. Signal Process, 2017, 137: 309–318
124 Liu W, Liu J, Huang L, et al. Distributed target detectors with capabilities of mismatched subspace signal rejection. IEEE Trans Aerosp Electron Syst, 2017, 53: 888–900
125 Hou C, Yang J, Ma X, et al. Adaptive detection of distributed targets with orthogonal rejection. IET Radar Sonar Navig, 2012, 6: 483–493

126 Liu W, Liu J, Du Q, et al. Distributed target detection in partially homogeneous environment when signal mismatch occurs. IEEE Trans Signal Process, 2018, 66: 3918–3928
127 Orlando D, Ricci G. A Rao test with enhanced selectivity properties in homogeneous scenarios. IEEE Trans Signal Process, 2010, 58: 5385–5390
128 Kalson S Z. An adaptive array detector with mismatched signal rejection. IEEE Trans Aerosp Electron Syst, 1992, 28: 195–207
129 Hao C, Liu B, Yan S, et al. Parametric adaptive radar detector with enhanced mismatched signals rejection capabilities. EURASIP J Adv Signal Process, 2010, 2010: 375136
130 Liu W, Xie W, Wang Y. Parametric detector in the situation of mismatched signals. IET Radar Sonar Navig, 2014, 8: 48–53
131 Bandiera F, Orlando D, Ricci G. One- and two-stage tunable receivers. IEEE Trans Signal Process, 2009, 57: 3264–3273
132 Raghavan R S, Qiu H F, McLaughlin D J. CFAR detection in clutter with unknown correlation properties. IEEE Trans Aerosp Electron Syst, 1995, 31: 647–657
133 Liu W, Xie W, Li R, et al. Adaptive detection in the presence of signal mismatch. J Syst Eng Electron, 2015, 26: 38–43
134 Liu W, Xie W, Zhang Q, et al. A doubly parameterized detector for mismatched signals. Chin J Electron, 2015, 24: 152–156
135 Liu J, Liu W, Chen B, et al. Modified Rao test for multichannel adaptive signal detection. IEEE Trans Signal Process, 2016, 64: 714–725
136 Liu J, Zhou S, Liu W, et al. Tunable adaptive detection in colocated MIMO radar. IEEE Trans Signal Process, 2018, 66: 1080–1092
137 Pulsone N B, Zatman M A. A computationally efficient two-step implementation of the GLRT. IEEE Trans Signal Process, 2000, 48: 609–616
138 Bandiera F, Besson O, Orlando D, et al. An improved adaptive sidelobe blanker. IEEE Trans Signal Process, 2008, 56: 4152–4161
139 Bandiera F, Orlando D, Ricci G. A subspace-based adaptive sidelobe blanker. IEEE Trans Signal Process, 2008, 56: 4141–4151
140 Hao C, Liu B, Cai L. Performance analysis of a two-stage Rao detector. Signal Process, 2011, 91: 2141–2146
141 Duan K, Liu M, Dai H, et al. A two-stage detector for mismatched subspace signals. IEEE Geosci Remote Sens Lett, 2017, 14: 2270–2274
142 Bandiera F, Orlando D, Ricci G. Advanced radar detection schemes under mismatched signal models. Synthesis Lect Signal Process, 2009, 4: 1–105
143 de Maio A, Orlando D. Feature article: a survey on two-stage decision schemes for point-like targets in Gaussian interference. IEEE Aerosp Electron Syst Mag, 2016, 31: 20–29
144 Liu J, Li K, Zhang X, et al. A weighted detector for mismatched subspace signals. Signal Process, 2017, 140: 110–115
145 Bandiera F, Besson O, Ricci G. An ABORT-like detector with improved mismatched signals rejection capabilities. IEEE Trans Signal Process, 2008, 56: 14–25
146 Briggs J N. Target Detection by Marine Radar. London: The Institution of Electrical Engineers, 2004
147 Genova J. Electronic Warfare Signal Processing. Boston: Artech House, 2018
148 Scharf L L, Friedlander B. Matched subspace detectors. IEEE Trans Signal Process, 1994, 42: 2146–2157
149 Behrens R T, Scharf L L. Signal processing applications of oblique projection operators. IEEE Trans Signal Process, 1994, 42: 1413–1424
150 Scharf L L, McCloud M L. Blind adaptation of zero forcing projections and oblique pseudo-inverses for subspace detection and estimation when interference dominates noise. IEEE Trans Signal Process, 2002, 50: 2938–2946
151 Besson O, Scharf L L, Vincent F. Matched direction detectors and estimators for array processing with subspace steering vector uncertainties. IEEE Trans Signal Process, 2005, 53: 4453–4463
152 Besson O, Scharf L L. CFAR matched direction detector. IEEE Trans Signal Process, 2006, 54: 2840–2844
153 Wang P, Fang J, Li H, et al. Detection with target-induced subspace interference. IEEE Signal Process Lett, 2012, 19: 403–406
154 Liu J, Zhang Z J, Cao Y, et al. Distributed target detection in subspace interference plus Gaussian noise. Signal Process, 2014, 95: 88–100
155 Bandiera F, de Maio A, Greco A S, et al. Adaptive radar detection of distributed targets in homogeneous and partially homogeneous noise plus subspace interference. IEEE Trans Signal Process, 2007, 55: 1223–1237
156 Liu J, Li J. False alarm rate of the GLRT for subspace signals in subspace interference plus Gaussian noise. IEEE Trans Signal Process, 2019, 67: 3058–3069
157 Liu W, Liu J, Huang L, et al. Rao tests for distributed target detection in interference and noise. Signal Process, 2015, 117: 333–342
158 Liu W, Liu J, Li H, et al. Multichannel signal detection based on Wald test in subspace interference and Gaussian noise. IEEE Trans Aerosp Electron Syst, 2019, 55: 1370–1381
159 Wang Z. Modified Rao test for distributed target detection in interference and noise. Signal Process, 2020, 172: 107578
160 Liu J, Li J. Analytical performance of rank-one signal detection in subspace interference plus Gaussian noise. IEEE Trans Aerosp Electron Syst, 2020, 56: 1595–1601
161 Liu W, Wang Y L, Liu J, et al. Performance analysis of adaptive detectors for point targets in subspace interference and Gaussian noise. IEEE Trans Aerosp Electron Syst, 2018, 54: 429–441
162 Liu W, Liu J, Gao Y, et al. Multichannel signal detection in interference and noise when signal mismatch happens. Signal Process, 2020, 166: 107268
163 Aubry A, Carotenuto V, de Maio A, et al. Coincidence of maximal invariants for two adaptive radar detection problems. IEEE Signal Process Lett, 2016. doi: 10.1109/LSP.2016.2587800
164 de Maio A, Orlando D. Adaptive radar detection of a subspace signal embedded in subspace structured plus Gaussian interference via invariance. IEEE Trans Signal Process, 2016, 64: 2156–2167
165 Ciuonzo D, de Maio A, Orlando D. A Unifying framework for adaptive radar detection in homogeneous plus structured interference-Part I: on the maximal invariant statistic. IEEE Trans Signal Process, 2016, 64: 2894–2906
166 Ciuonzo D, de Maio A, Orlando D. A unifying framework for adaptive radar detection in homogeneous plus structured interference-Part II: detectors design. IEEE Trans Signal Process, 2016, 64: 2907–2919
167 Ciuonzo D, de Maio A, Orlando D. On the statistical invariance for adaptive radar detection in partially homogeneous disturbance plus structured interference. IEEE Trans Signal Process, 2017, 65: 1222–1234
168 Bandiera F, Besson O, Orlando D, et al. GLRT-based direction detectors in homogeneous noise and subspace interference.

IEEE Trans Signal Process, 2007, 55: 2386–2394
169 Li W, Tong H, Li K, et al. Wald tests for direction detection in noise and interference. Multidim Syst Sign Process, 2018, 29: 1563–1577
170 Dong Y, Liu M, Li K, et al. Adaptive direction detection in deterministic interference and partially homogeneous noise. IEEE Signal Process Lett, 2017, 24: 599–603
171 Bandiera F, Besson O, Ricci G. Direction detector for distributed targets in unknown noise and interference. Electron lett, 2013, 49: 68–69
172 Richmond C D. Statistics of adaptive nulling and use of the generalized eigenrelation (GER) for modeling inhomogeneities in adaptive processing. IEEE Trans Signal Process, 2000, 48: 1263–1273
173 Richmond C D. Performance of a class of adaptive detection algorithms in nonhomogeneous environments. IEEE Trans Signal Process, 2000, 48: 1248–1262
174 Rabideau D J, Steinhardt A O. Improved adaptive clutter cancellation through data-adaptive training. IEEE Trans Aerosp Electron Syst, 1999, 35: 879–891
175 Bandiera F, de Maio A, Ricci G. Adaptive CFAR radar detection with conic rejection. IEEE Trans Signal Process, 2007, 55: 2533–2541
176 de Maio A, de Nicola S, Huang Y W, et al. Adaptive detection and estimation in the presence of useful signal and interference mismatches. IEEE Trans Signal Process, 2009, 57: 436–450
177 Svensson A, Jakobsson A. Adaptive detection of a partly known signal corrupted by strong interference. IEEE Signal Process Lett, 2011, 18: 729–732
178 Liu W, Liu J, Wang L, et al. Adaptive array detection in noise and completely unknown jamming. Digital Signal Process, 2015, 46: 41–48
179 Liu W, Liu J, Hu X, et al. Statistical performance analysis of the adaptive orthogonal rejection detector. IEEE Signal Process Lett, 2016, 23: 873–877
180 Besson O. Detection in the presence of surprise or undernulled interference. IEEE Signal Process Lett, 2007, 14: 352–354
181 Liu W J, Han H, Liu J, et al. Multichannel radar adaptive signal detection in interference and structure nonhomogeneity. Sci China Inf Sci, 2017, 60: 112302
182 Besson O, Orlando D. Adaptive detection in nonhomogeneous environments using the generalized eigenrelation. IEEE Signal Process Lett, 2007, 14: 731–734
183 Hao C, Orlando D, Hou C. Rao and Wald tests for nonhomogeneous scenarios. Sensors, 2012, 12: 4730–4736
184 Shang Z, Du Q, Tang Z, et al. Multichannel adaptive signal detection in structural nonhomogeneous environment characterized by the generalized eigenrelation. Signal Process, 2018, 148: 214–222
185 Tang P, Wang Y L, Liu W, et al. Adaptive subspace signal detection in a type of structure-nonhomogeneity environment. Signal Process, 2020, 173: 107600
186 Orlando D. A novel noise jamming detection algorithm for radar applications. IEEE Signal Process Lett, 2017, 24: 206–210
187 Addabbo P, Besson O, Orlando D, et al. Adaptive detection of coherent radar targets in the presence of noise jamming. IEEE Trans Signal Process, 2019, 67: 6498–6510
188 Yan L, Addabbo P, Hao C, et al. New ECCM techniques against noiselike and/or coherent interferers. IEEE Trans Aerosp Electron Syst, 2020, 56: 1172–1188
189 Raghavan R S. A CFAR detector for mismatched eigenvalues of training sample covariance matrix. IEEE Trans Signal Process, 2019, 67: 4624–4635
190 Besson O. Detection of Gaussian signal using adaptively whitened data. IEEE Signal Process Lett, 2019, 26: 430–434
191 Besson O. Adaptive detection using whitened data when some of the training samples undergo covariance mismatch. IEEE Signal Process Lett, 2020, 27: 795–799
192 Liu J, Liu W, Liu H. A simpler proof of rapid convergence rate in adaptive arrays. IEEE Trans Aerosp Electron Syst, 2017, 53: 135–136
193 Gerlach K. Outlier resistant adaptive matched filtering. IEEE Trans Aerosp Electron Syst, 2002, 38: 885–901
194 Rangaswamy M, Michels J H, Himed B. Statistical analysis of the non-homogeneity detector for STAP applications. Digital Signal Process, 2004, 14: 253–267
195 Han S, de Maio A, Carotenuto V, et al. Censoring outliers in radar data: an approximate ML approach and its analysis. IEEE Trans Aerosp Electron Syst, 2019, 55: 534–546
196 Besson O, Tourneret J Y, Bidon S. Knowledge-aided bayesian detection in heterogeneous environments. IEEE Signal Process Lett, 2007, 14: 355–358
197 Bidon S, Besson O, Tourneret J Y. A Bayesian approach to adaptive detection in nonhomogeneous environments. IEEE Trans Signal Process, 2008, 56: 205–217
198 Liu J, Han J, Zhang Z J, et al. Bayesian detection for MIMO radar in Gaussian clutter. IEEE Trans Signal Process, 2018, 66: 6549–6559
199 de Maio A, Farina A, Foglia G. Knowledge-aided Bayesian radar detectors & their application to live data. IEEE Trans Aerosp Electron Syst, 2010, 46: 170–183
200 Wang P, Sahinoglu Z, Pun M O, et al. Knowledge-aided adaptive coherence estimator in stochastic partially homogeneous environments. IEEE Signal Process Lett, 2011, 18: 193–196
201 Zhou Y, Zhang L-R. Knowledge-aided Bayesian radar adaptive detection in heterogeneous environment: GLRT, Rao and Wald tests. Int J Electron Commun, 2012, 66: 239–243
202 Bandiera F, Besson O, Coluccia A, et al. ABORT-like detectors: a Bayesian approach. IEEE Trans Signal Process, 2015, 63: 5274–5284
203 Bandiera F, Besson O, Ricci G. Adaptive detection of distributed targets in compound-gaussian noise without secondary data: a Bayesian approach. IEEE Trans Signal Process, 2011, 59: 5698–5708
204 Roman J R, Rangaswamy M, Davis D W, et al. Parametric adaptive matched filter for airborne radar applications. IEEE Trans Aerosp Electron Syst, 2000, 36: 677–692
205 Sohn K J, Li H B, Himed B. Parametric Rao test for multichannel adaptive signal detection. IEEE Trans Aerosp Electron Syst, 2007, 43: 921–933
206 Sohn K J, Li H, Himed B. Parametric GLRT for multichannel adaptive signal detection. IEEE Trans Signal Process, 2007, 55: 5351–5360
207 Li H B, Michels J H. Parametric adaptive signal detection for hyperspectral imaging. IEEE Trans Signal Process, 2006, 54: 2704–2715

208 Michels J H, Himed B, Rangaswamy M. Performance of STAP tests in Gaussian and compound-Gaussian clutter. Digital Signal Process, 2000, 10: 309–324
209 Alfano G, de Maio A, Farina A. Model-based adaptive detection of range-spread targets. IEE Proc Radar Sonar Navig, 2004, 151: 2
210 Sohn K J, Li H, Himed B. Recursive parametric tests for multichannel adaptive signal detection. IET Radar Sonar Navig, 2008, 2: 63–70
211 Abramovich Y I, Johnson B A, Spencer N K. Two-dimensional multivariate parametric models for radar applications-Part I: maximum-entropy extensions for Toeplitz-block matrices. IEEE Trans Signal Process, 2008, 56: 5509–5526
212 Abramovich Y I, Johnson B A, Spencer N K. Two-dimensional multivariate parametric models for radar applications-Part II: maximum-entropy extensions for hermitian-block matrices. IEEE Trans Signal Process, 2008, 56: 5527–5539
213 Abramovich Y I, Spencer N K, Johnson B A. Band-inverse TVAR covariance matrix estimation for adaptive detection. IEEE Trans Aerosp Electron Syst, 2010, 46: 375–396
214 Wang P, Li H, Himed B. A new parametric GLRT for multichannel adaptive signal detection. IEEE Trans Signal Process, 2010, 58: 317–325
215 Wang P, Li H, Himed B. A Bayesian parametric test for multichannel adaptive signal detection in nonhomogeneous environments. IEEE Signal Process Lett, 2010, 17: 351–354
216 Abramovich Y I, Rangaswamy M, Johnson B A, et al. Performance analysis of two-dimensional parametric STAP for airborne radar using KASSPER data. IEEE Trans Aerosp Electron Syst, 2011, 47: 118–139
217 Jiang C, Li H, Rangaswamy M. Conjugate gradient parametric detection of multichannel signals. IEEE Trans Aerosp Electron Syst, 2012, 48: 1521–1536
218 Jian T, He Y, Su F, et al. Adaptive detection of range-spread targets without secondary data in multichannel autoregressive process. Digital Signal Process, 2013, 23: 1686–1694
219 Wang P, Wang Z, Li H, et al. Knowledge-aided parametric adaptive matched filter with automatic combining for covariance estimation. IEEE Trans Signal Process, 2014, 62: 4713–4722
220 Shi B, Hao C, Hou C, et al. Parametric Rao test for multichannel adaptive detection of range-spread target in partially homogeneous environments. Signal Process, 2015, 108: 421–429
221 Mennad A, Younsi A, El Korso M N, et al. Adaptive detection of range-spread target in compound-Gaussian clutter without secondary data. Digital Signal Process, 2017, 60: 90–98
222 Gao Y, Li H, Himed B. Adaptive subspace tests for multichannel signal detection in auto-regressive disturbance. IEEE Trans Signal Process, 2018, 66: 5577–5587
223 Yan L, Hao C, Orlando D, et al. Parametric space-time detection and range estimation of point-like targets in partially homogeneous environment. IEEE Trans Aerosp Electron Syst, 2020, 56: 1228–1242
224 Fuhrmann D R. Application of Toeplitz covariance estimation to adaptive beamforming and detection. IEEE Trans Signal Process, 1991, 39: 2194–2198
225 Raghavan R S. CFAR detection in clutter with a kronecker covariance structure. IEEE Trans Aerosp Electron Syst, 2017, 53: 619–629
226 Wang Y, Xia W, He Z, et al. Polarimetric detection in compound Gaussian clutter with Kronecker structured covariance matrix. IEEE Trans Signal Process, 2017, 65: 4562–4576
227 Haimovich A M, Bar-Ness Y. An eigenanalysis interference canceler. IEEE Trans Signal Process, 1991, 39: 76–84
228 Wang Y L, Liu W J, Xie W C, et al. Reduced-rank space-time adaptive detection for airborne radar. Sci China Inf Sci, 2014, 57: 082310
229 Goldstein J S, Reed I S. Reduced-rank adaptive filtering. IEEE Trans Signal Process, 1997, 45: 492–496
230 Goldstein J S, Reed I S, Scharf L L. A multistage representation of the Wiener filter based on orthogonal projections. IEEE Trans Inform Theor, 1998, 44: 2943–2959
231 Goldstein J S, Reed I S, Zulch P A. Multistage partially adaptive STAP CFAR detection algorithm. IEEE Trans Aerosp Electron Syst, 1999, 35: 645–661
232 Pados D A, Karystinos G N. An iterative algorithm for the computation of the MVDR filter. IEEE Trans Signal Process, 2001, 49: 290–300
233 Fa R, de Lamare R C. Reduced-rank STAP algorithms using joint iterative optimization of filters. IEEE Trans Aerosp Electron Syst, 2011, 47: 1668–1684
234 Chen Z, Li H, Rangaswamy M. Conjugate gradient adaptive matched filter. IEEE Trans Aerosp Electron Syst, 2015, 51: 178–191
235 Chen W S, Mitra U, Schniter P. On the equivalence of three reduced rank linear estimators with applications to DS-CDMA. IEEE Trans Inform Theor, 2002, 48: 2609–2614
236 Scharf L L, Chong E K P, Zoltowski M D, et al. Subspace expansion and the equivalence of conjugate direction and multistage Wiener filters. IEEE Trans Signal Process, 2008, 56: 5013–5019
237 Broyden C G, Vespucci M T. Krylov Solvers for Linear Algebraic Systems. London: Elsevier, 2004
238 Dietl G K E. Linear Estimation and Detection in Krylov Subspaces. Berlin: Springer, 2007
239 Liu W J, Xie W C, Li R F, et al. Adaptive detectors in the Krylov subspace. Sci China Inf Sci, 2014, 57: 102310
240 Liu W, Xie W, Wang Y. Adaptive coherence estimator based on the Krylov subspace technique for airborne radar. J Syst Eng Electr, 2015, 26: 705–712
241 Gau Y-L, Reed I S. An improved reduced-rank CFAR space-time adaptive radar detection algorithm. IEEE Trans Signal Process, 1998, 46: 2139–2146
242 Reed I S, Gau Y-L. A fast CFAR detection space-time adaptive processing algorithm. IEEE Trans Signal Process, 1999, 47: 1151–1154
243 Reed I S, Gau Y L. Noncoherent summation of multiple reduced-rank test statistics for frequency-hopped STAP. IEEE Trans Signal Process, 1999, 47: 1708–1711
244 Liu W, Xie W, Wang Y. Adaptive detection based on orthogonal partition of the primary and secondary data. J Syst Eng Electron, 2014, 25: 34–42
245 Li H, Song W, Liu W, et al. Moving target detection with limited training data based on the subspace orthogonal projection. IET Radar Sonar Navig, 2018, 12: 679–684
246 Liu W, Xie W, Wang Y L. Diagonally loaded space-time adaptive detection. In: Proceedings of 2011 IEEE CIE International Conference on Radar, 2011. 1115–1119
247 de Maio A, Orlando D, Hao C, et al. Adaptive detection of point-like targets in spectrally symmetric interference. IEEE

Trans Signal Process, 2016, 64: 3207–3220
248 Nitzberg R. Application of maximum likelihood estimation of persymmetric covariance matrices to adaptive processing. IEEE Trans Aerosp Electron Syst, 1980, AES-16: 124–127
249 de Maio A. Maximum likelihood estimation of structured persymmetric covariance matrices. Signal Process, 2003, 83: 633–640
250 Liu J, Liu W, Liu H, et al. Average SINR calculation of a persymmetric sample matrix inversion beamformer. IEEE Trans Signal Process, 2016, 64: 2135–2145
251 Liu J, Orlando D, Addabbo P, et al. SINR distribution for the persymmetric SMI beamformer with steering vector mismatches. IEEE Trans Signal Process, 2019, 67: 1382–1392
252 Pailloux G, Forster P, Ovarlez J P, et al. Persymmetric adaptive radar detectors. IEEE Trans Aerosp Electron Syst, 2011, 47: 2376–2390
253 Hao C, Gazor S, Foglia G, et al. Persymmetric adaptive detection and range estimation of a small target. IEEE Trans Aerosp Electron Syst, 2015, 51: 2590–2604
254 Liu J, Cui G, Li H, et al. On the performance of a persymmetric adaptive matched filter. IEEE Trans Aerosp Electron Syst, 2015, 51: 2605–2614
255 de Maio A, Orlando D. An invariant approach to adaptive radar detection under covariance persymmetry. IEEE Trans Signal Process, 2015, 63: 1297–1309
256 de Maio A, Orlando D, Soloveychik I, et al. Invariance theory for adaptive detection in interference with group symmetric covariance matrix. IEEE Trans Signal Process, 2016, 64: 6299–6312
257 Cai L, Wang H. A persymmetric modified-SMI algorithm. Signal Process, 1991, 23: 27–34
258 Cai L, Wang H. A persymmetric multiband GLR algorithm. IEEE Trans Aerosp Electron Syst, 1992, 28: 806–816
259 Liu J, Li J. Mismatched signal rejection performance of the persymmetric GLRT detector. IEEE Trans Signal Process, 2019, 67: 1610–1619
260 Liu J, Liu W, Tang B, et al. Distributed target detection exploiting persymmetry in Gaussian clutter. IEEE Trans Signal Process, 2019, 67: 1022–1033
261 Hao C, Orlando D, Ma X, et al. Persymmetric detectors with enhanced rejection capabilities. IET Radar Sonar Navig, 2014, 8: 557–563
262 Casillo M, de Maio A, Iommelli S, et al. A persymmetric GLRT for adaptive detection in partially-homogeneous environment. IEEE Signal Process Lett, 2007, 14: 1016–1019
263 Hao C, Orlando D, Ma X, et al. Persymmetric Rao and Wald tests for partially homogeneous environment. IEEE Signal Process Lett, 2012, 19: 587–590
264 Gao Y, Liao G, Zhu S, et al. Persymmetric adaptive detectors in homogeneous and partially homogeneous environments. IEEE Trans Signal Process, 2014, 62: 331–342
265 Hao C, Orlando D, Foglia G, et al. Persymmetric adaptive detection of distributed targets in partially-homogeneous environment. Digital Signal Process, 2014, 24: 42–51
266 Wang Z, Li M, Chen H, et al. Persymmetric detectors of distributed targets in partially homogeneous disturbance. Signal Process, 2016, 128: 382–388
267 Ciuonzo D, Orlando D, Pallotta L. On the maximal invariant statistic for adaptive radar detection in partially homogeneous disturbance with persymmetric Covariance. IEEE Signal Process Lett, 2016, 23: 1830–1834
268 Liu J, Liu W, Gao Y, et al. Persymmetric adaptive detection of subspace signals: algorithms and performance analysis. IEEE Trans Signal Process, 2018, 66: 6124–6136
269 Liu J, Sun S, Liu W. One-step persymmetric GLRT for subspace signals. IEEE Trans Signal Process, 2019, 67: 3639–3648
270 Mao L, Gao Y, Yan S, et al. Persymmetric subspace detection in structured interference and non-homogeneous disturbance. IEEE Signal Process Lett, 2019, 26: 928–932
271 Liu J, Liu W, Tang B, et al. Persymmetric adaptive detection in subspace interference plus gaussian noise. Signal Process, 2020, 167: 107316
272 Liu J, Jian T, Liu W, et al. Persymmetric adaptive detection with improved robustness to steering vector mismatches. Signal Process, 2020, 176: 107669
273 Liu J, Liu W, Hao C, et al. Persymmetric subspace detectors with multiple observations in homogeneous environments. IEEE Trans Aerosp Electron Syst, 2020, 56: 3276–3284
274 Conte E, de Maio A. Distributed target detection in compound-Gaussian noise with Rao and Wald tests. IEEE Trans Aerosp Electron Syst, 2003, 39: 568–582
275 Gao Y C, Liao G S, Zhu S Q, et al. A persymmetric GLRT for adaptive detection in compound-Gaussian clutter with random texture. IEEE Signal Process Lett, 2013, 20: 615–618
276 Guo X, Tao H, Zhao H Y, et al. Persymmetric Rao and Wald tests for adaptive detection of distributed targets in compound-Gaussian noise. IET Radar Sonar Navig, 2017, 11: 453–458
277 Liu J, Liu S, Liu W, et al. Persymmetric adaptive detection of distributed targets in compound-Gaussian sea clutter with Gamma texture. Signal Process, 2018, 152: 340–349
278 Liu J, Li H, Himed B. Persymmetric adaptive target detection with distributed MIMO radar. IEEE Trans Aerosp Electron Syst, 2015, 51: 372–382
279 Liu J, Liu W, Han J, et al. Persymmetric GLRT detection in MIMO radar. IEEE Trans Veh Technol, 2018, 67: 11913–11923
280 Liu J, Han J, Zhang Z J, et al. Target detection exploiting covariance matrix structures in MIMO radar. Signal Process, 2019, 154: 174–181
281 Liu J, Han J, Liu W, et al. Persymmetric Rao test for MIMO radar in Gaussian disturbance. Signal Processing, 2019, 165: 30–36
282 Billingsley J B, Farina A, Gini F, et al. Statistical analyses of measured radar ground clutter data. IEEE Trans Aerosp Electron Syst, 1999, 35: 579–593
283 Conte E, de Maio A, Farina A, et al. Statistical tests for higher order analysis of radar clutter their application to L-band measured data. IEEE Trans Aerosp Electron Syst, 2005, 41: 205–218
284 Yan S, Massaro D, Orlando D, et al. Adaptive detection and range estimation of point-like targets with symmetric spectrum. IEEE Signal Process Lett, 2017, 24: 1744–1748
285 Foglia G, Hao C, Farina A, et al. Adaptive detection of point-like targets in partially homogeneous clutter with symmetric spectrum. IEEE Trans Aerosp Electron Syst, 2017, 53: 2110–2119
286 Wang P, Li H, Himed B. Knowledge-aided parametric tests for multichannel adaptive signal detection. IEEE Trans Signal

Process, 2011, 59: 5970–5982
287 Wang P, Sahinoglu Z, Pun M O, et al. Persymmetric parametric adaptive matched filter for multichannel adaptive signal detection. IEEE Trans Signal Process, 2012, 60: 3322–3328
288 Gao Y, Liao G, Zhu S, et al. Generalised persymmetric parametric adaptive coherence estimator for multichannel adaptive signal detection. IET Radar Sonar Navig, 2015, 9: 550–558
289 Ginolhac G, Forster P, Pascal F, et al. Exploiting persymmetry for low-rank space time adaptive processing. Signal Processing, 2014, 97: 242–251
290 Hao C, Orlando D, Foglia G, et al. Knowledge-based adaptive detection: joint exploitation of clutter and system symmetry properties. IEEE Signal Process Lett, 2016, 23: 1489–1493
291 Foglia G, Hao C, Giunta G, et al. Knowledge-aided adaptive detection in partially homogeneous clutter: joint exploitation of persymmetry and symmetric spectrum. Digital Signal Process, 2017, 67: 131–138
292 Carotenuto V, de Maio A, Orlando D, et al. Radar detection architecture based on interference covariance structure classification. IEEE Trans Aerosp Electron Syst, 2019, 55: 607–618
293 Klemm R. Adaptive airborne MTI: an auxiliary channel approach. IEE Proc, 1987, 134: 269–276
294 DiPietro R C. Extended factored space-time processing for airborne radar systems. In: Proceedings of the 25th Asilomar Conference on Signals, Systems and Computers, 1992. 425–430
295 Wang Y-L, Chen J-W, Bao Z, et al. Robust space-time adaptive processing for airborne radar in nonhornogeneous clutter environments. IEEE Trans Aerosp Electron Syst, 2003, 39: 70–81
296 Brown R D, Schneible R A, Wicks M C, et al. STAP for clutter suppression with sum and difference beams. IEEE Trans Aerosp Electron Syst, 2000, 36: 634–646
297 Zhang W, He Z, Li J, et al. A method for finding best channels in beam-space post-Doppler reduced-dimension STAP. IEEE Trans Aerosp Electron Syst, 2014, 50: 254–264
298 Cai Y, Wu X, Zhao M, et al. Low-complexity reduced-dimension space-time adaptive processing for navigation receivers. IEEE Trans Aerosp Electron Syst, 2018, 54: 3160–3168
299 Yang Z, Wang Z, Liu W, et al. Reduced-dimension space-time adaptive processing with sparse constraints on beam-Doppler selection. Signal Process, 2019, 157: 78–87
300 Wang H, Cai L J. On adaptive spatial-temporal processing for airborne surveillance radar systems. IEEE Trans Aerosp Electron Syst, 1994, 30: 660–670
301 Ayoub T F, Haimovich A R. Modified GLRT signal detection algorithm. IEEE Trans Aerosp Electron Syst, 2000, 36: 810–818
302 Jin Y W, Friedlander B. Reduced-rank adaptive detection of distributed sources using subarrays. IEEE Trans Signal Process, 2005, 53: 13–25
303 Besson O. Adaptive detection using randomly reduced dimension generalized likelihood ratio test. Signal Process, 2020, 166: 107265
304 Wang Z, Zhao Z, Ren C, et al. Adaptive detection of point-like targets based on a reduced-dimensional data model. Signal Process, 2019, 158: 36–47
305 Wang Z. Distributed target detection using samples filtered with normalized conjugate signal steering vector. Circ Syst Signal Process, 2020, 39: 4762–4774
306 Liu W, Liu J, Huang L, et al. Performance analysis of reduced-dimension subspace signal filtering and detection in sample-starved environment. J Franklin Institute, 2019, 356: 629–653
307 Wang Z. Adaptive detection of multichannel signals without training data. Signal Process, 2020, 176: 107710
308 Li J, Stoica P. MIMO Radar Signal Processing. Hoboken: Wiley, 2009
309 Haimovich A, Blum R, Cimini L. MIMO radar with widely separated antennas. IEEE Signal Process Mag, 2008, 25: 116–129
310 Li J, Stoica P. MIMO radar with colocated antennas. IEEE Signal Process Mag, 2007, 24: 106–114
311 Fishler E, Haimovich A, Blum R S, et al. Spatial diversity in radars' models and detection performance. IEEE Trans Signal Process, 2006, 54: 823–838
312 Du C, Thompson J S, Petillot Y R. Predicted detection performance of MIMO radar. IEEE Signal Process Lett, 2008, 15: 83–86
313 Tajer A, Jajamovich G H, Wang X, et al. Optimal joint target detection and parameter estimation by MIMO radar. IEEE J Sel Top Signal Process, 2010, 4: 127–145
314 Akcakaya M, Nehorai A. MIMO radar detection and adaptive design under a phase synchronization mismatch. IEEE Trans Signal Process, 2010, 58: 4994–5005
315 Gogineni S, Nehorai A. Polarimetric MIMO radar with distributed antennas for target detection. IEEE Trans Signal Process, 2010, 58: 1689–1697
316 Sheikhi A, Zamani A. Temporal coherent adaptive target detection for multi-input multi-output radars in clutter. IET Radar Sonar Navig, 2008, 2: 86–96
317 Liu J, Zhang Z J, Cao Y H, et al. A closed-form expression for false alarm rate of adaptive MIMO-GLRT detector with distributed MIMO radar. Signal Process, 2013, 93: 2771–2776
318 Li N, Cui G, Kong L, et al. MIMO radar moving target detection against compound-Gaussian clutter. Circ Syst Signal Process, 2014, 33: 1819–1839
319 Li N, Cui G, Yang H, et al. Adaptive detection of moving target with MIMO radar in heterogeneous environments based on Rao and Wald tests. Signal Process, 2015, 114: 198–208
320 Li N, Cui G, Kong L, et al. Moving target detection for polarimetric multiple-input multiple-output radar in Gaussian clutter. IET Radar Sonar Navig, 2015, 9: 285–298
321 He Q, Lehmann N H, Blum R S, et al. MIMO radar moving target detection in homogeneous clutter. IEEE Trans Aerosp Electron Syst, 2010, 46: 1290–1301
322 Wang P, Li H, Himed B. Moving target detection using distributed MIMO radar in clutter with nonhomogeneous power. IEEE Trans Signal Process, 2011, 59: 4809–4820
323 Akcakaya M, Nehorai A. MIMO radar sensitivity analysis for target detection. IEEE Trans Signal Process, 2011, 59: 3241–3250
324 de Maio A, Lops M, Venturino L. Diversity-integration tradeoffs in MIMO detection. IEEE Trans Signal Process, 2008, 56: 5051–5061
325 de Maio A, Lops M. Design principles of MIMO radar detectors. IEEE Trans Aerosp Electron Syst, 2007, 43: 886–898
326 Naghsh M M, Modarres-Hashemi M. Exact theoretical performance analysis of optimum detector in statistical multi-input multi-output radars. IET Radar Sonar Navig, 2012, 6: 99–111

327 Li N, Cui G, Kong L, et al. Rao and Wald tests design of multiple-input multiple-output radar in compound-Gaussian clutter. IET Radar Sonar Navig, 2012, 6: 729–738
328 Zhang T X, Cui G L, Kong L J, et al. Adaptive Bayesian detection using MIMO radar in spatially heterogeneous clutter. IEEE Signal Process Lett, 2013, 20: 547–550
329 Li N, Yang H, Cui G, et al. Adaptive two-step Bayesian MIMO detectors in compound-Gaussian clutter. Signal Process, 2019, 161: 1–13
330 Cui G, Kong L, Yang X. GLRT-based detection algorithm for polarimetric MIMO radar against SIRV clutter. Circ Syst Signal Process, 2012, 31: 1033–1048
331 Cui G, Kong L, Yang X, et al. Distributed target detection with polarimetric MIMO radar in compound-Gaussian clutter. Digital Signal Process, 2012, 22: 430–438
332 Kong L, Cui G, Yang X, et al. Rao and Wald tests design of polarimetric multiple-input multiple-output radar in compound-Gaussian clutter. IET Signal Process, 2011, 5: 85–96
333 Cui G, Kong L, Yang X, et al. The Rao and Wald tests designed for distributed targets with polarization MIMO radar in compound-Gaussian clutter. Circ Syst Signal Process, 2012, 31: 237–254
334 Bekkerman I, Tabrikian J. Target detection and localization using MIMO radars and sonars. IEEE Trans Signal Process, 2006, 54: 3873–3883
335 Cui G, Kong L, Yang X. Performance analysis of colocated MIMO radars with randomly distributed arrays in compound-Gaussian clutter. Circ Syst Signal Process, 2012, 31: 1407–1422
336 Li J, Xu L Z, Stoica P, et al. Range compression and waveform optimization for MIMO radar: a CramÉr-Rao bound based study. IEEE Trans Signal Process, 2008, 56: 218–232
337 Xu L Z, Li J, Stoica P. Target detection and parameter estimation for MIMO radar systems. IEEE Trans Aerosp Electron Syst, 2008, 44: 927–939
338 Liu W, Wang Y, Liu J, et al. Adaptive detection without training data in colocated MIMO radar. IEEE Trans Aerosp Electron Syst, 2015, 51: 2469–2479
339 Liu J, Li J. Robust detection in MIMO radar with steering vector mismatches. IEEE Trans Signal Process, 2019, 67: 5270–5280
340 Fortunati S, Sanguinetti L, Gini F, et al. Massive MIMO radar for target detection. IEEE Trans Signal Process, 2020, 68: 859–871
341 Lan L, Marino A, Aubry A, et al. GLRT-based adaptive target detection in FDA-MIMO radar. IEEE Trans Aerosp Electron Syst, 2021, 57: 597–613
342 Hassanien A, Vorobyov S A. Phased-MIMO radar: a tradeoff between phased-array and MIMO radars. IEEE Trans Signal Process, 2010, 58: 3137–3151
343 Fuhrmann D R, Browning J P, Rangaswamy M. Signaling strategies for the hybrid MIMO phased-array radar. IEEE J Sel Top Signal Process, 2010, 4: 66–78
344 Li H, Himed B. Transmit subaperturing for MIMO radars with co-located antennas. IEEE J Sel Top Signal Process, 2010, 4: 55–65
345 Xu J, Dai X Z, Xia X G, et al. Optimizations of multisite radar system with MIMO radars for target detection. IEEE Trans Aerosp Electron Syst, 2011, 47: 2329–2343
346 Chen P, Zheng L, Wang X, et al. Moving target detection using colocated MIMO radar on multiple distributed moving platforms. IEEE Trans Signal Process, 2017, 65: 4670–4683
347 Chao S, Chen B, Li C. Grid cell based detection strategy for MIMO radar with widely separated subarrays. Int J Electron Commun, 2012, 66: 741–751
348 Wang P, Li H, Himed B. A parametric moving target detector for distributed MIMO radar in non-homogeneous environment. IEEE Trans Signal Process, 2013, 61: 2282–2294
349 Li H, Wang Z, Liu J, et al. Moving target detection in distributed MIMO radar on moving platforms. IEEE J Sel Top Signal Process, 2015, 9: 1524–1535
350 Zhang Z J, Liu J, Zhao Y, et al. False alarm rate of the GLRT-LQ detector in non-Gaussian and heterogeneous clutter. Aerospace Sci Tech, 2015, 47: 191–194
351 Xu L, Li J. Iterative generalized-likelihood ratio test for MIMO radar. IEEE Trans Signal Process, 2007, 55: 2375–2385
352 Kong L, Cui G, Yang X, et al. Adaptive detector design of MIMO radar with unknown covariance matrix. J Syst Eng Electron, 2010, 21: 954–960
353 Cui G, Kong L, Yang X. Multiple-input multiple-output radar detectors design in non-Gaussian clutter. IET Radar Sonar Navig, 2010, 4: 724–732
354 Wang J, Jiang S, He J, et al. Adaptive subspace detector for multi-input multi-output radar in the presence of steering vector mismatch. IET Radar Sonar Navig, 2011, 5: 23–31
355 Gerlach K, Steiner M, Lin F C. Detection of a spatially distributed target in white noise. IEEE Signal Process Lett, 1997, 4: 198–200
356 Gini F, Bordoni F, Farina A. Multiple radar targets detection by exploiting induced amplitude modulation. IEEE Trans Signal Process, 2004, 52: 903–913
357 Carotenuto V, de Maio A, Orlando D, et al. Model order selection rules for covariance structure classification in radar. IEEE Trans Signal Process, 2017, 65: 5305–5317
358 Liu W, Wang L, Di Y, et al. Adaptive energy detector and its application for mismatched signal detection. J Radars, 2014, 4: 149–159
359 Muirhead R J. Aspects of Multivariate Statistical Theory. 2nd ed. Hoboken: Wiley, 2005
360 Anderson T W. An Introduction to Multivariate Statistical Analysis. 3rd ed. Hoboken: Wiley, 2003
361 Long T, Liang Z N, Liu Q H. Advanced technology of high-resolution radar: target detection, tracking, imaging, and recognition. Sci China Inf Sci, 2019, 62: 040301
362 Liu W J, Li J J, Wang P X, et al. Wald tests for signal detection when uncertainty exists in a target's spatial-temporal steering vector. Sci China Inf Sci, 2020, 63: 189304
363 Li Y, Song R, Wang W. Particle swarm optimization of compression measurement for signal detection. Circ Syst Signal Process, 2012, 31: 1109–1126
364 Wang Y G, Liu Z, Yang L, et al. Generalized compressive detection of stochastic signals using Neyman-Pearson theorem. Signal Image Video Process, 2015, 9: 111–120
365 Razavi A, Valkama M, Cabric D. Compressive detection of random subspace signals. IEEE Trans Signal Process, 2016, 64:

4166–4179
366 Wimalajeewa T, Varshney P K. Sparse signal detection with compressive measurements via partial support set estimation. IEEE Trans Signal Inf Process over Networks, 2017, 3: 46–60
367 Wimalajeewa T, Varshney P K. Compressive sensing-based detection with multimodal dependent data. IEEE Trans Signal Process, 2018, 66: 627–640
368 Ma J, Gan L, Liao H, et al. Sparse signal detection without reconstruction based on compressive sensing. Signal Process, 2019, 162: 211–220
369 Zhang X, Sward J, Li H, et al. A sparsity-based passive multistatic detector. IEEE Trans Aerosp Electron Syst, 2019, 55: 3658–3666
370 Carotenuto V, Orlando D, Farina A. Interference covariance matrix structure classification in heterogeneous environment. IEEE Signal Process Lett, 2019, 26: 1491–1495
371 Liu J, Biondi F, Orlando D, et al. Training data classification algorithms for radar applications. IEEE Signal Process Lett, 2019, 26: 1446–1450
372 Coluccia A, Fascista A, Ricci G. CFAR feature plane: a novel framework for the analysis and design of radar detectors. IEEE Trans Signal Process, 2020, 68: 3903–3916
373 Coluccia A, Fascista A, Ricci G. A k-nearest neighbors approach to the design of radar detectors. Signal Process, 2020, 174: 107609
374 Zaimbashi A, Li J. Tunable adaptive target detection with kernels in colocated MIMO radar. IEEE Trans Signal Process, 2020, 68: 1500–1514
375 Gerlach K. Spatially distributed target detection in non-Gaussian clutter. IEEE Trans Aerosp Electron Syst, 1999, 35: 926–934
376 Gini F, Greco M. Covariance matrix estimation for CFAR detection in correlated heavy tailed clutter. Signal Process, 2002, 82: 1847–1859
377 Sangston K J, Gini F, Greco M S. Coherent radar target detection in heavy-tailed compound-Gaussian clutter. IEEE Trans Aerosp Electron Syst, 2012, 48: 64–77
378 Jian T, He Y, Su F, et al. Cascaded detector for range-spread target in non-Gaussian clutter. IEEE Trans Aerosp Electron Syst, 2012, 48: 1713–1725
379 Chen X, Guan J, Bao Z, et al. Detection and extraction of target with micromotion in spiky sea clutter via short-time fractional fourier transform. IEEE Trans Geosci Remote Sens, 2014, 52: 1002–1018
380 Xu S, Shi X, Xue J, et al. Adaptive subspace detection of range-spread target in compound Gaussian clutter with inverse Gaussian texture. Digital Signal Process, 2018, 81: 79–89
381 Yang Y, Xiao S, Wang X, et al. Performance analysis of radar detection for correlated Gamma fluctuating targets in K distributed sea clutter. Digital Signal Process, 2018, 79: 136–141